Optimization of PV Modules Layout on High-rise Building Skins Using a BIM-based Generative Design Approach

Negar Salimzadeh

A Thesis

in the Department

of

Building, Civil, and Environmental Engineering

Presented in Partial Fulfillment of the Requirements

For the Degree of Doctor of Philosophy (Civil Engineering) at

Concordia University

Montreal, Quebec, Canada

July, 2021

CONCORDIA UNIVERSITY

School of Graduate Studies

This is to certify that the thesis prepared

By: Negar Salimzadeh

Entitled: **Optimization of PV Modules Layout on High-rise Building Skins Using a BIM-based Generative Design Approach**

and submitted in partial fulfillment of the requirements for the degree of

Doctor of Philosophy (Civil Engineering)

complies with the regulations of the University and meets the accepted standards with respect to originality and quality.

Signed by the final Examing Committee:

_____ Chair

Dr. Gosta Grahne

_____ External to Examiner

Dr. Walid Tizani

_____ External to Program

Dr. Yong Zeng

_____ Examiner

Dr. Osama Moselhi

_____ Examiner

Dr. Fuzhan Nasiri

_____ Thesis Supervisors

Dr. Amin Hammad

_____

Dr. Faridaddin Vahdatikhaki

Approved by

_____

Dr. Michelle Nokken, Chair of Department or Graduate Program Director

_____

Date of Defence

_____

Dr. Mourad Debbabi, Dean, Gina Cody School of Engineering and Computer Science

ABSTRACT

Optimization of PV Modules Layout on High-rise Building Skins Using a BIM-based Generative Design Approach

Negar Salimzadeh, Ph.D.

Concordia University, 2021

Growing urbanism and the resulting increase of energy demand coupled with depleting fossil energy resources are making the need for renewable energy resources progressively palpable and vital. In addition to reducing carbon dioxide emissions, renewable energy is crucial to improve health and well-being, and provide affordable energy access worldwide.

Photovoltaic (PV) solar energy, as a fast-evolving industry, has become a vital part of the global energy transformation in recent years that can contribute to the development of sustainable cities and the mitigation of global warming. In the urban environment, buildings are central to human activities. Given that buildings currently account for 40% of the global energy consumption, to achieve sustainable urban development, buildings are of particular importance for distributed renewable energy generation, which reduces energy transmission losses. PV panels are able to harvest the solar power and turn it into a clean source of energy. Furthermore, the increasing availability, affordability, and efficiency of PV panels are rendering them an attractive option for the users so that the worldwide use of photovoltaic electricity is growing rapidly by more than 50% a year.

Of different types of buildings in the built environment, high-rise buildings are of particular interest because of their high potentials for harvesting a considerable amount of PV energy on vertical and horizontal surfaces. Nevertheless, this high potential is seldom harnessed mainly because the deployment of PV modules on high-rise buildings requires considering a complex interplay between various factors that affect the installation of PV modules (e.g., neighborhood

shadow effect, modules self-shadowing effect, surface-specific PV modules, etc.). This renders the design of PV modules in high-rise buildings a complex optimization problem, one that requires a generative design approach. There are many tools and models, from simple 2D evaluation to more comprehensive and complicated 3D analysis, that can help simulate the solar radiation potential of surfaces of a building. However, the majority of the methods do not discriminate between different types of surfaces of the building and treat the entire envelope as a single surface. In recent years, and with the advent and rising popularity of the Building Information Modeling (BIM) concept, the apparatus for the implementation of such a comprehensive generative design approach is becoming increasingly available. However, to the best of the author's knowledge, there is currently no framework for the BIM-based generative design of PV modules for high-rise buildings.

Addressing the current issues, this research aims to: (1) Develop a parametric modeling platform for the design of surface-specific PV module layout on the entire skin of buildings, and (2) Develop a BIM-based generative design framework for the design of PV modules layout on high-rise building skins. In this framework, the surface-specific parametric model of PV modules is integrated with an optimization method to find the optimum design of PV modules layout considering the study period, profit margin, harvested PV energy, and cost. This framework will enable designers and investors to apply the generative design paradigm to the use of PV modules on building skin considering the complex interaction between building surface types (e.g., windows, walls, etc.), type of PV module (e.g., opaque, semi-transparent, etc.), their tilt and pan angles, and the financial aspect of the PV system (i.e., revenue vs. cost at different study periods).

The results generated by the elaborate case study demonstrated that the generative design framework is capable of offering more favourable solutions (i.e., either or both of reduced costs and increased energy revenue) compared to baseline scenarios. It is observed that in the majority of the studied scenario, the optimum solutions favored a more consistent orientation of the panels (i.e., consistent pan and tilt angles across all the panels).

Dedicated to my parents for their endless love and unwavering support.

ACKNOWLEDGEMENTS

I would like to extend my sincere gratitude to my supervisor, Professor. Amin Hammad for his intellectual guidance, patience, and continuous support of my research. I am grateful for his trust in me and allowing me to grow. Also, I would like to express my special appreciation to my co-supervisor, Dr. Faridaddin Vahdatikhaki for his technical support and perpetual enthusiasm. His insightful advice, influential guidance, and explicit criticism encouraged me to fulfill my Ph.D. thesis at my best.

I would also like to thank the members of my committee Dr. Walid Tizani, Dr. Osama Moselhi, Dr. Fuzhan Nasiri, and Dr. Yong Zeng for their invaluable inputs and precious time.

Words cannot express how indebted and grateful I am to my parents, and my brother, Amin, for always believe in me. Without their endless love and tremendous support, I would not have made it this far. My appreciation also goes out to the rest of my family especially my uncles, Dr. Javad Salimzadeh and Mehdi Salimzadeh who inspired me during these years.

I feel very fortunate for having my exceptional friends Dr. Dorna Sheikhi, Dr. Azin Eftekhari, Dr. Shide Salimi, Ms. Neshat Bolourian, and all my wonderful colleagues for their camaraderie and for a cherished time spent together. Their presence and support softened the difficulties of this journey.

This research was made possible by a scholarship from “Pierre Arbour Foundation” (special thanks to my mentor Ms. Diane Dechamplain) and “Sustainability Research Award” from Concordia. These supports are greatly appreciated.

I would also like to acknowledge Dr. Veronique Delisle and Dr.Sophie Pelland from CanmetENERY- Renewable Energy Integration Sector in Natural Resource Canada, for the precious opportunity they gave me to be involved in one of their projects as a research engineer to evaluate the PV potential of the rooftops for Canadian municipalities using LiDAR data.

TABLE OF CONTENTS

LIST OF FIGURES

LIST OF TABLES

LIST OF ABBREVIATIONS

2D	2-Dimensional
3D	3-Dimensional
API	Application Programming Interface
ATM	Atmospheric and Topographic Model
BAPV	Building Applied Photovoltaics
BIM	Building Information Model
BIPV	Building Integrated Photovoltaics
BOS	Balance of System
CAD	Computer Aided Design
CityGML	Geography Markup Language
DEM	Digital Elevation Model
DSM	Digital Surface Model
GA	Genetic Algorithm
GD	Generative Design
GIS	Geographical Information System
IRENA	International Renewable Energy Agency
JMSB	John Molson School of Business
LCC	Life Cycle Cost
LiDAR	Light Detection and Ranging
LoD	Levels of Development
MOEA	Multi-Objective Evolutionary Algorithms
NSGA	Non-Dominated Sorting Genetic Algorithm
PSO	Particle Swarm Optimization
PV	Photo Voltaic
ROI	Return on Investment
SGW	Sir George William
SVF	Sky View Factor
TFSC	Thin-Film Solar Cells

CHAPTER 1 INTRODUCTION

1.1 GENERAL BACKGROUND

About half of the world population lives in urban areas and, based on United Nation's estimate, this ratio will increase to 66% by 2050 (United Nations, 2015). The worldwide energy consumption records show a continuous increase in electrical energy demand (International Energy Agency, 2018). On the other hand, energy consumption is one of the most significant contributors to carbon dioxide (CO_2) emissions. In recent years, the significant amount of energy consumption in cities propelled researchers and practitioners to move in the direction of the decentralized energy generation and net-zero energy buildings in urban areas (Marszal et al., 2011). Furthermore, the sustainability of urban energy systems with regard to population growth, limited energy sources and global climate change are becoming the main focus of planners (Salimzadeh et al., 2016).

Renewable energy resources, such as hydroelectricity, wind and wave power, solar, and geothermal are clean and safe alternatives for future energy demands. Based on the Bloomberg New Energy Finance (BNEF) report, from the US$11.5 trillion global investment in renewable energy between 2018 and 2050, US$8.4 trillion will be in solar power technologies. As a result, solar photovoltaic capacity will grow 17-fold while the increase in wind power capacity will be 6-fold (Bloomberg New Energy Finance, 2018). As shown in Figure 1-1, the Canadian Solar Industries Association (CanSIA) also reported rapid growth in Canada's solar electricity sector in their roadmap (CanSIA, 2020).

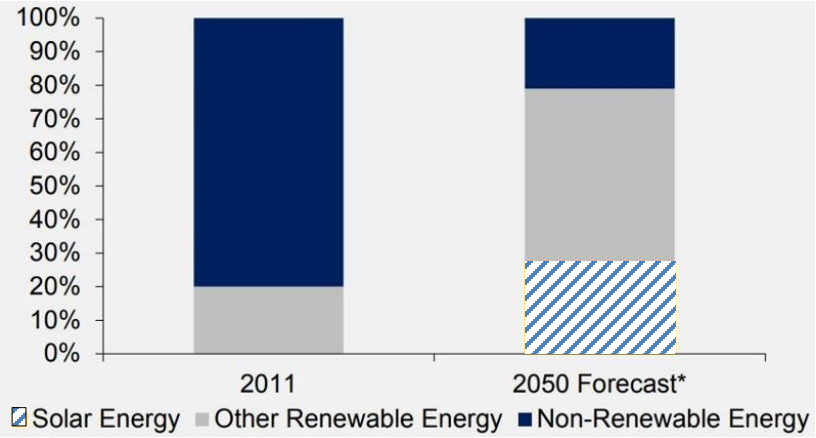

Figure 1-1 Global electricity mix in 2011 and 2050 forecast (CanSIA, 2020)

Growing urbanism and the higher level of energy demand in cities make photovoltaic (PV) technology an attractive option to generate energy. With the increasing global demand for energy and environmental concerns, as well as the continuous development of renewable technologies, PV energy is increasingly becoming a cost-effective operational energy option. Many of the global leading businesses have sensed this opportunity and started to leverage it. For instance, Apple and Amazon have an installed capacity of 393.3 MW, and 329.8 MW, respectively (SEIA, 2018). The worldwide use of PV electricity is increasing by more than 50% a year (Brown, 2015). Considering the decreasing cost of technology and the rising fossil fuel prices, the application of renewable energy technologies is promising. The application of PV systems in the built environment can reduce the need for electricity grid development and consequently minimize transportation loss (IRENA, 2021).

The application of PV modules has been widely explored in the built environment. However, the trend of PV application on building surfaces started by focusing on the rooftops of the buildings due to the simplicity of the process. Nevertheless, despite the lower radiation values on the vertical surfaces and the shadow effects of the surrounding objects, vertical surfaces (i.e., facades), especially of high-rise buildings, offer a great potential for the application of PV systems. Facades have fewer structural obstructions in comparison to rooftops such as chimneys, ventilation

systems, and antennas. Furthermore, the rate of snow accumulation on facade PV modules is lower.

This high potential is seldom harnessed mainly because the deployment of PV modules on high-rise buildings involves the consideration of a complex interplay between various factors that affect the installation of PV modules (Hong et al., 2014). Examples of these factors include climatic and geography related factors, building geometry and the build environment specifications, PV modules and hardware specifications, investment factors, etc. (Ning et al., 2017). Therefore, a successful design and implementation of PV modules on the facade of high-rise buildings need to be carried out in view of all these influential factors. When the economic aspect of deploying solar energy is added to the mentioned technical aspects, the PV modules design becomes a complex multi-objective optimization problem that requires a robust framework. In other words, a generative design methodology is needed to capture the complexities of PV module design for high-rise buildings.

In recent years, Building Information Modeling (BIM) has become an essential part of the design, architecture, and construction process. It provides all sorts of building data in an accessible 3D digital representation in advance of construction (Sydora & Stroulia, 2020). With the advent and rising popularity of the BIM concept, the apparatus for the implementation of such a comprehensive generative design approach is becoming increasingly available. Given that BIM models provide a rich repository of geometric and non-geometric data about the lifecycle of buildings, it has been successfully leveraged to solve complex building design optimization problems in the past (Liu et al., 2015). However, to the best of author knowledge, BIM has never been used for the application of generative design concepts to the design of PV systems on high-rise buildings. This is a major limitation in this domain because in the absence of semantically rich BIM models, the majority of approaches for PV system optimization resort to the indiscriminate treatment of building surfaces. This is an oversight because different types of surfaces on the building facade require different types of PV modules to maintain the economic edge of the design.

1.2 PROBLEM STATEMENT AND RESEARCH GAPS

The advent of various PV panels can extend the use of solar technologies considerably. However, there are still some limitations to the widespread use of solar panels in urban areas. On one hand, while the cost of solar panels has decreased considerably in recent years, the unsubsidized price is still high, especially for individual users. On the other hand, the relatively low efficiency of the PV panels, which exacerbates when they are applied on the façade, is another major deterrent in the adoption of the technology. Therefore, from a practical standpoint, for the use of PV panels to become economically viable and attractive for the end-users, the installation of PV modules on building skins must be thoroughly planned and optimized to adequately consider the diversity of available panels, their efficiencies, restrictions, costs, and payback periods. Only in view of such a comprehensive optimization would it be possible to generate viable strategies for the widespread implementation and application of the technology.

The analysis of solar radiation potential relies on computer simulations because many different factors play a major role in the radiation potential of a given external surface of a building. Examples of these factors include, but not limited to, (1) the location of the building, (2) the urban morphology of the surroundings, (3) the geometry and orientation of the building, (4) the mechanical installations on the rooftop, and (5) the size, type, and orientation of PV modules. Additionally, since a change in the size, shape, and orientation of PV modules can significantly change the shadow impact of the PV modules on themselves (especially on the vertical surfaces), radiation analysis is sensitive to the PV module layout. Therefore, for a given building, it is not sufficient to perform the radiation simulation only once, but instead, it needs to be performed for each alternative layout design.

Conventional simulation methods have a number of limitations: (1) Since PV modules have been conventionally considered only for rooftops, many of the existing simulation methods rely on the 2D and 2.5D models. These models cannot be used to analyze the vertical surfaces on the building facade (Carneiro et al., 2010; Esclapés et al., 2014); (2) The simulation methods that analyze the 3D models, do so only from the geometry perspective. This means that they do not distinguish

between different surfaces of the building facade and treat all of them equally (Catita et al., 2014; Liang et al., 2014). This can result in under- or over-design since there is a strong relationship between the type of surfaces and the type of PV modules that can be attached to them or integrated with them. Therefore, these simulation methods cannot be used for the design of a PV module layout where surface-restricted PV modules are considered (e.g., BIPV); (3) The majority of the existing simulation models do not consider the shape, size, and orientation of the PV modules in the radiation analysis (Bueno et al., 2015). In this sense, they cannot be used as a parametric modeling tool where the designer can easily investigate the impact of design changes (e.g., change of the size or orientation of the PV modules) on the overall performance of the PV system (Kim et al., 2015; Kim et al., 2015).

The emergence of BIM in recent years has provided a rich platform for object-based evaluation and analysis of buildings (Eastman et al., 2011; Eastman et al., 2011). Nonetheless, currently, BIM is not used for detailed and surface-specific simulation of building surfaces. Since BIM provides easy access to information about various elements of the building, it can be best used for various types of simulations, such as daylight, energy performance, and solar radiation (Wang & Chen, 2010; Abanda & Byers, 2016; Gourlis & Kovacic, 2017; Habibi, 2017). A research project in Germany is trying to integrate the energy active components into the building envelope based on BIM methodology (Solconpro, 2018). There are several software packages for BIM-based solar analysis, such as ECOTECT (Marsh, 2003) and Insight (Solar Analysis, 2021). However, these packages transform the BIM 3D objects into a polygon mesh. During this process, the semantic information about different objects is lost. As a result, these simulation packages also have the above-mentioned limitation about not being able to distinguish between different surfaces of building skin.

Given that the output of the PV system on building surfaces depends heavily on the layout design (i.e., the size, type, location, and orientation of the modules), it is imperative to perform detailed simulation of radiation potential on different surfaces of the buildings to find the most efficient PV layout. Existing simulation methods, which mostly use only the geometric model of buildings, cannot discriminate between different types of building surfaces. As a result, these methods cannot

be used to design PV layouts where different types of surface-restricted PV modules (e.g., PV modules that can be installed on windows) are incorporated.

In addition to the necessity of having accurate 3D building surfaces models, the PV locations and angles (i.e. tilt and pan) simultaneously on the building surfaces are critical especially when the target buildings are located in a complex built environment such as the dense urban areas where many factors (e.g. interference of shadow caused by the surrounding environment, lower yield contributed by solar radiation angle) affect the performance of the PV system. Therefore, these parameters need to be considered concurrently to find out where and how to apply or integrate the PV modules on the building surfaces to achieve optimum performance. Such an integrated platform, which consider the detail surface-specific building model and multiple design variables to find out the optimum PV layout is still missing among existing studies.

Therefore, the problems that justifies this research can be categorized into two main groups:

(1) Absence of a BIM-based approach for surface-specific simulation of solar potential to perform radiation simulation on a combination of desired surfaces of buildings.

(2) Absence of an optimization approach for planning the PV module layout on the entire building skin considering various design characteristics (e.g., size, type, pan, and tilt of panels), and the financial feasibility of the generated layouts.

1.3 RESEARCH OBJECTIVES

Based on the research gaps mentioned in the previous section, this research aims to: (1) Develop a parametric simulation modeling platform for the design of surface-specific PV module layout on the entire skin of buildings using the surface properties of the BIM model; (2) Develop a BIM-based generative design framework for PV module layout design on the whole exterior of high-rise buildings considering the complex interaction between building surface types (e.g., windows, walls, etc.), orientation of PV modules (e.g., tilt and pan angles), the efficiency of different PV modules, and the financial aspect of the PV system (i.e., revenue vs. cost at different study period);

and (3) Verifying and validating the proposed simulation modeling platform and generative design framework based on a detailed case study.

The objectives are set in a S.M.A.R.T (specific, measurable, achievable, realistic, timely) way to accurately measure the progress of the research toward the defined goals. They are specific by outlining a clear problem statement with respect to the identified research gaps. The numerical results can be used to make sure that the defined objectives are measurable and achievable. We assume that the objectives are realistic and timely.

1.4 OVERVIEW OF THE RESEARCH METHODOLOGY AND STRUCTURE OF THE THESIS

As shown in the overview of the research methodology in Figure 1-2, this research consists of multiple phases to develop the proposed framework and ensure it meets the research objectives and provides valid and reliable results. The research started with reviewing the related existing studies. During this review, relevant literature on solar radiation simulation methods in the built environment, PV modules' optimization approaches on building surfaces, and the generative design paradigm were reviewed. This phase resulted in identifying the research gaps in this domain. It is observed that the majority of the studies that focused on facade radiation potential analysis were based on the 2.5D models and they lack a sufficient level of details in representing the facade of buildings. In addition to the necessity of having accurate 3D building surfaces models, the PV locations and angles (i.e. tilt and pan) simultaneously on the building surfaces are critical especially when the target buildings are located in a complex built environment such as the dense urban areas where many factors (e.g. interference of shadow caused by the surrounding environment, lower yield contributed by solar radiation angle) affect the performance of the PV system. Therefore, these design parameters need to be considered concurrently in an integrated platform to find out where and how to apply or integrate the PV modules on the building surfaces to achieve the optimum performance.

In the problem analysis phase, the gaps in the literature were used to identify the requirements of the generative design framework in terms of the decision variables, pertinent objective functions, and constraints. Decision variables and objective functions were determined by considering all the controllable variables that constitute the PV system layout design (e.g., pan, tilt, location.) and the performance indicators that guide the selection of optimum design for asset managers (e.g., total radiation, cost, energy revenue, profit, etc.). In addition to the abovementioned design requirements, some other qualitative requirements were also considered, such as aesthetic values, constructability, and maintainability.

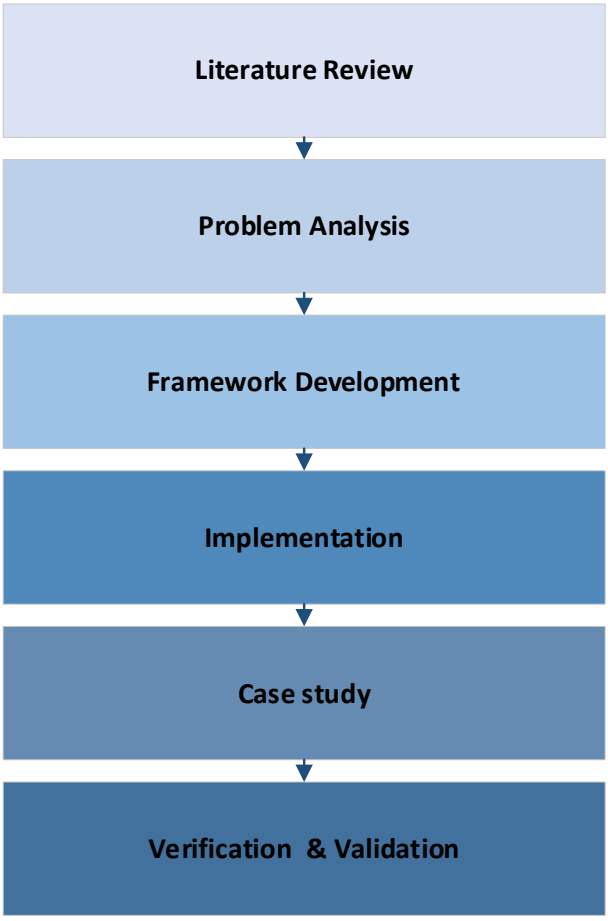

Figure 1-2 Overview of the research methodology

Building up on these design requirements, a framework was developed based on the integration of BIM with a generative design principle. This framework consists of two components, namely, parametric modeling and optimization module, as shown in Figure 1-3, which will be explained in Chapters 3 and 4, respectively.

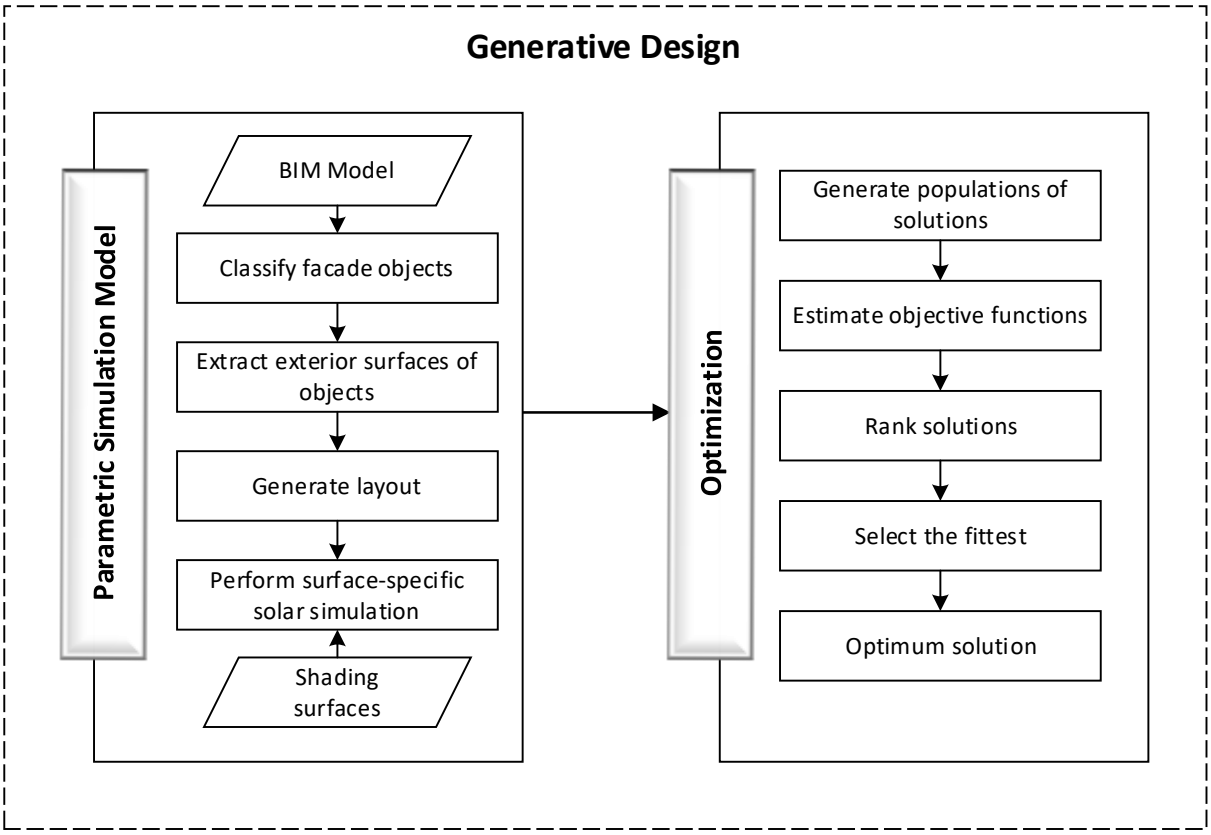

Figure 1-3 Proposed framework

The objective of first component is to develop a surface-specific solar simulation parametric model by creating classes of surfaces that associate with different types of building objects (e.g., exterior walls, roofs, curtain walls, windows, etc.) using BIM capabilities. For this purpose, BIM and CityGML models are used to define the constraints of the PV application. This component comprises of four different steps including façade object classification, extraction of exterior

surfaces, generation of a specific layout, and performing solar radiation simulation. This component is explained in detail in Chapter 3. This component is verified by applying sensitivity analysis.

After developing and verifying the parametric model, a simulation-based generative design approach is developed to integrate the parametric model and the optimization module to satisfy the objective functions of the optimal layout of the PV modules, as shown in Figure 1-3. Then, the developed framework is implemented in a prototype. To test the feasibility of the developed prototype, a case study was conducted on a building in Montreal, Canada. The functionality of the developed prototype is validated by comparing the results with other studies and comparing with the baseline design scenarios' outputs. This component is explained in Chapter 4.

Finally, summary, conclusions and future work of the research are presented in Chapter 5.

CHAPTER 2 LITERATURE REVIEW

2.1 INTRODUCTION

In recent years, many studies focused on renewable energy as a clean and sustainable alternative to fossil fuel. Diversification of energy resources would have a significant role to guarantee the future energy supply. Considering the fact that the free irradiation energy that the earth is receiving daily from the sun is 10,000 times more than human daily energy use, Photovoltaic (PV) energy has a very promising future for the development of sustainable cities by providing a viable solution for the growing energy demand and global warming detrimental effects. It provides clean, silent, and easy access to energy by enabling onsite power generation and reducing the transmission costs. According to International Energy Agency (IEA) analysis, solar PV will generate 20 to 25% of world electricity by 2050 (IEA, 2018). The main challenge is collecting and converting this energy to a usable form of energy with a reasonable cost. PV systems are getting more popular due to the continuous technological advancements and the decreasing cost of solar panels. Additionally, compared to other power generators, PV systems have less space requirements for the installation, especially when mounted on building surfaces (Charabi et al., 2010).

This chapter is structured as follows: First, the transition of solar radiation measurements and assessment models and tools from conventional GIS-based solutions to BIM-based integrated approaches are reviewed. Then photovoltaic systems and their components, PV panel types, and their application in the built environment are reviewed. In addition, the status of current practices in PV system optimization on building surfaces are reviewed and the limitations and the research gaps in the existing works are highlighted. Furthermore, the generative design approach and its application in different research works are reviewed.

2.2 SOLAR RADIATION MEASUREMENTS

In addition to a direct beam of solar irradiance that reaches the surface, there is also a diffuse component that comes to the earth after multiple scattering from water vapor molecules, dust

particles and clouds, which is the main difference of many available radiation models. The summation of direct and diffuse radiations determines the total global radiation in watt-hours per square meter (Jelle et al., 2012). Various factors, such as weather condition, topography, ground surface characteristics, latitude, the time, and seasons affect the distribution of radiation coming from the atmosphere (Redweik et al., 2013; Martín et al., 2015).

The following quantities associated with solar radiation are commonly measured:

Direct beam irradiance (G_n) is the energy of the solar radiation (W/m^2) incoming from the solid angle subtended by the sun's disk perpendicular to the rays.

Direct horizontal irradiance (G_b) is measured on a flat horizontal plane in contrast to direct beam irradiance. Since the incidence angle of the solar beam is equal to the sun the zenith angle, then:

$$G_b = G_n \cos\theta_z \qquad \text{Eq. 2-1}$$

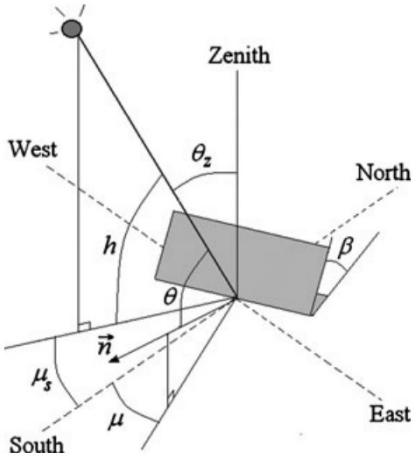

Figure 2-1 Angles representing the position of the surface and the sun (Paulescu et al., 2012)

Diffuse irradiance (G_d) represents the radiation incoming from the entire sky dome on a horizontal surface. *Global irradiance (G)* is the sum of the direct horizontal and diffuse components.

$$G = G_b + G_d \qquad \text{Eq. 2-2}$$

As shown in Figure 2-1, the incidence angle (Θ), which is important in fenestration and solar technology, is the angle between the sun direction and the surface's normal. This factor affects the intensity of the direct solar radiation striking the surface. Tilt (slope) angle (β) and surface azimuth angle (μ) are the other angles that describe the position of the surface. On the other hand, zenith angle (Θz) measured from vertical; elevation angle (h) measured up from the horizon, and azimuth angle (μs) represent the position of the sun (Paulescu et al., 2012).

2.3 EVOLUTION OF SOLAR RADIATION ASSESSMENT MODELS AND TOOLS

Modeling solar radiation potential has a key role in evaluating the feasibility of PV system implementation. Although solar power is considered as an available and accessible source of energy, the received amount of insolation by any surface is affected by multiple factors of the surrounding area and also the characteristics of the radiation receiving surfaces. In more complex environments, such as urban areas, the radiation assessment become more sophisticated due to the existence of numerous obstacles and shadow effects. Radiation models, coupled with simulation tools, provide a better representation of this complex environment in order to come up with more accurate radiation estimation.

According to the literature, to assess the solar radiation potential, several approaches have been developed in different timelines for various purposes (Figure 2-2). For example, earlier studies analyzed the solar radiation potential from a physical and geographical standpoint using numerical models (Paulescu et al., 2012). By introducing the computational approaches and simulation tools, some research investigated the solar potential in the urban areas (Chow et al., 2014). Increasing the energy demand and introducing renewable energy motivated the analyses of solar radiation potential in the built environment. Early studies mostly focused on analyzing the solar radiation on rooftop surfaces. Then, by the improvement of PV modules technology, the vertical surfaces of the buildings started to be considered as potential options. However, the majority of the studies were developed based on 2.5D models. In recent years, by introduction of the BIM based radiation

simulation tools, some studies started to consider BIM-based solar radiation analysis (Brown, 2016).

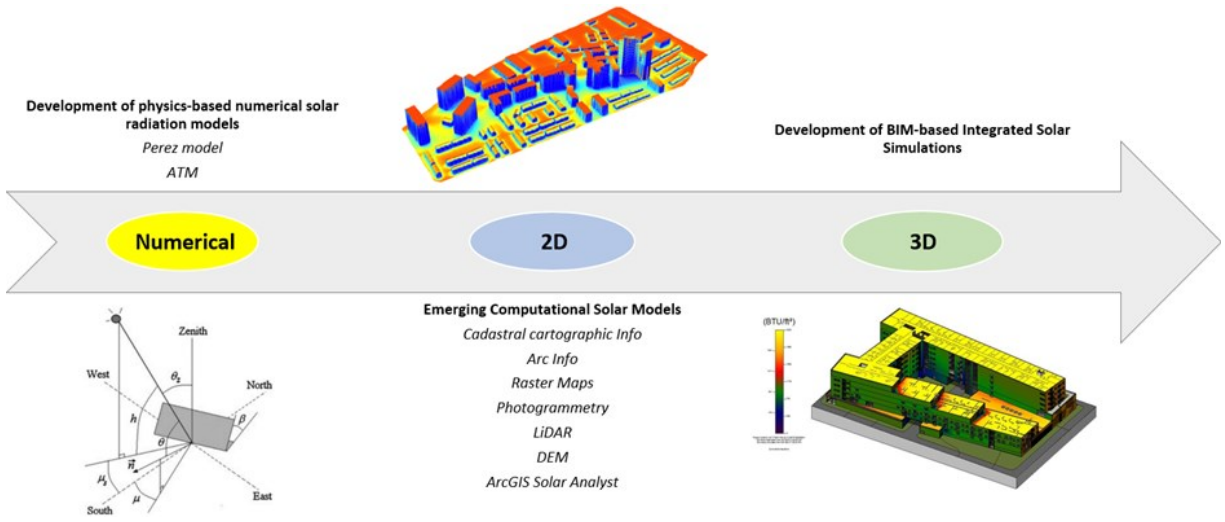

Figure 2-2 Solar energy technology timeline (adopted from Paulescu et al., 2012; Chow et al., 2014; Brown, 2016).

Table 2-1 represents research works that investigated the solar radiation potential directly or indirectly for the purpose of evaluating a PV system on building surfaces. As shown in this table, earlier studies analyzed the solar radiation from a physical and geographical standpoint using numerical models.Atmospheric and Topographic Model (ATM) is the first topographical solar image-based model that considered the geography and climate in large-scale calculations (Dubayah & Rich, 1995). SolarFlux is a radiation evaluation model that was developed in the ArcInfo platform to use the topographic data and calculate the total direct and diffuse radiation with respect to the Sky View Factor (SVF) (Hetrick et al., 1993). This model was later improved by considering the Digital Elevation Model (DEM) of the area and the specific period of time for the study (Kumar et al., 1997). Furthermore, Redweik et al. (2013) developed an approach for evaluating the SVF on the vertical surfaces and discovered that less than half of the sky hemisphere is visible from a vertical façade point. These computational solar models give an insight into the physics involved in PV panels by investigating behaviors of radiation factors and shadow effects in association with different topographical characteristics of large areas. However, the large-scale analysis of how PV systems work in a complex urban context requires more comprehensive

simulation models. Therefore, several techniques, e.g., vector cartographic maps, cadastral information, Geographic Information Systems (GIS), aerial or satellite images and Light Detection and Ranging (LiDAR), were applied to collect the required information and parameters for modeling buildings (Jochem et al., 2009). For example, Karteris et al. (2013) developed a statistical model to calculate the horizontal roof surfaces. The output was validated with the building's real measurement in Greece. A study in Los Angeles estimated the solar potential of rooftops considering several factors, such as energy radiation amount, the suitable rooftop size, slope and orientation (Ludwig et al., 2009). Likewise, the annual electricity generation by different solar technologies has been evaluated based on a GIS solar radiation map in Oman (Gastli & Charabi, 2010). In another study, the annual potential of PV systems was evaluated for three different categories of residential buildings in Spain, including detached and/or semi-detached houses, row houses, and high-rise buildings. Two types of PV modules with different dimensions and power rates were considered on flat and pitched rooftop areas in calculating the energy production (Ordóñez et al., 2010).

RADIANCE is a powerful and reliable software which considers the physical behavior of light and reflections in a volumetric 3D model and curved geometries using a light-backward ray-tracing algorithm. The foundation of this extensively used simulation software is based on the idea of the Perez diffuse radiation model (Perez et al., 1990). RADIANCE is used to determine the solar potential on building surfaces for both purposes of daylight analysis and power generation (Ward, 1994). Several models, which were introduced later on, were inspired and created based on RADIANCE, such as Cumulative Sky approach for generating annual irradiation images (Robinson & Stone, 2004). While Daysim is able to analyze the annual daylighting at each point in and around buildings. The climate data, shading factor, and reflections on a 3D geometrical model are considered in the calculations of Daysim (Mardaljevic, 2000).

Table 2-1 Comparison of solar radiation assessment models

Reference	Method/Tool	Considered Factors				
		Physical/ Geographical	Shading	Rooftop Surface	Facade Surface	PV (Type, Slope, Azimuth)
(Dubayah & Rich, 1995)	ATM / Image-based	✓	-	-	-	-
(Hetrick et al., 1993)	SolarFlux / Arc Info	✓	-	-	-	-
(Kumar, Skidmore, & Knowles, 1997)	SolarFlux / DEM	✓	-	-	-	-
(Ward, 1994)	Perez Model / RADIANCE	✓	-	✓	✓	-
(Mardaljevic, 2000)	Daylight coefficient method / Daysim	✓	✓	-	-	-
(Redweik et al., 2013)	SVF	✓	-	✓	✓	-
(Carl, 2014), (Fu & Rich, 1999), (Wiginton et al., 2010), (Brito et al., 2012)	ArcGIS Solar Analyst / LiDAR	✓	-	✓	-	-
(Hofierka & Suri, 2002), (Šúri & Dunlop, 2005), (Hofierka & Kaňuk, 2009)	r.sun / PVGIS Optimized for European Climate	✓	-	✓	-	-
(Tooke et al., 2012)	Solar penetration through urban vegetation canopy / LiDAR	✓	-	✓	✓	-
(Melo et al., 2013)	Solar3DBR / Google SketchUp plug-in	✓	✓	-	-	-
(Erdélyi et al., 2014)	SORAM	✓	✓	-	-	✓
(Gastli & Charabi, 2010)	GIS-based solar radiation map	✓	-	-	-	✓
(Ludwig et al., 2009), (Jochem et al., 2009), (Nguyen et al., 2012), (Gooding et al., 2013), (Martín et al., 2015)	GIS / LiDAR & DEM	✓	-	✓	-	-
(Carneiro et al., 2010)	Hay model, SVF / Vector maps, Airborne LiDAR	✓	-	✓	✓	-
(Hofierka & Kaňuk, 2009), (Hofierka & Zlocha, 2012)	v.sun / Raster maps, GRASS GIS platform	✓	-	✓	✓	-
(Jakubiec & Reinhart, 2013)	Perez model / Airborne LiDAR, Daysim	✓	-	✓	✓	-
(Catita et al., 2014)	SOL / Matlab, Airborne LiDAR, ArcGIS	✓	-	✓	✓	-
(Esclapés et al., 2014)	Cadastral cartographic Info	✓	-	✓	✓	-
(Byrne et al., 2015)	Cartographic Info, Statistic & GIS	✓		✓	-	✓

Since the energy output of PV panels depends on the amount of the solar radiation they receive, a major part of the previous studies focused on the geographical analysis using GIS for the evaluation of the radiation potential. The radiation gradient is defined by different factors at different levels of studies. Elevation, slope, orientation and the shadow effects of the intended surfaces are the elements that influence the radiation at the local scale, while the rotation of the earth around the sun and its topographical characteristics are considered for evaluating the global radiation (Šúri et al., 2007).

The advances in GIS improved the function of the radiation models in recent years by providing faster and more integrated platforms for processing complex solar radiation models. ArcGIS Solar Analyst extension was developed and added to the ArcGIS platform by ESRI (ArcGIS, 2021). This tool enables users to evaluate the temporal and spatial variability of incident solar radiation on the landscape with higher resolution (Carl, 2014). Location, elevation, orientation, and atmospheric transmission are the main factors in the analysis (Fu & Rich, 1999). Several studies employed Solar Analyst and other GIS tools to determine the suitable rooftop area for implementing PV systems (Wiginton et al., 2010; Brito et al., 2012).

r.sun (r.sun, 2006) is a tool based on GRASS GIS software using the clear sky model. It was developed to solve the limitations of the earlier models, such as Solei-32, SolaFlux, SolarAnalyst, and SRAD by enabling large-scale analysis (Hofierka & Suri, 2002). Besides creating the radiation raster maps shadow and reflectance maps, this model was optimized especially for the European climate conditions with horizontal or inclined surfaces (Šúri & Dunlop, 2005). Solar3DBR (Melo, 2021) which was introduced as a plug-in to Google SketchUp, can simulate the shadow around the PV panels created by nearby buildings. Consuming less processing time for modeling and providing more detailed representation are considered as the advantages of this tool compared to the previous ones (Melo et al., 2013).

The majority of the aforementioned models are only able to assess the radiation potential of the PV panels installed on flat surfaces. This limitation is resolved by SORAM, which can calculate the radiation on slanted PV panels (Erdelyi et al., 2014). This algorithm considers the 3D shading

caused by surrounding obstacles based on Google Maps and, thus, generates more accurate results compared to the improved Perez model.

2.3.1 Solar Radiation Simulation Considering Vertical Surfaces

As addressed in Section 2.3, significant efforts have been made to develop a wide range of numerical and conceptual solar radiation models with different characteristics. These models were only able to provide some information about the building's classification, their footprint, orientation, and elevation related data. However, quantifying PV potential at urban scale requires a better representation of the geometry of the buildings in addition to detailed information about their surrounding environment. Therefore, a number of studies have been conducted to create solar radiation analysis by considering vertical surfaces of buildings (Martín et al., 2015). For example, research focused on the assessment of PV adaptability on urban facades (Esclapés et al., 2014). In this research, solar radiation data from the Spanish Meteorological Agency were collected to generate 3D solar maps based on the cadastral cartographic information. In this study, the detailed model of the façade area was not considered in the radiation evaluation.

Since the data collection methods and technologies, in general, depend on the scale of the study areas and the complexity of the built environment, the use of LiDAR for collecting height information of urban areas has gained more popularity in recent years (Martín et al., 2015). For instance, a study in Kingstone, Ontario, used LiDAR data to analyze the PV potential on buildings' rooftops at the regional scale (Nguyen et al., 2012).

The rooftop PV capacity of seven main UK cities was calculated using GIS-based digital surface models and LiDAR data (Gooding et al., 2013). A 2.5D urban surface model was generated for the city of Geneva, using buildings footprint 2D vector maps and the elevation information from Airborne LiDAR (Carneiro et al., 2010). In this study, any surfaces with a slope greater than 60^{o} are considered vertical and the remaining surfaces are treated as flat or tilted rooftops; then the radiation was evaluated for all surfaces. Finally, the algorithm total outputs were plotted graphically on the intended surfaces. Although it was claimed that the vertical surfaces were

involved in the radiation calculation, the details of the building surfaces, such as windows and related geometrical properties were not considered.

In another study, r.sun model was employed in another vector-based model, called v.sun, on the GRASS GIS platform (Hofierka & Zlocha, 2012). A combined vector-voxel approach was used to analyze the 3D vector data of the urban area in a way that the smaller voxel size results in a higher accuracy and more spatial details but more computation time. In this research, the solar radiation was investigated on the flat rooftops and vertical facades based on the 3D model of Presov, Slovakia, provided by a photogrammetric method in the Level of Development (LOD1).

In another urban-oriented study, a 2.5D model of Cambridge, USA, was constructed using airborne LiDAR data. The collected points were divided into the ground and buildings levels for 3D triangulation. The rooftops with a slope greater than 60^{o} were considered as vertical surfaces (Jakubiec & Reinhart, 2013). The irradiation simulation followed the detailed Perez sky model and the cumulative sky method using Daysim software on an hourly basis. The accuracy of the created model was validated by a real rooftop PV system installed on the neighborhood buildings and also simulations from Solar Analyst, r.sun, Daysim, and PVWatts. The range of annual errors was from 3.6% to 5.3%. Like the aforementioned studies, the surfaces in this model were also represented with low geometric accuracy.

SOL is a Matlab-based algorithm that was developed for the evaluation of the radiation potential at a larger scale (Catita et al., 2014). However, this calculation was conducted regardless of the position of the points whether they are located on the ground, roof or façade. This algorithm works based on the geo-referenced LiDAR data rasterized to 1×1 m^2 pixels. All pixels with a slope greater than 72° were considered 90° to represent the vertical walls. This model was applied to the Science Faculty of Lisbon University (Figure 2-3).

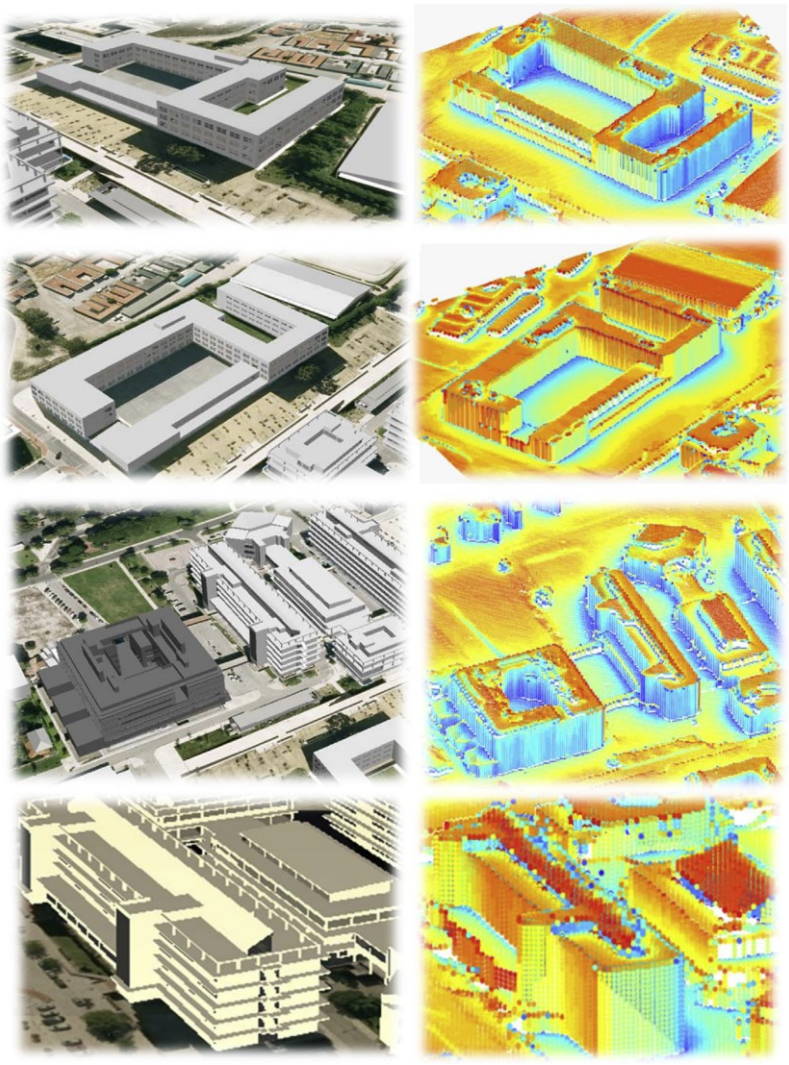

Figure 2-3 Annual solar radiation on vertical surfaces based on 2.5D model (Catita et al., 2014)

The results represented a higher level of received solar radiation on the south facing facades than the roofs in winter time (Catita et al., 2014). The geometric accuracy to assess the radiation on building surfaces in this model, like many other previous studies, was limited (Figure 2-4).

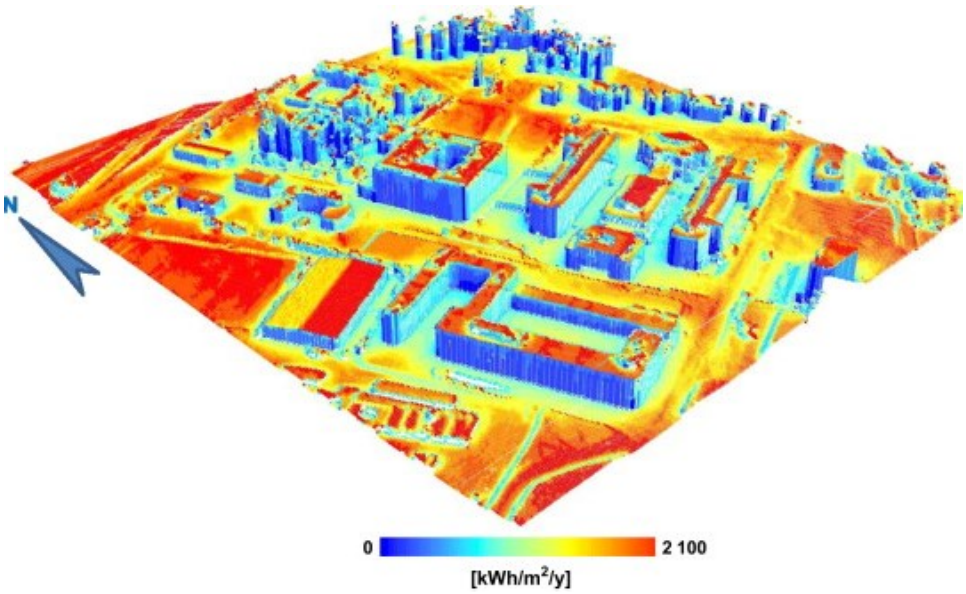

Figure 2-4 Annual global radiation based on 2.5D models (Catita et al., 2014)

Although 2.5D models are capable of providing the necessary input for the analysis of the vertical surfaces of the buildings, they lack a sufficient level of details in representing the façade of buildings. The accurate representation of the vertical geometry is especially crucial when considering the installation of BIPVs.

2.4 PHOTOVOLTAIC SYSTEMS

A PV system is basically composed of PV modules and some other elements, such as inverters, batteries, electrical components and mounting systems (IEA, 2018). The basic unit of a PV system is a semiconductor material, which is called a PV cell. These cells convert solar energy into direct-current electricity.

Progressive technical improvement of the PV modules is making them an increasingly attractive and viable solution for the large-scale use of renewable energy on high-rise buildings. Building rooftops and facades can be equipped with a new generation of efficient and aesthetically appealing PV modules (Li & Liu, 2018). In other words, the emersion of highly transparent solar cells can transform the metropolises from power consumers to power plants (Husain et al., 2018). With highly transparent solar cells, a significant part of the built environment surfaces has potential to harvest solar energy without affecting their main functionality (Traverse et al., 2017). Although the efficiency of these cells is about 5%, because of their installation flexibility, they can be used on a wider range of surfaces compared to the opaque ones, therefore, a large surface area of buildings can help compensate for the reduced power (Traverse et al., 2017). Currently, multiple semi-transparent photovoltaic technologies are under development to achieve reasonable efficiency and transparency at the same time. This is the challenging part of the material fabrication since the PV cells should be able to efficiently absorb the photons and convert them to power, and at the same time let the photons pass through to satisfy the transparency and visual comfort requirements (Husain et al., 2018). Recent studies on semitransparent PV cells material and fabrication show that translucent polymer- and perovskite-based photovoltaic cells have promising characteristics from the electrical and optical point of view and they do not have the limitations of silicon-based cells (Shin & Choi, 2018).

2.4.1 PV Panel Types

Monocrystalline Silicon Solar Cells are the most expensive opaque modules with the highest efficiency rates, which is typically 18-20%. Since these types of panels produce electricity up to

four times more than thin films, they are space-efficient. Their life cycle is longer than the other types and they perform more efficiently in cold weather. Although Polycrystalline Silicon Solar Cells have lower cost and less silicon waste compared to monocrystalline, they have lower heat tolerance. Their efficiency is 15-17%, so a larger surface is needed to get higher output. Thin-Film Solar Cells (TFSC) consist of non-silicon semiconductor material. They are responsible for almost 10% of the global market with 11% efficiency. Although they are cheaper, they require a lot of space and degrade faster (Energysage, 2021).

New PV systems comprise various types of panels that make them suitable to be applied on different surfaces. As shown in Table 2-2, different types of panels could be installed either independently or integrated on surfaces for different purposes. For example, at the local scale, they can be attached to buildings' rooftops or to the vertical surfaces. They are also used on a large scale in such infrastructures as solar plants, public parking shades, and gas station structures. PV foils, tiles, modules, and solar cell glazing can be named as various categories of BIPVs. Different studies focused on the architectural aspect of using BIPV (Biyik et al., 2017).

Within the built environment, PV systems can be categorized into two main groups. The PV systems that are added to the existing buildings (e.g. conventional rooftop applications) are called building-applied photovoltaics (BAPV). BIPV are usually used as a part of building components and are integrated into the building skin (Natural Resources Canada, 2019). They can be multifunctional as a part of the building envelope replacing the regular materials and generating energy at the same time (Jelle et al., 2012). The advantages of BIPV over the non-integrated panels are that they do not require dedicated space, they can reduce the total material and labor cost, and they do not require extra installation or assembly (Raugei & Frankl, 2009).

Table 2-2 PV panels types and application surfaces

Panel Types		Monocrystalline (Opaque)	Polycrystalline	Thin-Film	Transparent / Semi-Transparent
Efficiency (%)		18 - 20	15 - 17	11	2-5
Price ($)/Watt		0.21 - 0.35			0.45 - 1.10
Applicable Surfaces	Rooftops	✓	✓	-	-
	Façades & Balconies	✓	✓	-	✓
	Windows	-	-	✓	✓
	Shades and Blinds	-	-	✓	✓
	Infrastructures	✓	✓	✓	✓

Furthermore, as shown in Figure 2-5, there are many opportunities for using BIPV systems in an innovative architectural design. For example, using PV panels as balcony fences, or applying semi-transparent modules for designing spaces like atrium roofs or facades can improve aesthetical aspects (Norton et al., 2011). Certain types of PV products such as amorphous silicon tiles can replace the common tiled roofs. Some other types could be applied as shading techniques or semi-transparent fenestration (Jelle et al., 2012). Besides generating energy, they do not compromise the aesthetic value and enable light penetration into the building (Peng et al., 2011). The curtain walls provide multiple possibilities for the integration of PV panels into buildings. PV glasses for curtain walls come frameless and could be assembled into different types of buildings. In addition to generating power, the transparency of PV glass maintains the functionality of the windows and allows the natural lighting and unobstructed views (Onyx Solar , 2019).

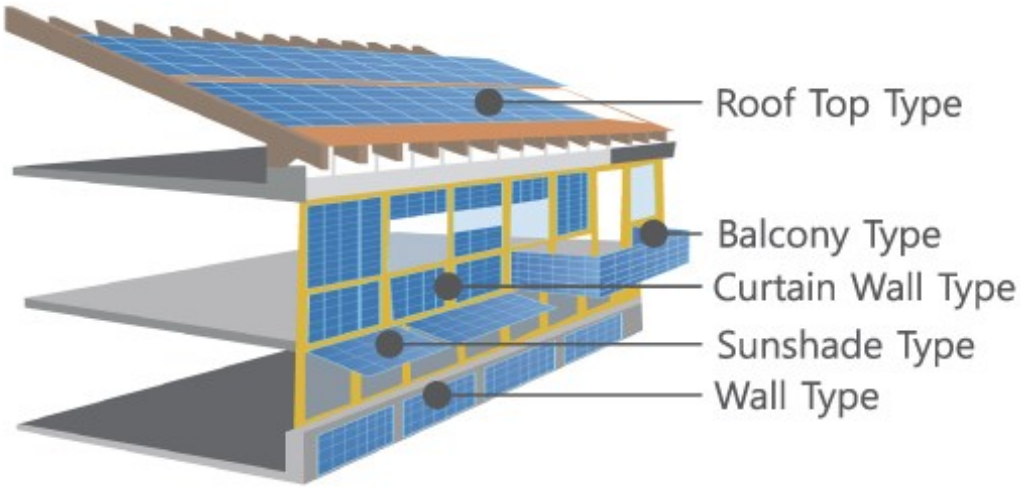

Figure 2-5 BIPV installation examples (S-Energy, 2018)

2.4.2 Curtain Wall Systems

Generally, a curtain wall is a kind of light exterior building enclosure (Figure 2-6). The structure of curtain walls, as a part of the façade, makes them flexible and potential candidate for applying BIPV systems. Although they are considered as a structural element, they carry no vertical structural load except their own weight. There are different classifications of curtain walls but some forms of curtain walls are more common.

Figure 2-6 Curtain wall system

Stick built and unitized curtain walls are two main types of curtain wall systems that are classified based on the manufacturing procedure (CWCT 'Cladding Forum', 2000). A stick-built curtain wall is fabricated in the company and the pieces are assembled and glazed at the site. Therefore, the site labor cost and the construction time are considerable for the installation of this type of curtain walls. In contrast, the whole component of a unitized curtain wall comes as a single unit from the factory. Since this type of curtain walls is fully manufactured in advance, it has higher quality; and due to the faster construction, it is usually used in high-rise buildings (Morris, 2013).

2.4.3 PV Panels in the Built Environment

Currently, building owners and designers can consider a PV module layout where different types of PV modules are installed in different parts of the building skin depending on the cost, characteristics, and efficiency of the modules, the suitability of a PV module for a given surface, and the geometry of the building. The layout design of PV modules on the building skin requires a detailed analysis in order to identify surfaces that receive enough radiation for an economically justifiable investment. This is because not all the surfaces have equal radiation potentials and building owners normally operate under budgetary limitations.

There are several unique buildings which have PV modules applied on their façades. For example, in a Danish school project in Copenhagen, 12,000 solar panels have been used to cover the building's façade with a total area of 6,048 m^2 (Dezeen, 2017). This project aims to provide 50% of the annual school electricity demand (Figure 2-7). In this project, a pixelated pattern was created on the building exterior surfaces using PV modules. A random tilting is applied on the installed blue color PV modules that resonate with the surrounding water to satisfy the aesthetic purposes (Dezeen, 2017).

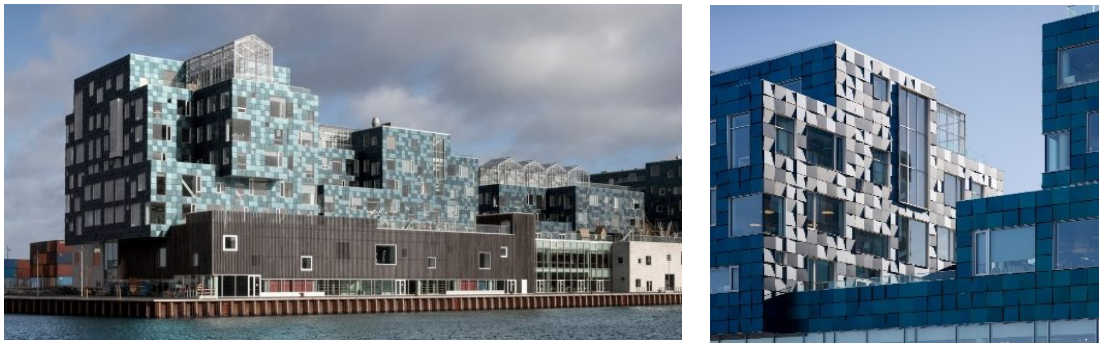

(a) Overall view (b) Detailed view

Figure 2-7 Copenhagen International School with BIPV, (a) Overall view, (b) Detailed view (Dezeen, 2017)

The new head office of the Federation of Korean Industries is an example of using BIPV on the southwest and northwest façades (Figure 2-8). In addition to generating PV energy through BIPV and providing maximum access to views, the exterior wall of this 50-story building is designed to comply with energy efficiency strategies and reduce the internal heating and cooling loads. Besides the architectural aspects, the optimization of the PV panels' positions is a driving factor in the development of this project to fulfill the district and city requirement. According to city regulations, the new generation of large-scale commercial buildings should be able to generate a minimum of 5% of their required energy. In order to maximize the amount of collected energy in this project, PV modules are tilted by 30° toward the sun **(Smith & Gill, 2014)**.

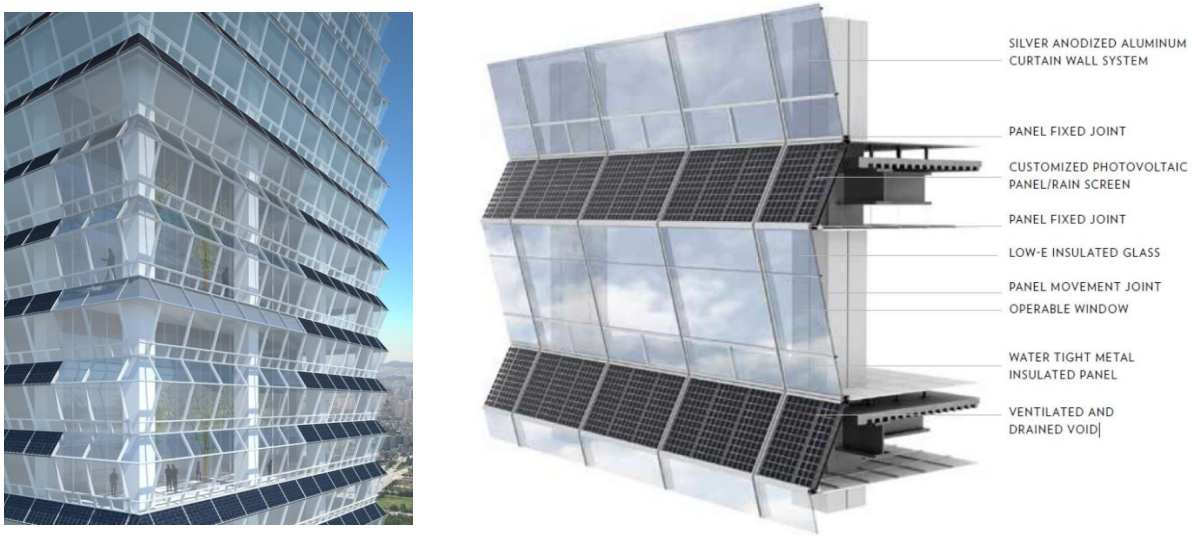

(a) Picture of the facade (b) Schematic view

Figure 2-8 Building of Federation of Korean Industries with BIPV (Smith & Gill, 2014)

2.4.4 Components of PV System and Cost Breakdown

Multiple factors can affect the amount of generated electricity by PV modules. Some of these factors, such as the size, position, number, and efficiency of the utilized PV modules, are design variables. However, some other factors, such as daylight hours and weather condition, are location-specific, and therefore not controllable.

In PV system terminology, all components of a PV system other than the modules, such as the inverters, electrical and structural components, etc., are called the Balance of System (BOS). These components contribute to how the system functions. The total cost of a PV system can be categorized into two major parts, including the hardware costs (i.e., PV modules and the BOS) and the soft costs, such as the labor costs, permits, and customer acquisition costs (Hagerty & Cormican, 2019). According to a price breakdown of the PV system, almost 13% of the total price of a PV system belongs to the modules, and the remaining covers the BOS and the soft costs (Fu et al., 2018). A standard PV module has an input rate of around 1000 W/m2. However, the available modules have 15-20% efficiency at best (The eco experts, 2021). As shown in Figure 2-9, the estimated cost of a PV module including all fees is $2.8 per Watt (SUNMetrix, 2021).

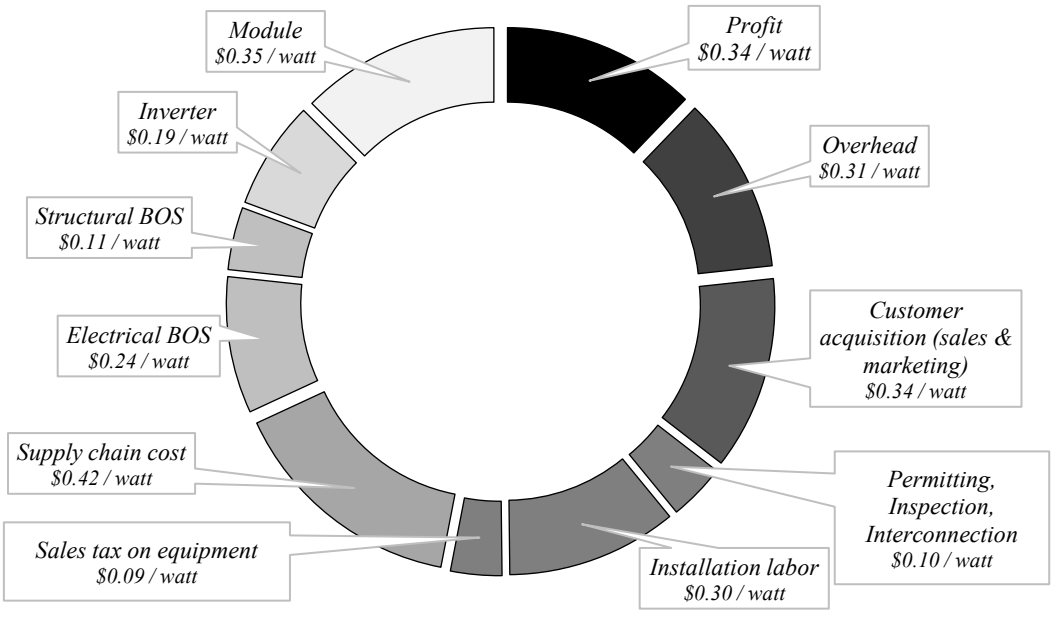

Figure 2-9 Cost of PV system breakdown (adapted from SUNMetrix, 2019)

According to Fu et al. (2018) in US National Renewable Energy Laboratory, the cost of PV systems has had a significant reduction of up to 60% since 2009. In addition to the utility rate, higher tax credits and incentive programs can significantly improve the financial feasibility of the PV systems. Concerning the significance of the economic aspects in prospering sustainable energy development, some studies explored the application of PV systems from cost-benefit perspectives. For example, in a techno-economic analysis, the life cycle cost (LCC) of the PV modules is combined with a method for visualizing economic performances of the application of PV modules on building envelopes (Li & Liu, 2018). Considering the installation and maintenance cost, the investment payback period is calculated as an economic indicator in pixel units in an empirical study. However, most of the critical but controllable design variables, which are essential in the efficiency of a BIPV system, are not included in this study.

The absence of an approach that can consider the building surface PV suitability with the optimum PV modules' configurations simultaneously, as well as the economic aspect necessitates the adoption of an integrated platform that considers all these key factors for designing a financially feasible PV system with the maximum PV energy generation level.

2.5 OPTIMIZATION TECHNIQUES

Optimization is a mathematical approach to find the maxima and/or minima of the objective functions considering the constraints. A number of objective functions and the certainty in decision variables can define the type of the optimization problem. The problems with one objective function are called single objective problems and the ones with more than one objective are defined as multi-objective problems. If the value of the objective functions can be determined with certainty, it is a deterministic optimization; otherwise, it is considered as stochastic (Mawlana, 2015). Based on the form of the equations of the objective functions and constraints, the optimization can be linear or non-linear. Linear optimization is for the problems with linear objective functions and constraints, while nonlinear optimization has nonlinear objective functions and constraints (Diwekar, 2008). Integer programming, mixed integer linear programming, and mixed integer nonlinear programming are three types of discrete optimization, which usually have

discrete decision variables. In integer programming, the decision variables are integers with linear or nonlinear constraints, while the mixed integers are the combination of integers and continuous decision variables (Mawlana, 2015).

Multi-objective optimization has more than one optimal solution (Abraham & Jain, 2005). The basic mathematical formulation of multi-objective optimization is shown as follows:

$$minimize\ [f_1(x), f_2(x), \dots, f_k(x)] \qquad \text{Equation 2-3}$$

subject to m inequality constraints:

$$g_i(x) \leq 0 \qquad i = 1,2, \dots, m \qquad \text{Equation 2-4}$$

and p equality constraints:

$$h_i(x) = 0 \qquad i = 1,2,\dots, p \qquad \text{Equation 2-5}$$

where, $x = [x_1, x_2,\dots, x_n]$ is the vector of decision variables. The number of objective functions is indicated by *k*. The set of objectives to be minimized is *f(x)* and the function of the first objective is defined as $f_1(x)$. The equality and inequality constraints are shown in $g_i(x)$ and $h_i(x)$ functions.

The objective functions in multi-objective optimization problems are usually negatively correlated to each other so that the improvement of one comes at the cost of compromising the other. Therefore, instead of a single optimal solution, this type of optimization generates a set of optimal solutions. These solutions are called Pareto front or solutions that are not dominated by the other solutions. In other words, none of these solutions is objectively superior to the rest (Deb et al., 2002).

2.5.1 Selection of Optimization Algorithm

Due to the limitations of conventional optimization algorithms in finding optimality, metaheuristic methods were developed. These methods evolutionarily guide the search space to obtain near-optimal solutions (Mellouk et al., 2015). John Holland and his colleagues invented Genetic

Algorithm (GA) in the mid-1970s at Michigan University. GA, which is inspired by the theory of natural evolution, is one of the well-known meta-heuristic methods that can solve complex multi-objective optimization problems. In other words, the "evolutionary optimization" is based on the genetics and evolution principals, which follow the "survival of the fittest" rule in selecting and generating the individuals (design solutions) that are adapted to the situation (design objectives/constraints). Therefore, favorable characteristics will evolve and continue in the population genomes during the iterations, and the weaker ones will be eliminated (Schmitt, 2001).

The process starts with a set of individuals, which is called a population. The characteristics of these individuals are formed by genes that represent the variables. A set of these genes (variables) in a string represents the chromosomes, which are called solutions. The fitness function provides a fitness score for each individual. This score defines the probability that an individual can be selected for the reproduction. Then, the offsprings are generated by crossover based on exchanging genes among parents at random points. Mutations that are done on certain proportion of top ranked solutions preserve the diversity in the population characteristics and prevents the premature convergence. These process of selection, crossover, mutation, and computing the fitness are iterated until the population has converged to the near-optimal solutions (Mallawaarachchi, 2021).

Particle Swarm Optimization (PSO), that was developed by Kennedy and Eberhart in the mid-1990s, is based on the concept of "collective intelligence". The collaborative behavior and swarming in biological populations, such as flocks of birds, helps them to adapt to their environment by implementing an "information sharing" approach to avoid the predators and find the proper food sources. In this method, randomly generated solutions are like initial swarms, using the shared information among the members to move towards the optimal solution. Every movement of these masses within the design space is considered as an iteration (Kennedy & Eberhart, 1995).

GA is inherently discrete, therefore it is compatible with discrete design variables, while PSO is basically continuous and it has to be modified for discrete design variable cases. Studies show that the difference in the computational efficiency between GA and PSO is related to the problem. In problems with unconstrained nonlinear nature and continuous design variables, PSO outperforms

GA; while their performance does not have a significant difference when the problem is constrained nonlinear with continuous or discrete design variables. Although the computational cost for GA is much higher, it is commonly used in academia and industry because of its easier implementation, intuitiveness, and effectiveness in solving nonlinear, mixed integer optimization problems (Hassan et al., 2005).

The Non-Dominated Sorting Genetic Algorithm (NSGA) is one of the multi-objective evolutionary algorithms (MOEAs) that creates Pareto solutions (Srinivas & Deb, 1994). To alleviate some of the problems associated with NSGA, such as the computational complexity, lack of elitism, and the need for sharing parameters, a better and faster algorithm, called NSGA-II, was introduced (Deb et al., 2002). NSGA-II, which has the ability to effectively solve multi-objective optimization problems, is known as a mature multi-objective optimization algorithm (Wang, 2016). Moreover, NSGA-II has the flexibility to be applied to a wide range of optimization problems of significant complexity (McCall et al., 2002). It is also widely used due to the simplicity of its computational steps, especially when it is integrated with simulation models.

2.6 PV SYSTEM MODELING AND OPTIMIZATION APPROACHES ON BUILDING SURFACES

Modeling and optimizing the PV system on building surfaces are among the main challenges of the application of PV in municipalities. In this domain, many researchers considered PV for rooftop surfaces in the built environment. Some merely focused on the 3D modeling (Karteris et al., 2013; Brito et al., 2012) or solar radiation simulation aspects (Erdélyi et al., 2014; Melo et al., 2013). In some other studies, the optimization of the PV system yield is discussed just from hardware and technical configuration aspects (Celik et al., 2015).

As shown in Table 2-3, several optimization approaches were proposed for rooftop PV layout. However, the majority of them did not use the BIM model in the optimization process. For example, in a study by Cheng et al. (2009) to find out the optimal PV angle, 20 south-oriented tilted rooftops are selected and the correlation between the performance of the PV system and the

tilt angle are studied. The results revealed that the optimum performance of the roof-mounted PV system is achieved when the tilt angle is equal to the site latitude.

An integrated Geographic Information System (GIS), optimization, and simulation framework is developed by Kucuksari et al. (2014) to determine the optimal PV size and location on the Arizona University campus. In this study, the best candidate rooftops with higher radiation potential are simply identified using (ArcGIS, 2021) and the Digital Elevation Model (DEM). Then, considering the area of these candidate locations, the maximum number of panels is calculated based on a certain PV panel size. Finally, an optimization module is used to maximize the total profit of the PV deployment, considering the installation, operation, and maintenance costs within a 20-year time horizon. The optimization method is formulated in Equation 2-6 to Equation 2- 9. The total benefit from saving in the electricity bills is formulated as follows:

$$TB = ASH \times dr \times \sum_{t=0}^{T} \frac{UR_t}{(1+r)^t} \sum_{\tau=0}^{t} \sum_{k=1}^{K} \sum_{m=1}^{M} n_{\tau km} \times e_{k,t-\tau} \qquad \text{Equation 2-6}$$

TB calculates the power output of PV panels as a function of the age of the panel ($e_{k,t}$), since degradation of the PV panels reduces their power output. In addition, a derate factor (*dr*) is considered to represent system losses caused by wires, inverters, and connectors.

where,

ASH is annual sunny hours (hrs).

dr is derate factor representing system losses caused by wires, inverters, and connectors.

UR_t is utility rate in period *t* ($/kWh).

$n_{\tau km}$ is the number of panel type *k* installed in period *t* on building *m*.

$e_{k,t-\tau}$ is output power of panel type *k* at age *t* (kW).

τ is the installation year and r is discount year.

The total installation cost, which includes fix and variable costs is calculated by Equation 2-7.

$$IC = \sum_{t=0}^{T} \sum_{k=1}^{K} \sum_{m=1}^{M} \frac{1}{(1+r)^t} \left(y_{tm} \times F_t + n_{tkm} \times e_{k0} \times NSC_{tk}\right) \qquad \text{Equation 2-7}$$

where,

y_{tm} is 1 if PV panels are installed on building m in period t or 0 otherwise

F_t is fixed cost of PV panels installed in period t ($)

n_{tkm} is number of panel type k installed in period t on building m

e_{k0} is output power of panel type k with age t (kW)

NSC_{tk} is net variable cost of PV installation in period t for panel type k ($/kW)

Since the inverter lifecycle is shorter than that of a solar panel, the inverter replacement cost is considered in the calculations as shown in the following equation:

$$IRC = \rho \sum_{t=0}^{T} \frac{C_t\,(X_t - I_t)}{(1+r)^t} \qquad \text{Equation 2-8}$$

IRC contains the costs of inverters purchased with the new PV installations (I_t) each time period as well as the cost of new inverters needed to replace the failed ones.

where,

ρ is average commercial inverter size (kW)

C_t is inverter replacement cost in period t ($/kW)

X_t is total number of inverters installed in period t

I_t is number of inverters installed in year t for newly installed panels

The periodical cleaning of PV panels and inspection of electrical connections are formulated as operation and maintenance costs:

$$OMC = \alpha \sum_{f=0}^{T} \sum_{t=0}^{f} IC_t \qquad \text{Equation 2-9}$$

α is operation and maintenance cost ratio
IC_t is installation cost of PV panels in period t ($)

However, in this study, no BIM model is considered and the rooftop analysis is simply based on the DEM model. In addition, the PV location is presented as the only decision variable in the optimization process. GIS-based DEM is a 2.5D model that is simply generated using building's footprint 2D vector maps and the elevation information. The DEM model treats the building skin as a set of polygons and does not provide any surface-specific and semantic information. Therefore, a detailed surface-specific PV layout optimization is not feasible without discriminating between different types of surfaces and their geometrical information.

In another example, a GIS-based optimization model is developed to find out the maximum annual PV energy generation on rooftops after performing a sensitivity analysis considering the azimuth and the tilt angle of the installed panels simultaneously (Hong et al., 2014). An integrated multi-objective optimization model was developed by Koo et al. (2016) to find the best scenario for implementing the rooftop PV system. However, no BIM model is used in this study, and the analysis was done based on a GIS model.

As shown in Table 2-3, some of the studies used a BIM-based approach for the rooftop PV optimization but in most of the cases, only a few factors were considered as variables in the optimization process. A BIM-based design and analysis platform for the BIPV on the building surfaces was developed by (Ning et al., 2018). The results of the radiation and power flow analysis for a BIPV case study showed that by the implementation of a BIM-based BIPV design, the cost of the PV system was reduced by 11.7% and the power transmission loss decreased by 2.95%. Although this platform is also used for optimization, the focus was only on optimizing the PV array of the rooftop surface.

In addition to the forms and locations of the building exteriors, the shadow of the surrounding objects would highly influence the output of PV modules. For this matter, a tool is developed by

Ning et al. (2017) to improve the design efficiency of the rooftop PV analysis by performing the shadow and radiation simulation based on the BIM model (Figure 2-10).

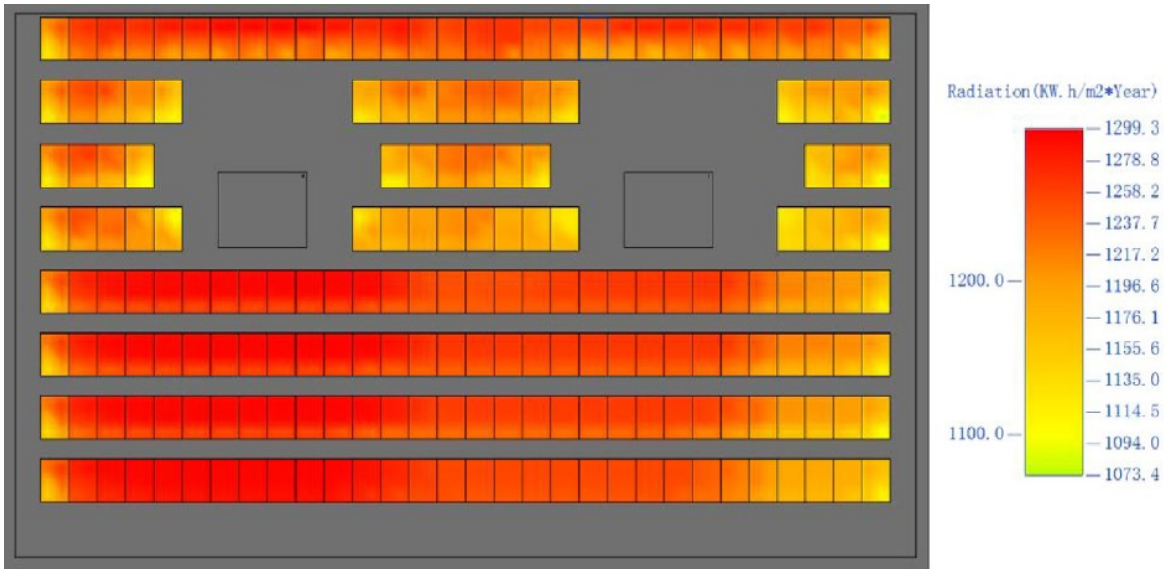

Figure 2-10 BIM-based PV optimization on rooftop (Ning et al., 2017)

Table 2-3 Various PV system optimization approaches on building surfaces

Reference	Sensitivity Analysis	Optimization							Approach	Modeling Tools
		Target surfaces		Objective(s)	Decision Variables					
		Roof	Facade		PV type	PV tilt	PV orientation	PV location		
(Cheng, Jimenez, & Lee, 2009)	✓	✓	-	Max PV energy generation	-	✓	✓	-	GIS-based	PVSYST
(Hwang, Kang, & Kim, 2012)	✓	-	✓	-	✓ F	✓ V	✓ V	✓ V	BIM-based	eQUEST
(Kucuksari, et al., 2014)	-	✓	-	Max total profit of PV installation	-	-	-	✓ V	GIS-based	ArcGIS
(Hong, Koo, Park, & Park, 2014)	✓	✓	-	Max annual PV energy generation	-	✓ V	-	-	GIS-based	RETScreen
(Freitas, Serra, & Brito, 2015)	-	✓	✓	Max PV energy generation, Min system cost	-	✓ F	✓ F	✓ V	GIS-based	SOL (3D solar radiation model)
(Koo, Hong, Lee, & Kim, 2016)	-	✓	-	Max PV energy generation, Min initial cost	✓ V	✓ V	-	-	GIS-based	RETScreen
(Ning, et al., 2017)	-	✓	-	Min capital investment per unit power output		✓ V	-	✓ V	BIM-based	Revit
(Ning, Kan, Zhifeng, Weihua, & Geert, 2018)	✓	✓	✓	Max PV energy generation, Min cost	-	-	-	✓ V	BIM-based	Revit
(Al-Janahi, Ellabban, & Al-Ghamdi, 2020)	-	✓	-	Max PV energy generation	-	-	-	✓ V	BIM-based	Revit
Present study	✓	✓	✓	Max PV energy generation, Min cost	-	✓ V	✓ V	✓ V	BIM-based	Dynamo, Refinery
F: Fixed for all panels, V: Variable per panel										

In a study by Al-Janahi et al. (2020) the BIM platform was used for the integration of BIPV modules on the rooftop of a metro station with a complex shape in Qatar. First, the rooftop area was divided into 45 main parts, then a certain number of PV modules were considered for each part. The solar feasibility analysis was conducted based on the average annual solar irradiance using Revit. A GA was used to optimize the layout of the PV arrays in terms of their electrical connection between those 45 zones in a way to maximize the currents in the rows by reducing the mismatch losses in the strings due to the partial shading. However, in this study, the PV modules with a certain size were directly integrated with the rooftop surfaces and no variation of tilt and pan angles were considered in the process of PV layout optimization.

Lin et al. (2021) mentioned the absence of an integrated framework for the design of PV systems, including building modeling and PV simulation. They developed a BIM-based solar tool, which is called PV Link, to integrate the PV system design phases considering various design variables and the feasibility analysis for rooftops. Although the PV placement based on the solar radiation potential on the rooftop is automated in this tool, the optimization approach is still missing in this integrated platform.

Considering the significant amount of potential solar power that could be harvested from high-rise building surfaces, many studies focused on the application of PV modules on the vertical surfaces of the buildings. Some of the researchers that considered facade PV application, investigated the performance of PV system based on the comparison of various influential factors such as the shadow effect, PV module type, orientation, and architectural aesthetic values. For example, a study by Peng et al. (2011), combined aesthetic criteria of BIPV installation with consideration of issues related to functionality, cost, and technical aspects of the applied PV modules.

In a practical application of BIPV on the front facade windows of a building, the impact of the orientation and shadow effect on the performance of the transparent thin film is monitored by (Yoon et al., 2011). The analysis of results confirmed that the shadow effect and the orientation of the PV modules can result in 47% improvement in PV systems' performance. However, no optimization is done to find out the optimum trade-off between these factors. In another study, two identical PV systems are applied on two different facades of a building in Turkey with different

shading conditions. Comparison of the output for two systems confirmed the criticality of the shading effect on the performance of PV modules (Eke & Demircan, 2015).

The application of two types of PV modules on a commercial building facade with different tilt angles was simulated and compared by (Bueno et al., 2015). Although no cost analysis is conducted in this study, the feasibility of the approach from a financial perspective is found to be viable considering the falling PV system prices.

To assess the PV system performance on the facades of two office buildings, an extensive sensitivity analysis is done by Hwang et al. (2012). The sensitivity analysis results showed that with a certain configuration of the PV modules, 1-5% of the electricity need of an office building can be covered by the installed PV system. Although the impact of multiple factors (e.g. type of the PV module, PV tilt, and orientation) are investigated in the PV energy simulation, no optimization is done to determine the best combination of the multiple parameters, and no cost analysis is considered within the process.

In a study done by a research group at Lisbon University, extensive work has been done to study the PV potential on building facades (Freitas et al., 2015). In this study, two reliable simulation approaches are used to prove the feasibility of the facade PV application. As shown in Figure 2-11, to find out the best facade PV design that maximizes the total irradiation yield, six irregular facade layouts were modeled in horizontal and vertical forms of rotating or folded louvers in addition to ellipsoid and hexagonal wall geometrical shapes. The Rhinoceros 3D software and Grasshopper were used for the parametric modeling of facade PV layout and annual solar radiation analysis with a 0.1 m^2 grid resolution. The generated energy is calculated by multiplying the total amount of annual solar radiation received by each facade by an average solar cell efficiency of 15%. The results indicated that the horizontal rotated PV layouts on the facade contribute to a higher level of PV energy generation. A multi-objective GA optimization approach is developed to find out the optimum tiling for PV modules string, which leads to maximizing the annual PV energy yield and minimizing the system cost. The optimization results revealed that the layouts with more but shorter PV strings achieve higher energy yields. The operation costs and the discount rate were not considered in the cost calculation. Furthermore, the BIM model was not considered in the

analyses and the simulation process was performed based on the Digital Surface Model (DSM) (Freitas & Brito, 2015).

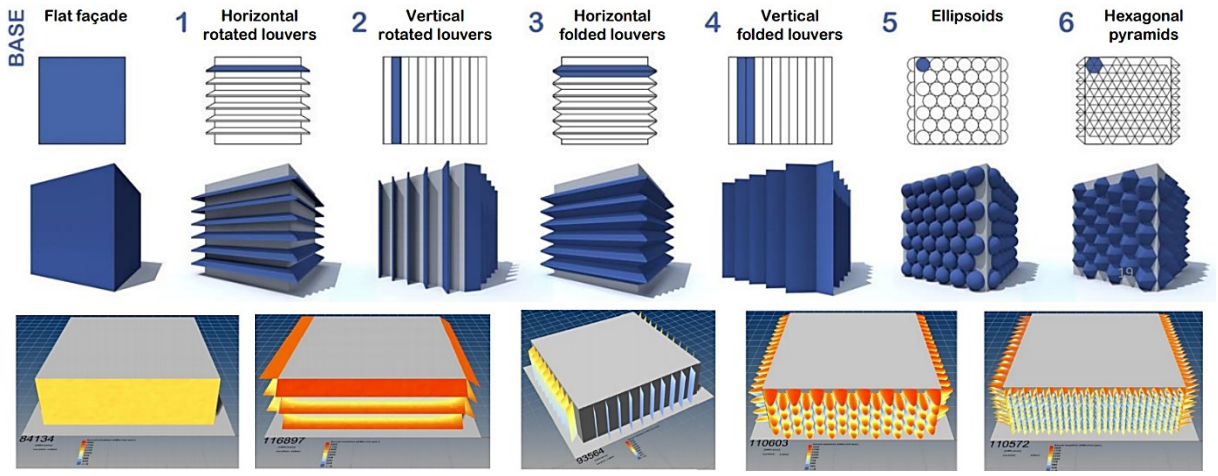

Figure 2-11 Studied facade layouts and their respective radiation simulations (Freitas & Brito, 2015)

Considering the PV locations and angles (i.e. tilt and pan) simultaneously on the building surfaces is critical especially when the target buildings are located in a complex built environment such as the dense urban areas where many factors (e.g. interference of shadow caused by the surrounding environment, lower yield contributed by solar radiation angle) affect the performance of the PV system. Therefore, these parameters need to be considered concurrently to find out where and how to apply or integrate the PV modules on the building surfaces to achieve optimum performance.

The integration of 3D modeling platforms and BIPV simulation tools is proposed in a study by (de Sousa Freitas, Cronemberger, Soares, & Amorim, 2020) to investigate the feasibility of rooftop and facade BIPV by comparing several design alternatives to retrofit some institutional buildings from the architectural and energy perspective. The design steps, including building 3D modeling, solar radiation assessment, and PV energy generation calculation, are performed using Rhinoceros Grasshopper software (Rhinoceros, 2021) and Ladybug (Ladybug Tools, 2021). Then, the energy balance is calculated using the BIPV generated energy and the building energy demand. Three design alternatives for facades are proposed as tilted sun-shading elements and double skin facades. Also, three design alternatives with certain tilt and pan angles are proposed for the

rooftops along with their energy generation. However, no optimization is considered in the process of modeling and assessment.

2.7 GENERATIVE DESIGN

Computer Aided Design (CAD) improved the efficiency of the design procedure and enabled the architects to create more precise and editable designs without redrawing the original one. However, the CAD tools were not flexible enough in case of automatically applying parametric changes in complex modeling. Therefore, Generative design (GD) was introduced as a solution to deal with its challenges (McCormack et al., 2004).

GD was defined for the first time by Mitchell in the 1975 as "devices capable of generating potential solutions to a given problem". Later, the GD was described as automating the creation of a large number of designs using the user-defined criteria and constraints (Caetano et al., 2020). Automation of generating various alternative designs, versus tedious manual procedures, offers the potential for more creativity and selecting the design, which best fits the wide range of criteria. The process of GD can be categorised into a series of steps including generate, analyze, rank, evolve, explore, and integrate (Figure 2-12).

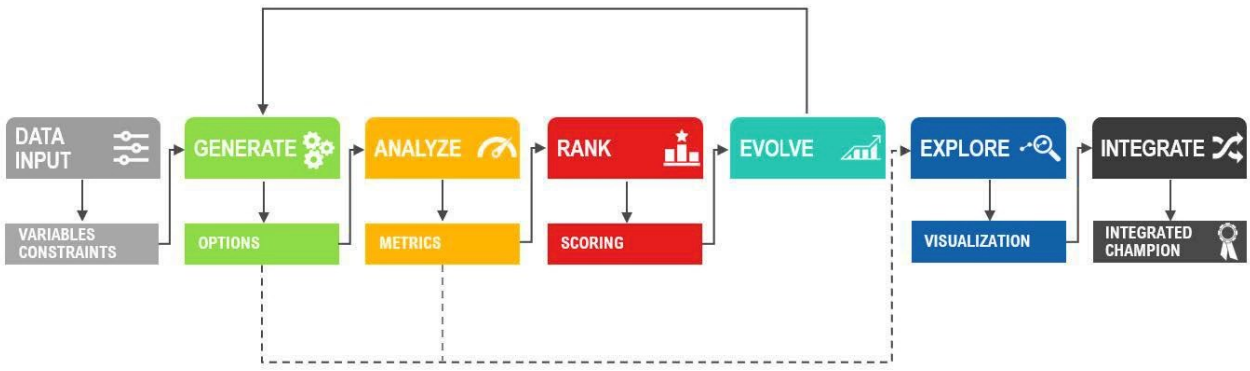

Figure 2-12 Generative design process (Vermeulen & El Ayoubi, 2021)

In the generating stage, the design options are created using the algorithm and the parameters defined by the designer. Next, the generated designs are analyzed and ranked based on how they meet the criteria defined by the designer. Then the designs will be evolved based on the ranking

results. The generated designs will be compared and explored; then the best fitting design option will be selected to be used or integrated into the project (Vermeulen & El Ayoubi, 2021).

The generative design approach was used in different domains in recent years. For example, since CAD applications are replaced by BIM tools, Ferreira & Leitão (2015) proposed a GD solution with a set of abstractions created for BIM tools. Fernando et al. (2012) investigated the advantage of connecting BIM and parametric modeling with explorative design modeling. By providing semantically rich BIM models, a link can be made between the conceptual and developed stages of the design process. In another study, a BIM-based rule language is developed by Sydora & Stroulia (2020) to automate the generation of interior design models.

In a study by Zhang et al. (2021), a parametric generative algorithm was developed to design buildings with respect to the energy conservation perspectives, which can improve the energy efficiency of the building in the early design phase and optimize the cost. Touloupaki & Theodosiou (2017) used a GD approach to optimize the energy performance of buildings for the case of near-zero energy buildings. In this study, GA and energy simulation were integrated through Grasshopper for Rhinoceros 3D (Rhinoceros, 2021) to explore the performance-based design alternatives in the building. For this purpose, software tools were developed to solve the automation and interoperability issues by facilitating the modeling procedure and interdisciplinary collaborations. Wang et al. (2020) proposed a GD urban design framework to explore a practical way of generating designs and applying them in the real project scheme. In this study the CityEngine (ESRI, 2021) modeling was used to generate the texture of blocks similar to the actual blocks in urban design.

Ma et al. (2021), (Ma, Wang, Wang, Xiang, & Sun, 2021) reviewed the approaches and requirements of BIM-based GD. They categorized the objectives of developing GD in BIM into two groups: (1) Solving specific design tasks (e.g., such as coping with design changes, the design period shortening, generating parametric models, exploring building forms or generating façade designs automatically) and (2) Supporting design processes (e.g., automating the design evaluation, reducing construction waste by proposing an early design workflow, improve the applicability of BIM in different design steps, developing a portable platform for application of

GD in BIM, and customizing the design tools). They defined the following future research directions: (1) development of more sophisticated and systematic GD-BIM to support more design processes, and (2) facilitating GD-BIM development by reducing programming difficulties for designers.

2.8 SUMMARY

Based on the review, the early research mostly focused on analyzing the solar radiation behavior using numerical and physics models. Then, by the introducing the computational models and various software, considering other factors, such as the geographical and topographical aspects became possible in evaluating the solar radiation. Later on, urban developments, and consequently the increasing trend of energy demand within the cities, propelled researchers and practitioners to move towards the decentralized energy generation. Solar PV energy has a very promising future both for its economic viability and environmental sustainability. It provides clean, silent, and easy access to energy by enabling onsite power generation and reducing the transmission costs.

Traditionally, PV panels are only used on farmlands or the rooftops of buildings. However, the improvement of PV technology and introduction of BIPV give them more flexibility to be applied to urban elements. Since urban development is mostly happening vertically in recent years, there is a considerable potential, especially on high-rise building facades, for generating PV energy. The complexity of the urban structure necessitates a thorough analysis of a wide range of parameters and factors including the surrounding environment and the building itself. Considerable progress has been made in reconstructing building 3D models with the continuous improvement in the level of accuracy and automating the process. However, the current tools are not geared toward the surface-specific solar analysis of the building, which is essential for a comprehensive design of PV solar modules

As highlighted in Table 2-3, most of the existing studies focused on PV optimization for rooftop surfaces, and various approaches were proposed by considering different decision variables. However, the majority of them did not use BIM models, and therefore did not consider surface-suitability for different types of PV modules. Although some studies included the facade surfaces

for the application of PV modules, a comprehensive optimization approach based on a surface-specific model, which considers multiple decision variables to optimize the energy yield, cost, and profit, is not developed yet.

Therefore, this study aims to develop a BIM-based method for a detailed solar simulation of building envelope using its surface properties, which will satisfy the ultimate goal of the study to determine the optimal layout of the PV modules on the building surfaces considering the number, type, location, and orientation of the PV modules on the building exterior surfaces.

CHAPTER 3 PARAMETRIC MODELLING AND SURFACE-SPECIFIC SENSITIVITY ANALYSIS OF PV MODULE LAYOUT ON BUILDING SKIN USING BIM [1]

3.1 INTRODUCTION

This chapter builds on the advent of BIM to develop a parametric modeling platform for the design of surface-specific PV module layout on the entire skin of buildings using the surface properties of the BIM model. This parametric modeling will be integrated with the optimization module to perform GD as explained in Chapter 4. In addition, using this platform, designers will be able to (1) perform radiation simulation on any, or a combination of, desired surfaces of buildings, (2) study the impact of various design characteristics (e.g., size and orientation), (3) develop complex scenarios for the layout of PV modules on the buildings, and (4) perform detailed cost-benefit analysis of the best scenario to investigate the cost implications (e.g. payback period) with respect to the number of installed panels.

The remainder of this chapter is structured as follows. First, the presentation of the proposed parametric simulation model. Next, the verification of the model through implementation and case study is presented. Subsequently, sensitivity analysis and a cost-benefit analysis are discussed. Finally, the summary and conclusions are presented.

3.2 PARAMETRIC SIMULATION MODEL

Figure 3-1 presents an overview of the proposed method for the parametric modeling of PV modules. In this method, first, the required data are collected. It is assumed that the BIM model of the studied building is available. Also, the CityGML model of the surroundings of the target

[1] This chapter is based on the following paper:
Salimzadeh, N., Vahdatikhaki, F., and Hammad, A. (2020). Parametric Modelling and Surface-specific Sensitivity Analysis of PV Module Layout on Building Skin Using BIM. *Energy and Buildings,* 216, 109953.

building needs to be obtained from the publicly available data. Next, the BIM model is decomposed in order to distinguish and classify different types of objects on the building skin (e.g., exterior walls, roofs, curtain walls, windows, etc.). Subsequently, within each class, the external surfaces of the objects are extracted. This step is important because the inclusion of inner surfaces, which receive no radiation, in the radiation simulation would add significantly to the computational efforts. Once relevant and classified surfaces are identified, the user-defined configurations (pan, tilt, size) for each PV module are used to generate PV modules on the surfaces. Finally, the BIM-based radiation simulation is applied on all the PV modules considering the shadow effects of (1) the surrounding buildings, (2) the objects on the studied building, and (3) PV modules.

Next, the results from the parametric modeling platform can be used to (1) perform sensitivity analysis by defining several PV module layout scenarios (i.e., different pan, tilt, and sizes for solar panels) then (2) perform a cost-benefit analysis to investigate the payback period of each scenario.

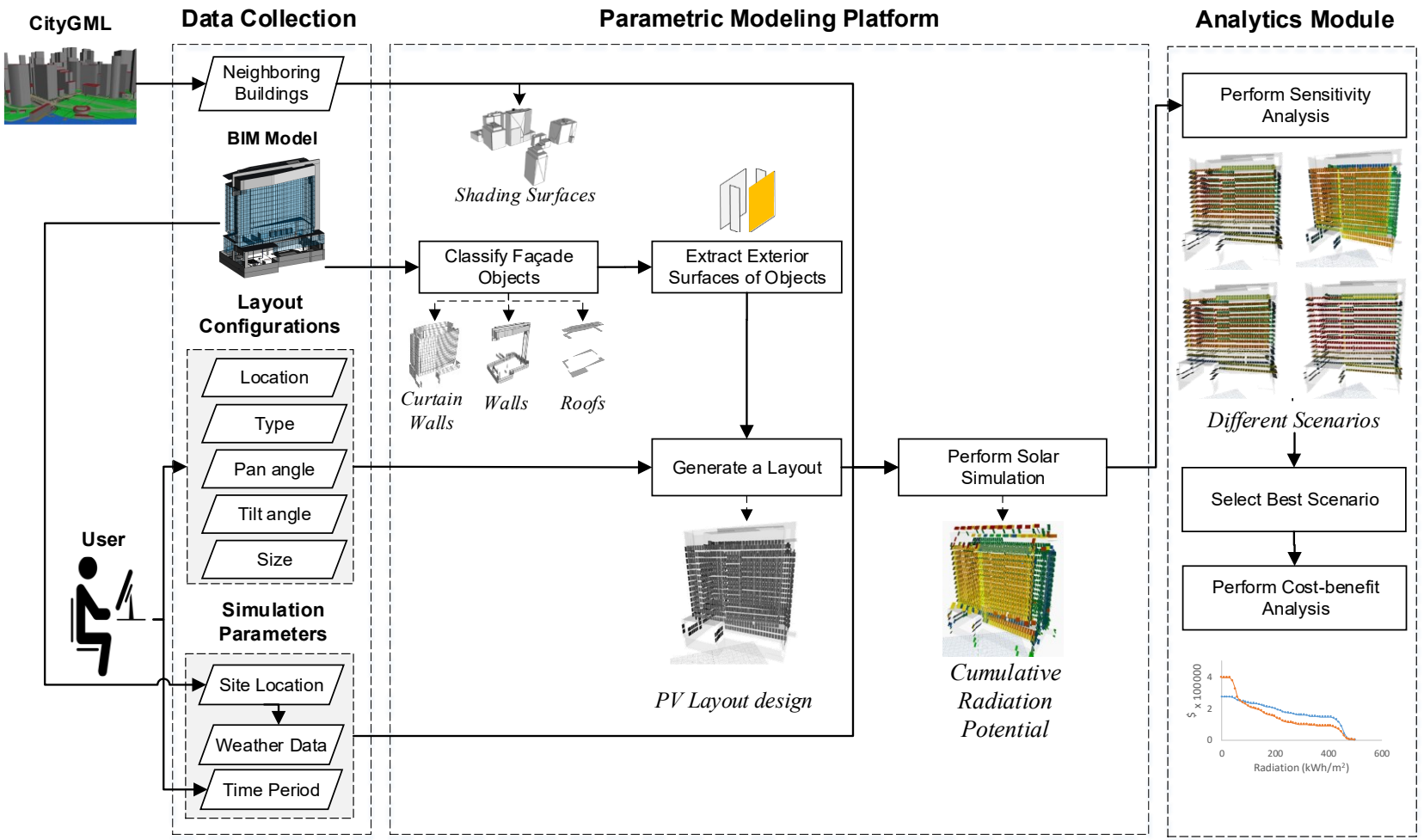

Figure 3-1 Overview of the simulation model

3.2.1 Data Collection

To be able to use the BIM model for PV panel planning, the model needs to be at a certain level of maturity in terms of the data available in the model. According to the definition of the American Institute of Architecture (AIA), Level of Development (LOD) represents the minimum dimensional, spatial, quantitative, and qualitative data in a model element. For example, LOD 100 includes the conceptual geometry with a generic representation, and LOD 200 describes the approximate geometry in terms of quantities, shape, and size of the objects. While LOD 300 shows the precise geometry of a specific object including size, shape, and location. In addition to the graphical representation, this LOD may include some non-graphic information (AIA, 2021). For the purpose of PV layout planning, the LOD 300 is sufficient. At this LOD, the type and geometry (i.e., size, shape, location, and orientation) of building objects are known (Bedrick, 2008).

To represent the surrounding objects that have a shading effect on the target building, the 3D models of neighborhood buildings are used. As shown in Figure 3-2(a), many cities are already using CityGML to provide high-quality geo-referenced semantic models of their jurisdictions (City of Montreal, 2021). Therefore, these models are becoming increasingly available in different areas. The CityGML model should be trimmed to include only buildings in the effective region of the building under consideration in order to reduce the computational effort of the simulation. The boundaries of the effective region are marked by the furthest buildings in different directions that can cast a shadow on the building under consideration. Then, as shown in Figure 3-2(b) the surfaces of the neighborhood buildings from CityGML model are merged with the BIM model of the building under consideration before running the solar radiation simulation. Another input required from the user is about the layout of the PV system. The layout is determined in terms of location, pan, and tilt angles, and size of the modules. This input is provided in the form of the matrix shown in Equation 3.1. First, as shown in Figure 3-1. the user needs to determine whether or not there is a module at the potential installation spot.

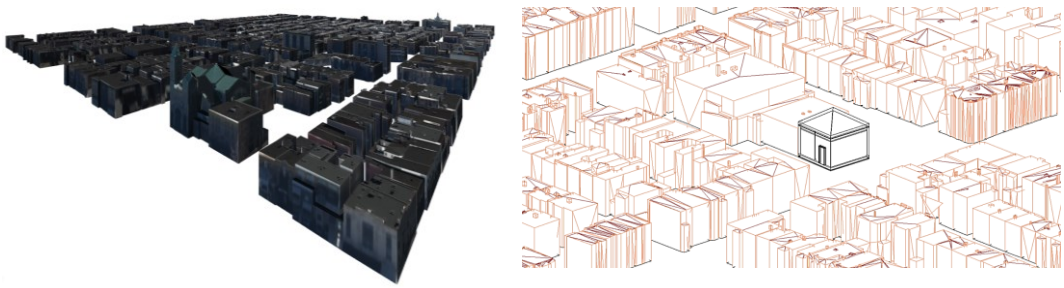

(a) (b)

Figure 3-2 (a) An example of CityGML file of Montreal, (b) BIM and CityGML integration

3.2.2 Parametric Modeling Platform

As will be explained in detail in Section 3.2.2.1 to Section 3.2.2.4, Figure 3-3 presents the overall concept behind the parametric model used in this research. The overall problem of finding the optimum configurations for the PV modules can be translated to (1) identifying the locations where solar panels need to be installed, and (2) finding the tilt and pan angles of these panels (the pan angle is applied only for PV modules on the roof). It should be highlighted that this problem must be solved concurrently for the various variables (i.e., finding optimum locations, pans, and tilts together) rather than sequentially (i.e., to first find the optimum locations and then optimum pans and tilts). This is important because considering the shadow effect of panels on one another, placing PV modules with specific angles on the lower-radiation locations but with a low shadow effect can possibly yield better results than simply placing PV modules on the top-ranking locations from the radiation potential perspective but with a high shadow effect.

The first step in developing viable solutions is to identify all candidate locations considering the suitability of different types of PV modules (e.g., opaque or transparent) on different types of exterior objects (roofs, walls, etc.). Therefore, this research proposes the use of a BIM model as input because the embedded semantics in the BIM model allows considering object-specific PV modules. For example, the use of transparent or semi-transparent panels can be considered only for windows while opaque panels can be considered for the walls (Figure 3-3 (a)). Additionally,

the semantics in the BIM model allows excluding areas where PV modules cannot be installed (e.g., because of mechanical installations or openings).

Once the candidate exterior objects are identified, they can be trimmed to only retain the exterior surface. This is needed because the solar radiation simulation is essentially surface-based. Keeping other surfaces of objects in the model, thus, slows down the simulation considerably. After filtering the redundant surfaces, the remaining surfaces need to be rasterized into a grid, as shown in Figure 3-3(b). The size of this grid is determined by the size of the panels being considered for each specific surface. Each cell in this grid is a potential location for the installation of PV modules. Ultimately, the entire exterior of the building is represented by K potential locations for PV modules.

Upon the generation of the simulation grid, a potential solution can be developed. At this stage, the decisions to be made are: (1) should a panel be placed at any of the K locations?, (2) what is the tilt angle of each panel?, and (3) if the panel is on the horizontal surface, what is the pan angle?, as shown in Figure 3-3(c) and Figure 3-3(d). It should be highlighted that the pan angle for the facade PV modules is not considered mainly because of aesthetics reasons and installation challenges. As mentioned by Attoye et al. (2017), in some cases aesthetical consideration or other design objectives (e.g., maximum daylight and view) requires compromising the energy performance. The decision about the consideration or rejection of cell k for the installation of PV modules can be mathematically represented by a binary value for P_i, where 0 represents no PV module and 1 represents the use of a PV module on location i. Eventually, a specific solution for PV module installation can be represented by the matrix shown in Equation 3.1.

$$S_i = \begin{bmatrix} P_{i,1} & \cdots & P_{i,k} & \cdots & P_{i,K} \\ \theta_{i,1} & \cdots & \theta_{i,k} & \cdots & \theta_{i,K} \\ \beta_{i,1} & \cdots & \beta_{i,k} & \cdots & \beta_{i,K} \\ A_{i,1} & \cdots & A_{i,k} & \cdots & A_{i,K} \end{bmatrix} \quad \text{Eq. 3.1}$$

where:

S_i: Potential solution i
$P_{i,k}$: a binary value representing presence (1) or absence (0) of PV module at location k in solution i
$\theta_{i,k}$: the tilt angle of PV module at location k in solution i where $0° \leq \theta_{i,k} \leq 90°$
$\beta_{i,k}$: the pan angle of PV module at location k in solution i where $0° \leq \beta_{i,k} \leq 360°$
$A_{i,k}$: the size of PV module at location k in solution i

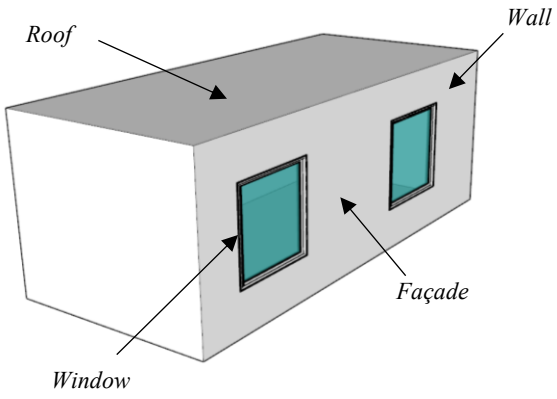

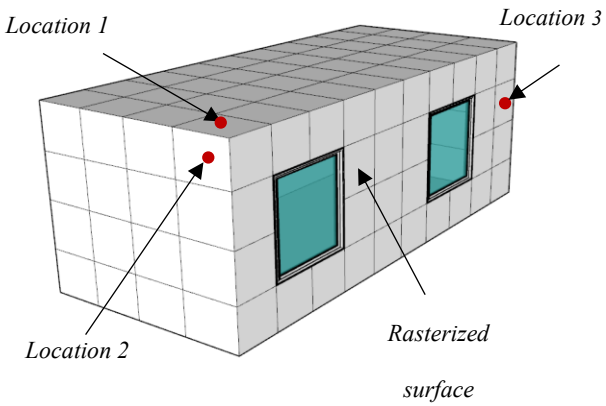

(a) Separation of surfaces

(b) Surface rasterization

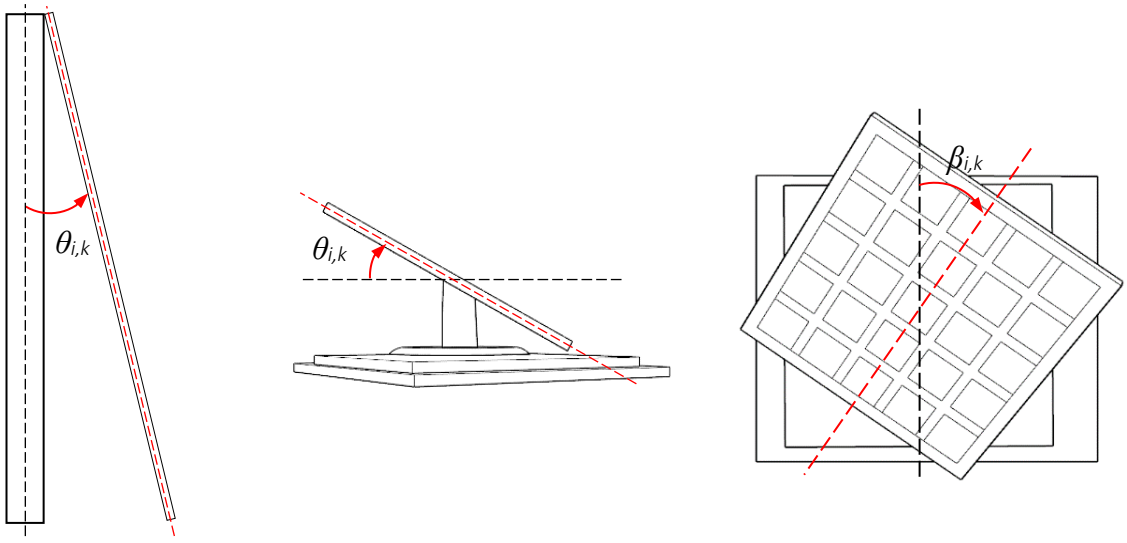

(c) Application of Tilt (θi,k) and Pan (βi,k) angles on created PV modules

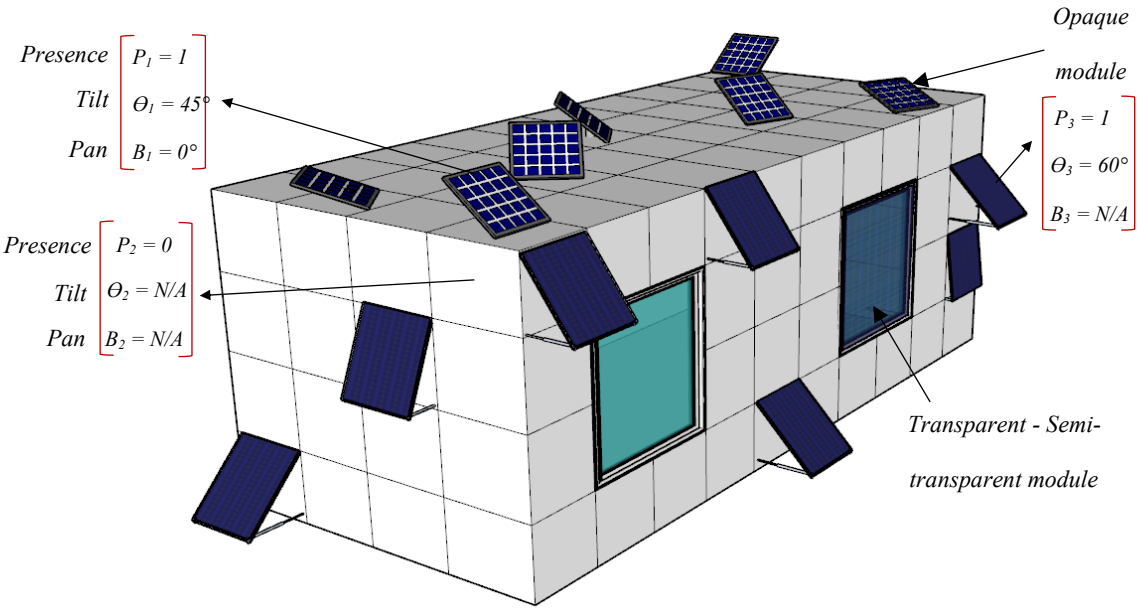

(d) Generation of a potential solution

Figure 3-3 Process of preparing the parametric model

It should be noted that before the solar radiation simulation can be executed on the generated solution, the simulation engine requires a 3D representation of the surrounding buildings for consideration of their shadow effect on the PV modules. This model can be obtained from available CityGML models or generated using public GIS data. When the 3D models of the surrounding buildings are imported, the solar radiation simulation can run. This simulation estimates the annual cumulative radiation potential of each panel ($R_{i,k,\theta,\beta}$).

3.2.2.1 Facade object classification

The BIM model provides the basis for the classification of different objects of the building façade (e.g. roof, walls, and windows). Depending on the considered types of PV modules, the classification can be further expanded using the attributes of the objects. For instance, the length and width of the windows can be used to classify the windows into sub-categories based on their

sizes. Such detailed classification helps to select suitable PV modules for the objects based on their materials or sizes. However, the consideration of detailed attributes (e.g., materials) may necessitate a higher LOD of the BIM model.

3.2.2.2 Extraction of exterior surfaces

After the classification, all the objects in each class are decomposed into the constituent surfaces. The main goal of this step is to identify the exterior surfaces which can receive solar radiation. Therefore, for each object, only the exterior surface is kept, and the remaining surfaces are filtered out as they are irrelevant for the solar simulation. As shown in Figure 3-4, after identifying all walls of the provided BIM model, the internal ones, which are not receiving the solar radiation, are removed. In the next step, the external walls are decomposed into surfaces to be able to filter out the horizontal surfaces and keep only the vertical surfaces for the solar simulation purpose. Finally, the exterior faces of the distinguished surfaces are identified using their normal vectors to determine the analysis surfaces for the solar radiation simulation.

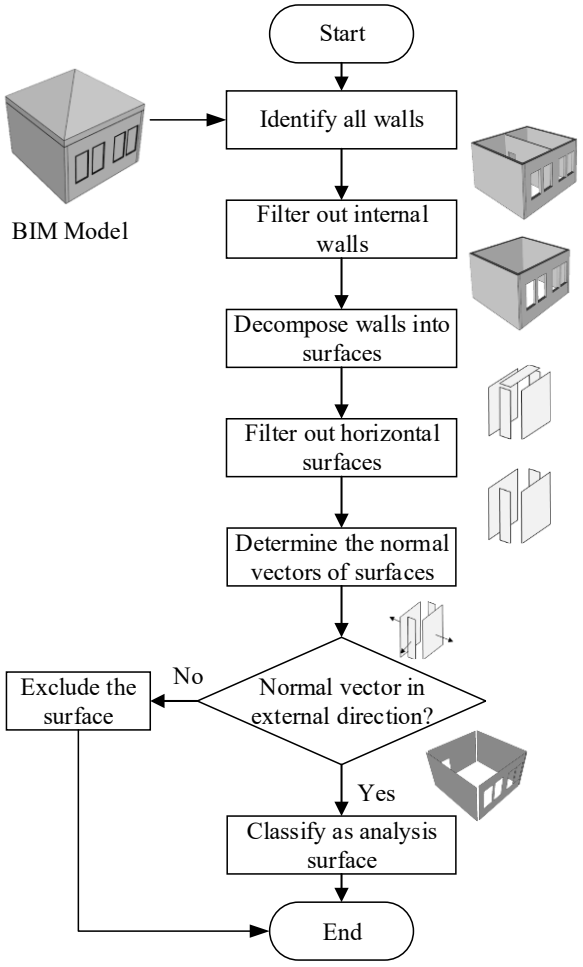

Figure 3-4 Flowchart for extraction of exterior surfaces from wall objects

3.2.2.3 Generate a layout

In this step, the user-defined configurations, as shown in Equation 3.1, are used to generate a layout. The resolution is determined based on the defined module sizes. The resolution specifies how many analysis points on each surface should be considered.

3.2.2.4 Solar radiation simulation

User-defined simulation parameters are used to perform solar radiation simulation. While the simulation period can be of any length and from any starting date, since the PV module optimization procedure is based on the annual cumulative solar potential, it is recommended to use

a whole year for the time period. The site location can be obtained from the coordinates of the site, which is available in the BIM model. Based on the location of the building, the weather data can be retrieved from national meteorological databases (Historical Climate Data, 2018). The shading caused by surrounding objects is calculated using the ray-tracing shading algorithm, where a shadow ray is traced from the light source toward each beam of light. If any opaque object (e.g., trees, buildings) is found between the PV module surface and the light source, the surface is in shadow and the light does not illuminate it (Introduction to Shading, 2021).

3.2.3 Analytics Module

3.2.3.1 Sensitivity analysis

The performance of the PV modules on the building surfaces depends on different factors. Some of these factors (i.e. the size of the PV module, the shading effects of the modules on each other, their installation tilt angle, and the orientation) have a significant effect on the amount of the received solar radiation. Therefore, to investigate the importance of each factor, sensitivity analysis is performed for different scenarios, where different configurations of tilt angle are considered for a certain PV dimension. Then, the simulated radiation value is analyzed for each scenario.

3.2.3.2 Cost-benefit analysis

Since different levels of radiation are received by different PV modules, each of them would have a certain return on investment. Performing the cost-benefit analysis provides the possibility to find at which level of generated energy it is reasonable to invest, given a certain payback period.

The first step in performing the cost-benefit analysis is to determine the number of PV modules that have a solar potential higher than a given threshold. Therefore, the present value of the generated energy revenue by PV modules at each threshold during their life cycle of *T* years is quantified as shown in Equation 3.2.

$$ER_{\mathrm{i}}^{T} = \mathrm{V} \times D_T \sum_{k=1}^{K} P_{i,k} \times R_{ik\theta\beta} \times e_{i,k} \times PR \qquad \text{Eq. 3.2}$$

where:

V: the present value of the energy unit cost ($/kWh)
D_T: the present value of a growing annuity for T years
K: the number of possible locations of PV modules
$P_{i,k}$: a binary value representing presence (1) or absence (0) of PV module at location k in solution i
$R_{ik\theta\beta}$: the global annual radiation received by PV module k with tilt (θ), and pan (β,only for roof) for solution i (kWh)
$e_{i,k}$: efficiency of PV module k for the solution i (%)
PR: the performance ratio of the PV system (%)

D_T can be calculated using the equation for the present value of a growing annuity as shown in Equation 3.3 (Finance Formulas, 2021), which calculates the present value of a series of future periodic payments that increase at a proportionate rate (i.e., inflation rate).

$$D_T = \frac{1}{r-g}\left[1 - \left(\frac{1+g}{1+r}\right)^T\right] \quad \text{Eq. 3.3}$$

where:
r: the discount rate
g: the inflation rate

On the other hand, the total cost of PV modules includes the initial cost (i.e., acquisition and installation) and the maintenance cost, as shown in Equations 3.4. Since the maintenance cost should be considered for the whole life cycle of the PV system, the D_T factor must be considered.

$$TC_i^T = CM \sum_{k=1}^{K} a_{i,k}(1 + \alpha \times D_T) \quad \text{Eq. 3.4}$$

where:

CM: the cost of PV module per square meter ($/m^2)
$a_{i,k}$: the area of module k for the solution i (m^2),
α: the percentage of the initial cost of the PV system spent on annual maintenance and operation

3.3 IMPLEMENTATION AND CASE STUDY

The proposed method is implemented in a prototype. In this implementation, Revit (Autodesk, Revit, 2021) is used as the platform for integrating the BIM model and the CityGML model to capture both the object properties of a certain building and the surroundings of this building. In order to implement the method in Revit, Dynamo visual programming is used (Dynamo, 2021). Dynamo runs within Revit and works as an Application Programming Interface (API). Dynamo can make the custom analysis possible, which is not covered in Revit solar analysis. Also, it allows rapid programming within Revit and provides seamless integration between the Revit model and various simulation tools.

To implement the proposed method, different graphs are developed in Dynamo using Python scripts. For example, Figure 3-7 shows the implementation of the wall object detection and surface extraction as previously described in Section 3.2.2.2. In addition, Figure 3-5 shows the implementations steps of the graph developed in Dynamo for creating the PV modules with adjustable size, and tilt and pan angles.

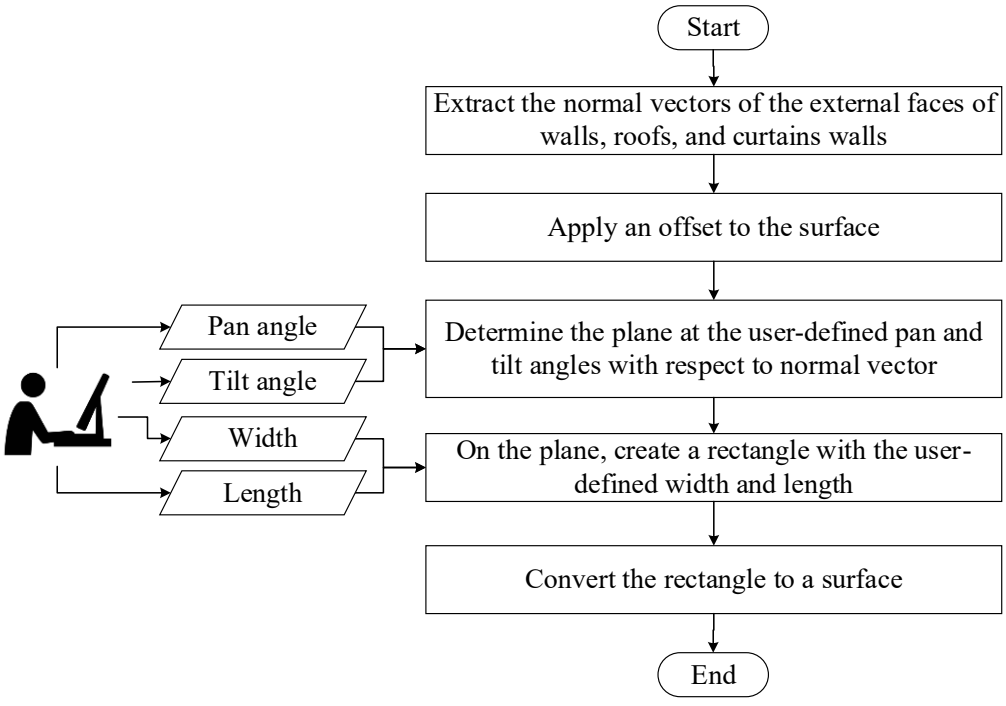

Figure 3-5 Implementation steps for creating PV modules and applying pan and tilt angles

The created rectangles, defined as PV modules, are converted to surfaces at the end to be used as input to the "SolarAnalysis" node. A separate node is used to generate the shading surfaces of the study site. The output of this node is also considered as one of the inputs to the solar analysis node. Also, as shown in Figure 3-6**,** another graph is developed to visualize the result of the solar radiation simulation using the information of the surfaces and the radiation values.

The feasibility of the proposed method is tested by carrying out a case study. The case study is conducted in Sir George William (SGW) campus of Concordia University in downtown Montreal. The building of John Molson School of Business (JMSB) is selected for the analysis because of its specific architecture, which includes curtain walls, windows, walls, rooftops, and projected horizontal surfaces at a different level. This complex architecture requires a detailed and surface-specific simulation of the building envelope.

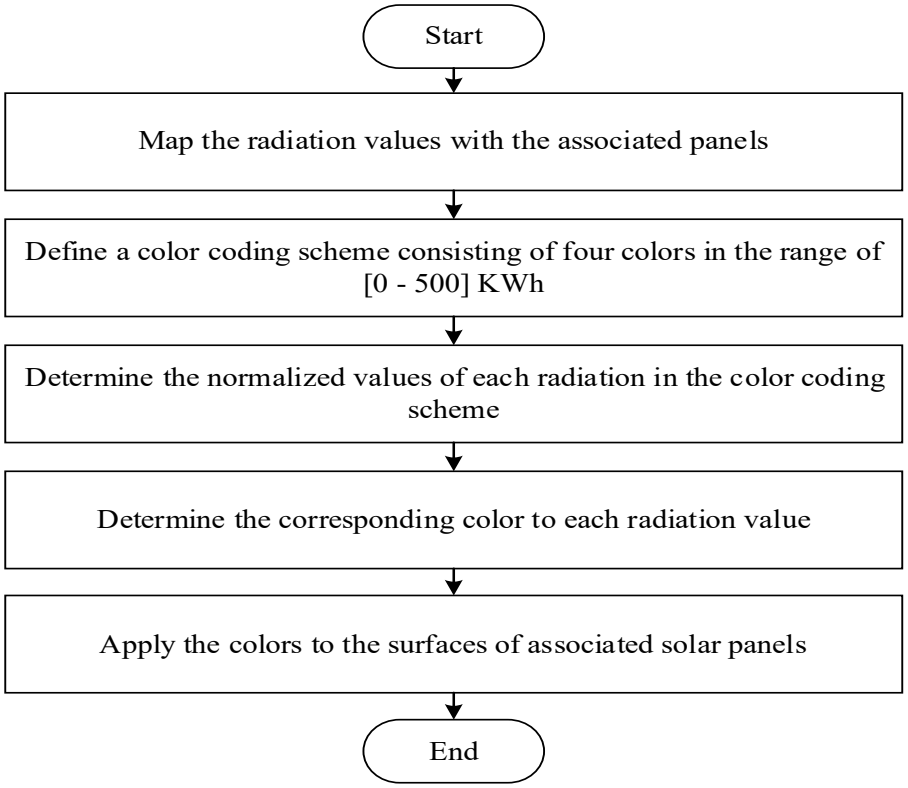

Figure 3-6 Visualization of solar radiation simulation

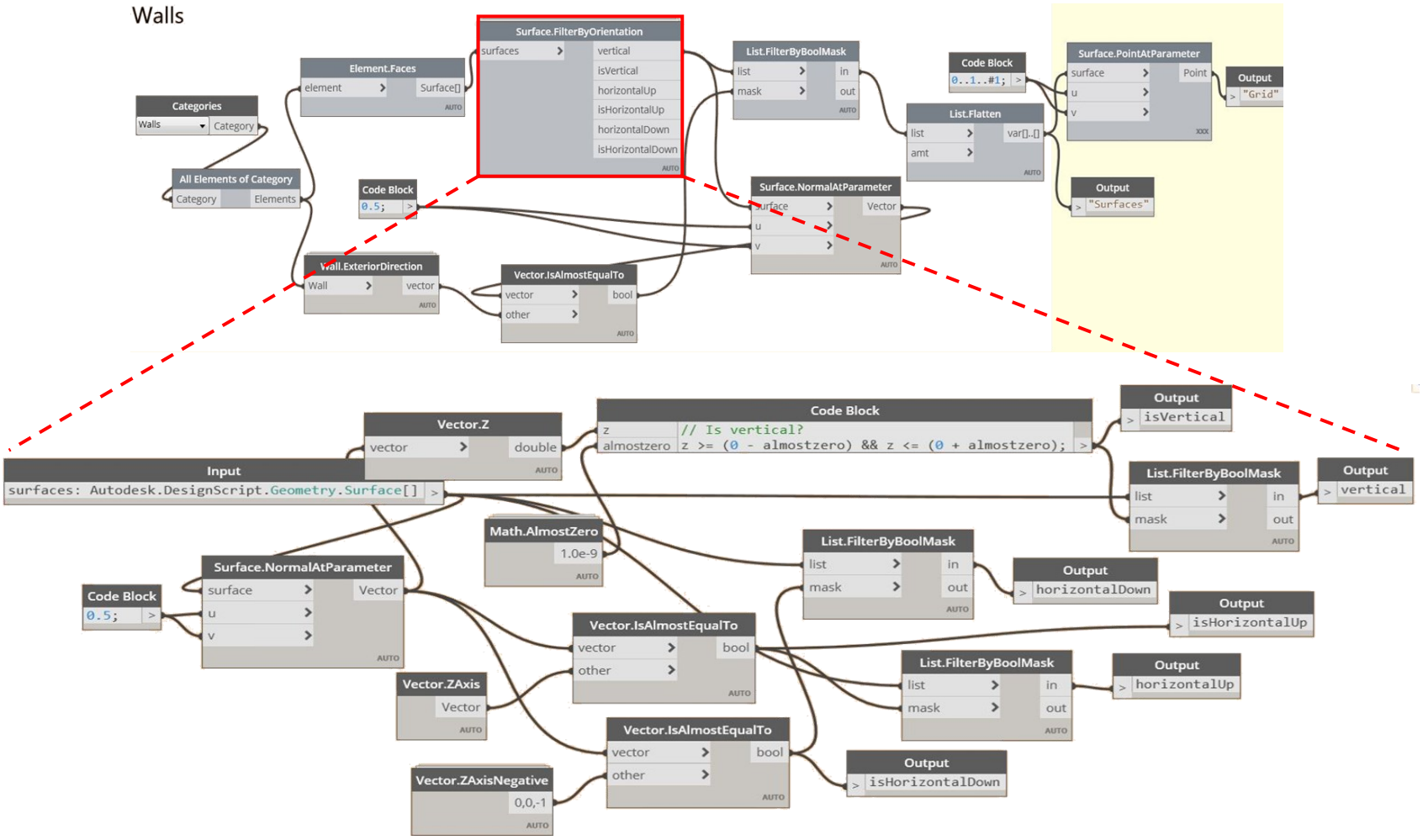

Figure 3-7 Implementation of wall detection and surface extraction in Dynamo

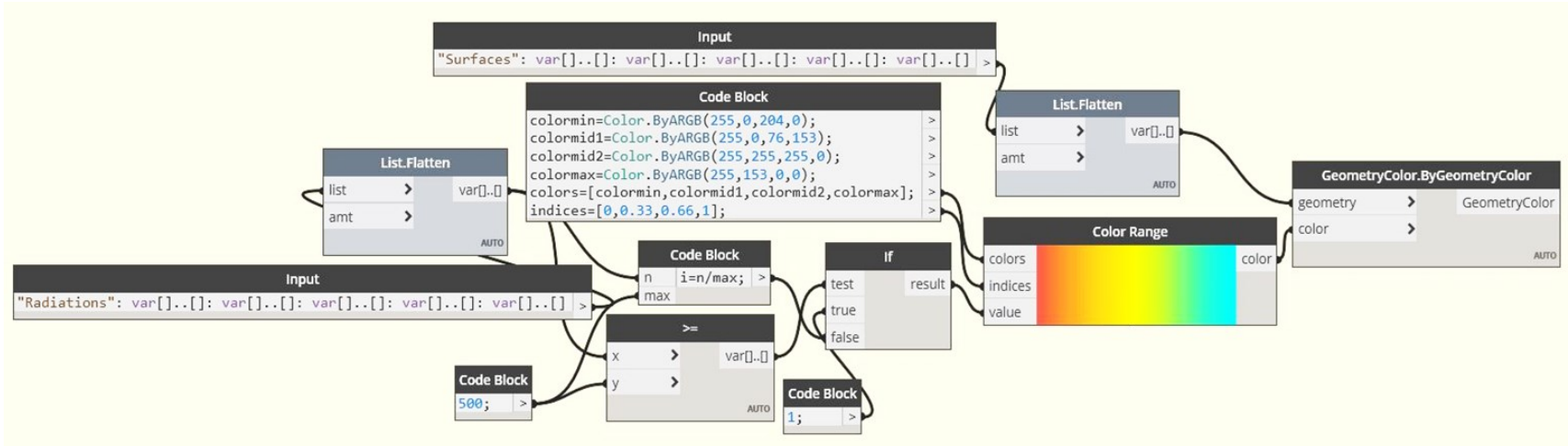

Figure 3-8 Visualization of solar radiation simulation

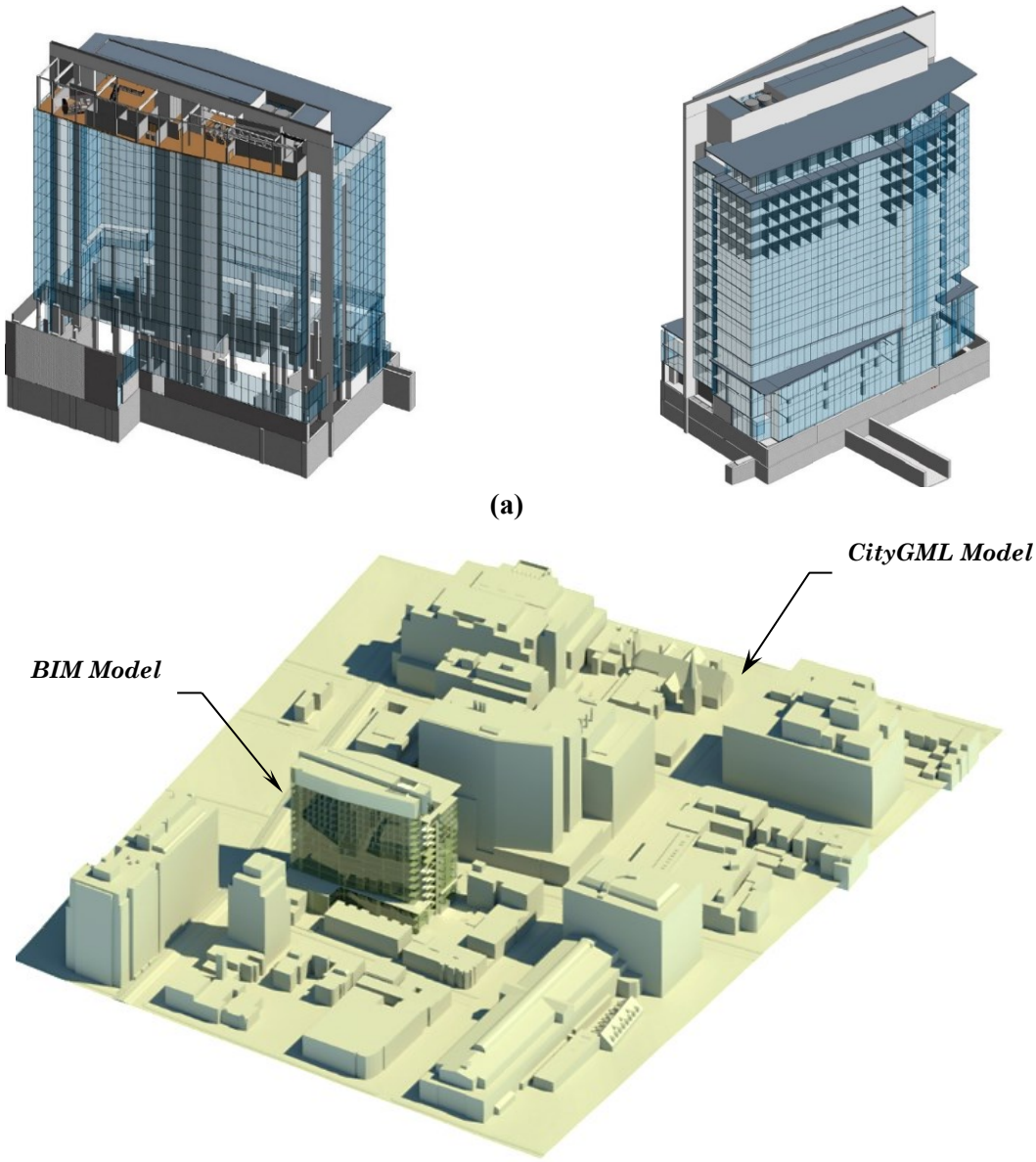

Figure 3-9 (a) JMSB BIM model, (b) Integration of the BIM Model and CityGML in Revit

The BIM model of JMSB building is created and imported into Revit. To consider the shadow effect of the neighborhood buildings in solar simulation, the city blocks around the JMSB building are extracted from the CityGML model (City of Montreal, 2021). CityGML data is converted into a FBX file and then merged with the BIM model as a unique site family in Revit (Figure 3-9).

Three classes of objects are considered in this case study, namely, roofs, walls, and curtain walls. Figure 3-10 (a, b, and c) show the external surfaces of these elements. The extraction of the exterior surfaces of the classified objects is implemented on the target building based on the steps explained in Section 4.2.2.2. It is important for the implementation that elements are modelled using appropriate families and attributes in the BIM model. For the resolution of the simulation analysis, a grid with a spacing of 1 m is used, as shown in Figure 3-10 (d, e, and f).

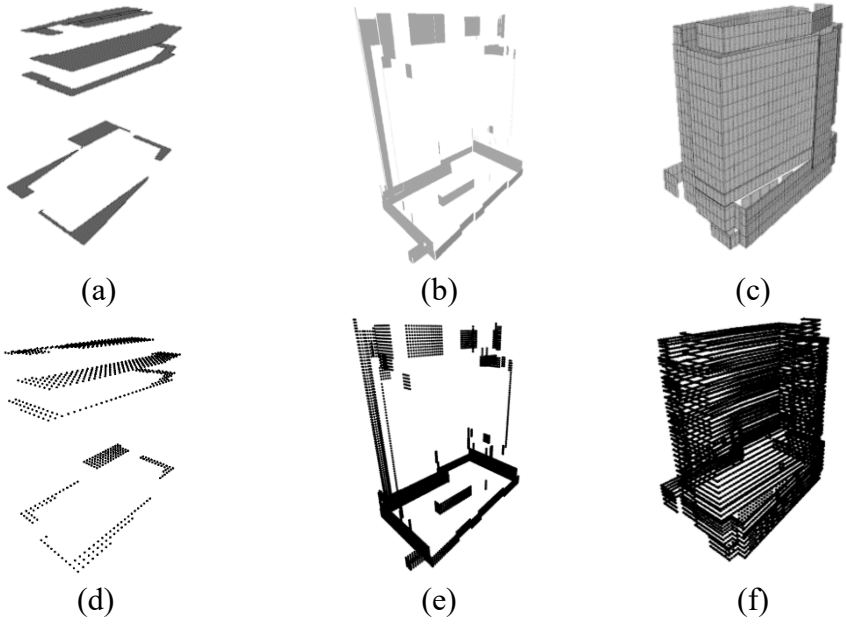

Figure 3-10 Extraction of external surfaces of (a) roofs, (b) walls, (c) curtain walls, and resolution of simulation analysis for (d) roofs, (e) walls, and (f) curtain walls

To generate the layout, different configurations such as the PV location, size, type, tilt and pan angles are defined by the user. The next step is to apply the solar radiation simulation in Dynamo using the predefined node. The weather data is automatically determined based on the site location, and the annual solar radiation is calculated for one year. After running the solar analysis on the created modules considering various configurations, the developed Dynamo graph is used to visualize the cumulative radiation results using a color-coding scheme (Figure 3-8). The solar radiation analysis is done for all classes of surfaces.

3.4 SENSITIVITY ANALYSIS

As mentioned in Section 3.2.3.1, a sensitivity analysis is performed on the façade curtain walls and rooftop of the target building. This analysis aims to investigate the performance of different PV modules' layouts with various configurations of size and tilt/pan angles.

3.4.1 Curtain Wall PV Layout Sensitivity Analysis

Based on the available BIM model, the distance between two floors on the façade is covered by the curtain panels of 4 *m* high and 2 *m* wide. It is assumed that 25% of the floor height is dedicated to the window section and the remaining part is a wall. Having this information, two sets of scenarios are developed for the curtain wall PV layout with a certain size of the module for each set. In the first set, modules with the size of 1.5 *m* by 3 *m* are considered to be installed on the opaque area between two consecutive rows of windows (Figure 3-11). The opaque type of PV modules with a minimum efficiency of 16% is used for this layout. In addition, a horizontal space of 0.5 *m* is assumed between PV modules as the workspace for the installation and maintenance purposes. Then, the radiation simulation is implemented with five different configurations of the tilt angle. The average radiation value for each scenario is obtained by dividing the annual cumulative radiation by the total panelized area. The overall panelized area for each set is calculated considering all 1,937 PV modules previously generated on the curtain wall multiplied by the specified dimension for each set.

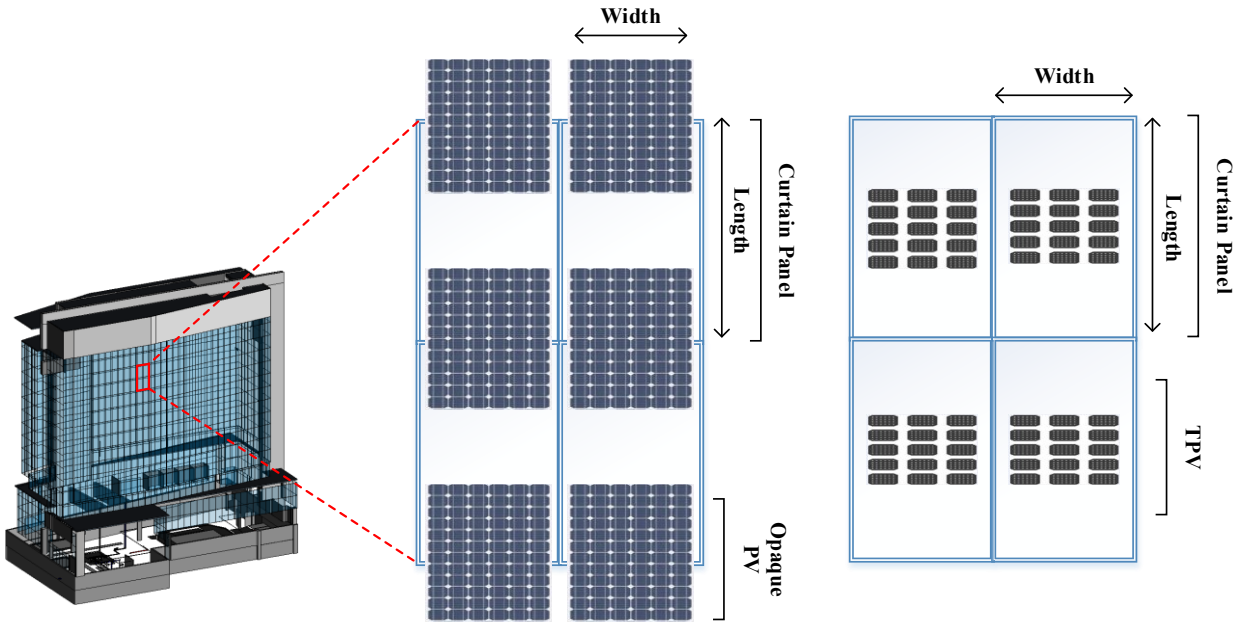

Figure 3-11 Installation of (a) opaque and (b) semi-transparent PV modules on the facade

In Scenario A1, the tilt angle for all PV modules is set at 0°, i.e., parallel to the facade. The output of the simulation with no tilt angle provides a baseline to evaluate the sensitivity of the radiation to the tilt angle. In Scenario B1, all modules are set at 45°, which is the site latitude for the target building. According to previous studies, the optimum tilt angle for PV modules is equal to the latitude of the area (Kemery et al., 2012). As presented in Table 3-1, the PV layout with this tilt angle has higher average radiation compared to the other scenarios in the first set. In Scenario C1, the tilt angle of PV modules is gradually increased downward through to the lower level of the building. It was expected that increasing the tilt angle at the lower levels will increase the chance of capturing radiation by PV modules and will decrease the shadow effect of the upper-level modules on the lower ones. As can be seen in Table 3-2, the average radiation of this setting is higher than Scenario A1 but slightly lower than Scenario B1. Opposite to Scenario C1, in Scenario D1 the tilt angle is gradually decreased downward and according to the radiation value, the shadow effect of the upper levels reduced the received radiation. In Scenario E1, the tilt angle of the upper levels is set at 45°, equal to the latitude, to capture more radiation, and the lower level is set at 75°

to enhance the chance of receiving solar radiation. Nevertheless, the output was not as good as Scenario C1.

Table 3-1 Curtain wall PV layout output based on tilt angle (set 1)

Scenario	Tilt Angle *(Degree)*	PV Module Dimensions		Total Panelized Area *(m2)* **[A]**	Annual Cumulative Radiation *(MWh)* **[R]**	Percentage *(%)*	Average Radiation **(***kWh/m2)* **[R/A]**
		W *(m)*	**L** *(m)*				
A1	0	1.5	3	8716.5	1,576	100	180.80
B1	**45**	**1.5**	**3**	**8716.5**	**1,655**	**105**	**189.87**
C1	Increasing tilt downward (0 - 90)	1.5	3	8716.5	1,632	103.5	187.23
D1	Decreasing tilt downward (90 - 0)	1.5	3	8716.5	1,593	101	182.77
E1	Increasing tilt downward (45 - 75)	1.5	3	8716.5	1,617	102.6	185.51

In the second set of scenarios, the radiation simulation is repeated with the same configurations of tilt angle but with a smaller size of PV modules, as shown in Table 3-2. The dimension of the PV modules is considered 1.5 *m* by 2 *m* for this set to analyze the effect of reducing the module size, and consequently reducing the shadow effect of the modules on each other. According to Table 3-2, comparing Scenario A2 and B2 shows the better performance of modules at 45° compared to the vertical modules. Comparing Scenarios B2 and C2 shows a slight increase in Scenario C2. However, this increase did not happen when comparing B1 and C1 in Set 1 because of the bigger shadow effect of the PV modules on each other due to their larger size. This indicates the intricate and complex correlation between size and tilt angles and demonstrates that an accurate analysis of PV layout indeed requires a parametric modeling platform that can capture this complexity.

Table 3-2 Curtain wall PV layout output based on tilt angle (set 2)

Scenario	Tilt Angle *(Degree)*	PV Module Dimensions		Total Panelized Area *(m2)* **[A]**	Annual Cumulative Radiation *(MWh)* **[R]**	Percentage *(%)*	Average Radiation **(***kWh/m2)* **[R/A]**
		W *(m)*	**L** *(m)*				
A2	0	1.5	2	5,811	1,060	100	182.00
B2	45	1.5	2	5,811	1,233	116	212.00
C2	**Increasing tilt downward (0 - 90)**	**1.5**	**2**	**5,811**	**1,236**	**116.6**	**212.77**
D2	Decreasing tilt downward (90 - 0)	1.5	2	5,811	1,162	109.6	199.89
E2	Increasing tilt downward (45 - 75)	1.5	2	5,811	1,222	115	210.00

A pair-wise comparison of the scenarios of the two sets shows that although the annual cumulative radiation values for Set 1 are higher due to a larger area of PV modules, PV modules in Set 2 receive higher average radiation per m^2. The visualized results of these scenarios are presented in Figure 3-12 and Figure 3-13.

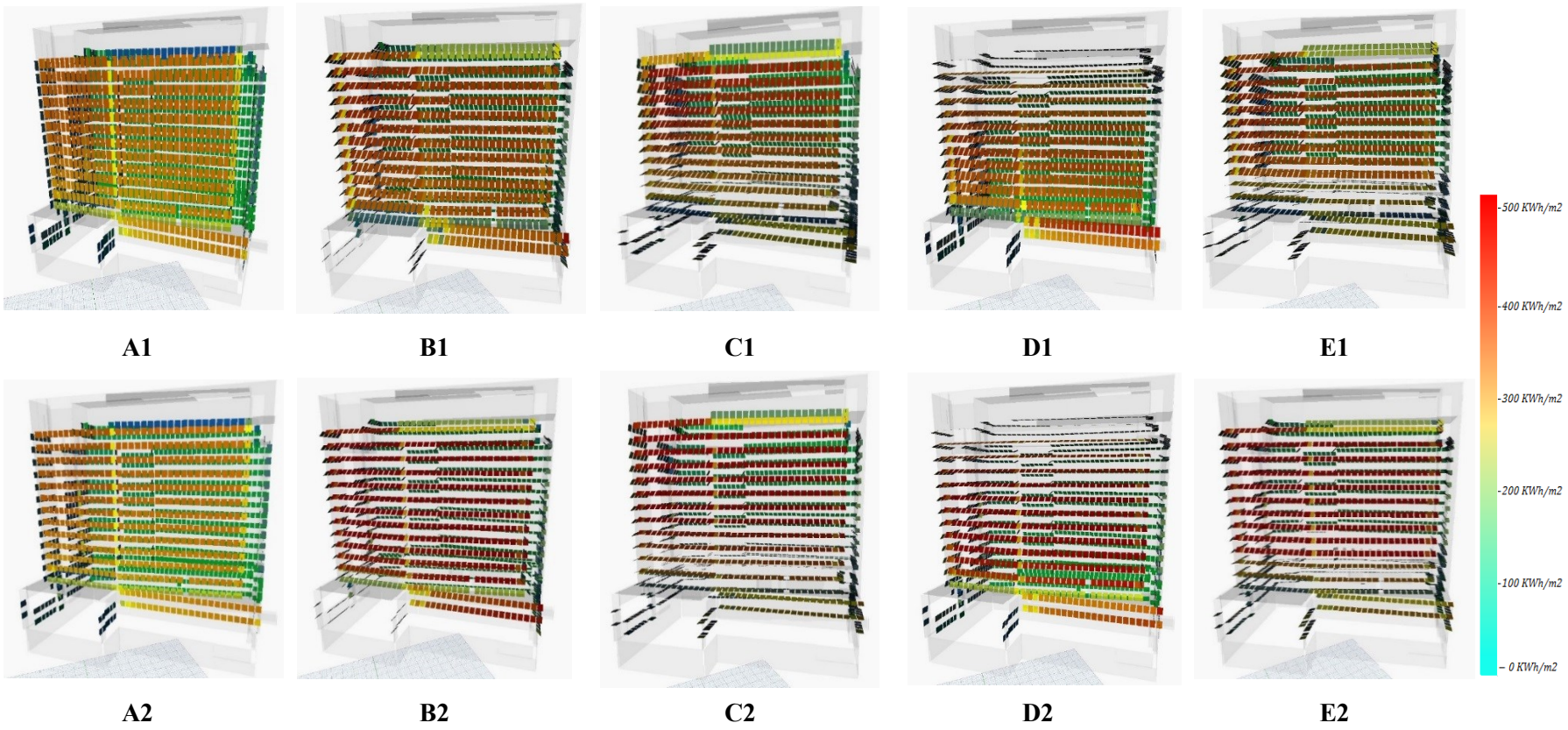

Figure 3-12 Visualized results for curtain wall PV layout scenarios (South facade)

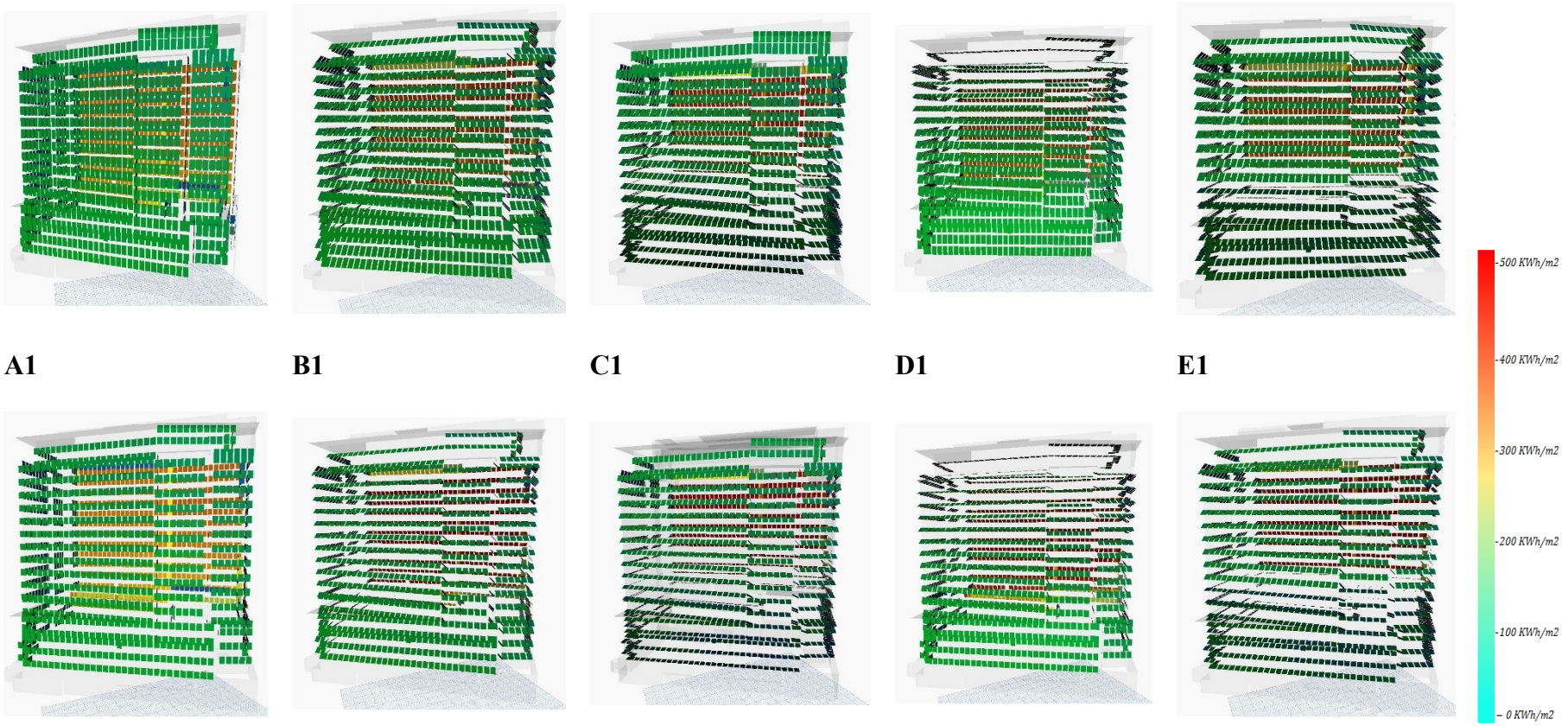

Figure 3-13 Visualized results for curtain wall PV layout scenarios (North facade)

Two examples of the visualized results of solar radiation simulation of the facades from Set1 are presented in Figure 3-14. Due to less shadow effect caused by the neighbouring buildings, the south facade of the building Figure 3-14(a) receives more radiation, compared to the north facade (Figure 3-14(b)).

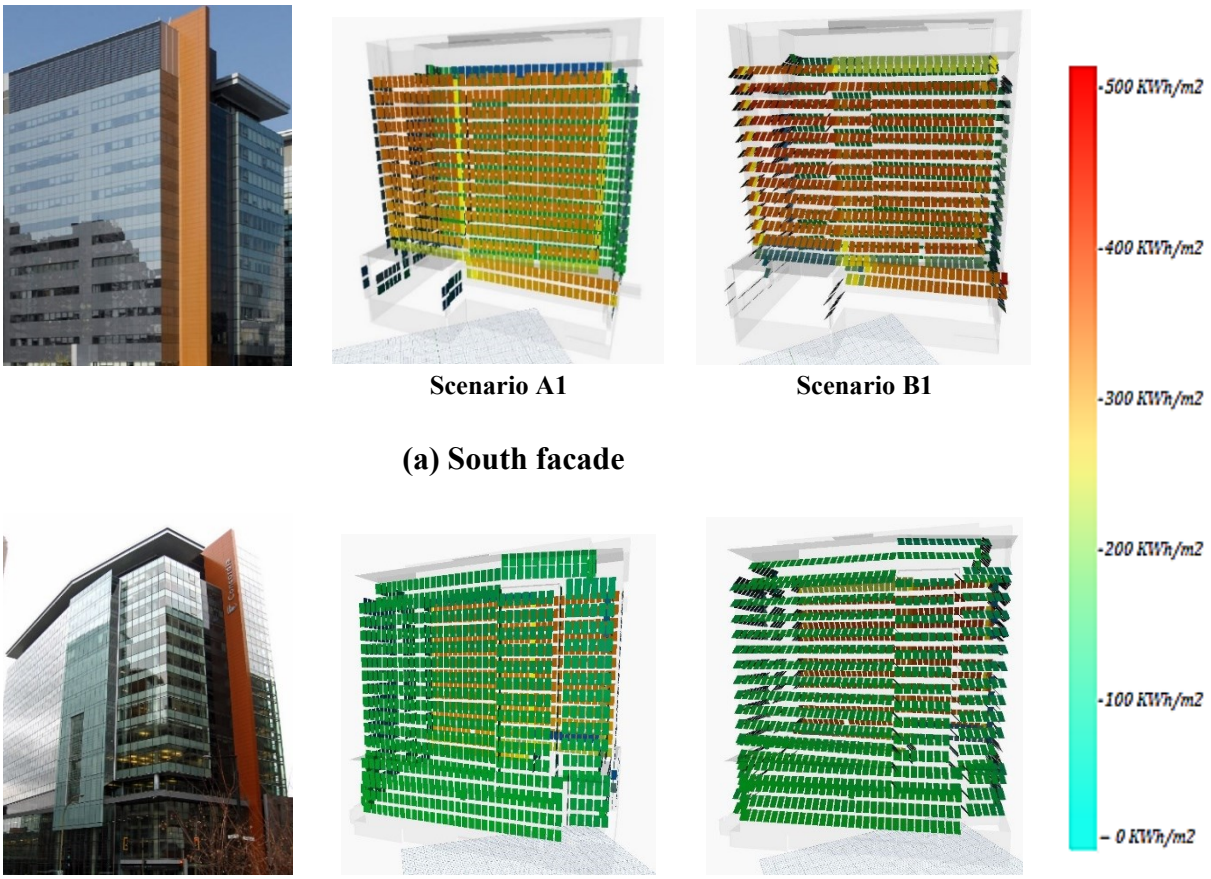

Scenario A1 Scenario B1

(a) South facade

Scenario A1 Scenario B1

(b) North facade

Figure 3-14 Two examples of visualized results for curtain wall PV layout scenarios

3.4.2 Rooftop PV Layout Sensitivity Analysis

To analyze the radiation on the rooftop, multiple scenarios are defined with different configurations of tilt and pan angles. Because of the higher flexibility of the rooftop space for the installation of PV modules, the size of the modules is assumed 3 *m* by 3 *m*. Then, the sensitivity

analysis is done based on changing the modules' tilt and pan angles Figure 3-15. The first group of analysis (A-E) is done by changing the pan angle of the modules while fixing the tilt angle at 45°. As shown in Table 3-3, the highest average radiation is received when the modules are facing south (i.e. pan angle = 270°).

Table 3-3 Comparing rooftop PV layout output based on pan angle

Scenario	**Tilt** *(Degree)*	**Pan** *(Degree)*	**PV Module Dimensions**		**Annual Cumulative Radiation** *(MWh)*	**Percentage** *(%)*	**Average Radiation** (*kWh/m2)*
			W *(m)*	**L** *(m)*			
A	0	0	3	3	319	100	295.00
B	45	0	3	3	162	50.7	149.78
C	45	90	3	3	158	49.5	146.64
D	45	180	3	3	364	114	336.88
E	**45**	**270**	**3**	**3**	**371**	**116**	**343.57**

In the next set of analysis, using Scenario E as the starting point, the orientation of all modules is set to south direction (i.e. pan angle = 270°) and different tilt angles (10°-50°) were analyzed for this orientation. As shown in Table 3-4, the modules with the tilt angle of 30° and 40° are receiving a higher amount of radiation.

Table 3-4 Comparing rooftop PV layout performance based on tilt angle

Scenario	**Tilt** *(Degree)*	**Pan** *(Degree)*	**PV Module Dimension**		**Annual Cumulative Radiation** *(MWh)*	**Percentage** *(%)*	**Average Radiation** (*kWh/m2)*
			W *(m)*	**L** *(m)*			
F	10	270	3	3	347	100	321.00
G	20	270	3	3	366	105.5	338.84
H	**30**	**270**	**3**	**3**	**374**	**107.8**	**346.00**
I	**40**	**270**	**3**	**3**	**374**	**107.8**	**346.00**
J	50	270	3	3	367	105.7	339.64

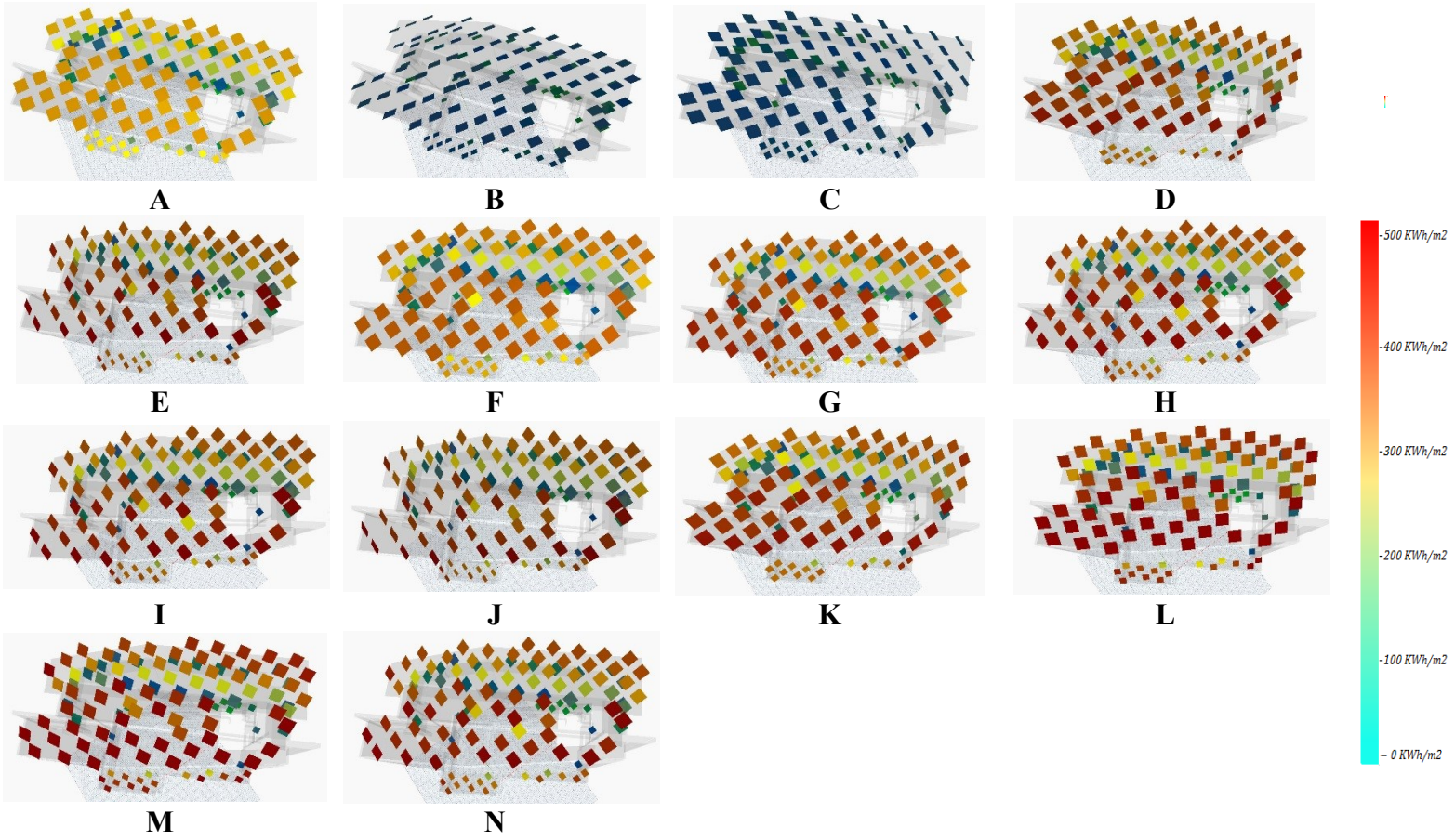

Figure 3-15 Rooftop PV layout sensitivity analysis

Based on the best average radiation of the two previous sets of scenarios for the rooftop PV layout, the promising range of tilt angles and orientations are selected for defining a new set. As shown in Table 3-5, a tilt angle of 35° is analyzed for a range of the pan angle (180-270) with 30° increment. The results of the simulation with these configurations revealed that the optimum performance is at 35° tilt angle and 240° pan angle. The best and worst scenarios (M and C, respectively) for the rooftop PV layout are visualized in Figure 3-16 to highlight the importance of the configurations in receiving a higher level of radiation.

Table 3-5 Rooftop PV layout output with a selection of tilt angle and pan angle

Scenario	**Tilt** *(Degree)*	**Pan** *(Degree)*	**PV Module Dimension**		**Annual Cumulative Radiation** *(MWh)*	**Percentage** *(%)*	**Average Radiation** (*kWh/m2)*
			W *(m)*	**L** *(m)*			
K	35	180	3	3	367	100	340.00
L	35	210	3	3	396	107.9	366.66
M	**35**	**240**	**3**	**3**	**399**	**108.7**	**369.00**
N	35	270	3	3	375	102	347.50

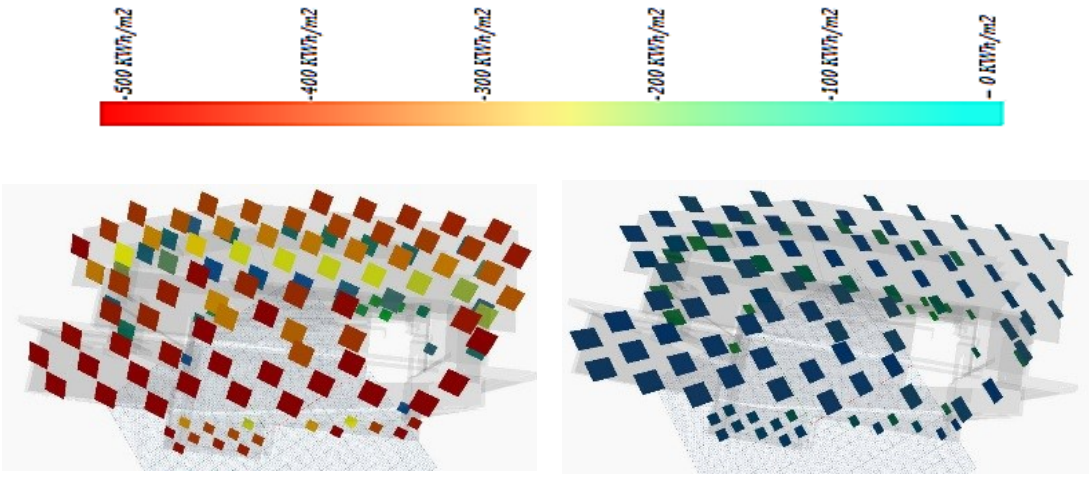

Scenario M **Scenario C**

Figure 3-16 Rooftop PV layout best scenario (M) versus worst Scenario (C)

Comparing the best results of the facade and rooftop analysis shows that facade PV modules receive a lower average radiation 212.77 kWh/m^2 than rooftop PV modules 369.00 kWh/m^2. However, the larger installation area on façades (5,811 m^2) resulted in a total radiation value of 1,236 *MWh*, compared to the 399 (*MWh*) for the rooftop area (1,080 m^2). This huge amount of energy that is potentially generated on the facade is largely ignored in the current practice. Since facade surfaces seem to have a great potential for the installation of solar modules, in the next step, a cost-benefit analysis is performed to investigate the economic viability of such an undertaking.

3.4.3 Cost-Benefit Analysis

Defining a number of thresholds for the radiation amount provides a distribution of the cumulative solar radiation received by PV modules. This analysis is done for Scenario B1 as an example. As shown in Figure 3-17, all 1,937 PV modules on the façades are able to receive at least 40 *kWh* of radiation. By increasing the radiation threshold, the number of PV modules that are able to capture that level of radiation decreases. For example, the number of modules is almost half when the threshold is raised to 150 *kWh*, and only 117 of PV modules (6% of the total) are able to receive at least 460 *kWh* of radiation.

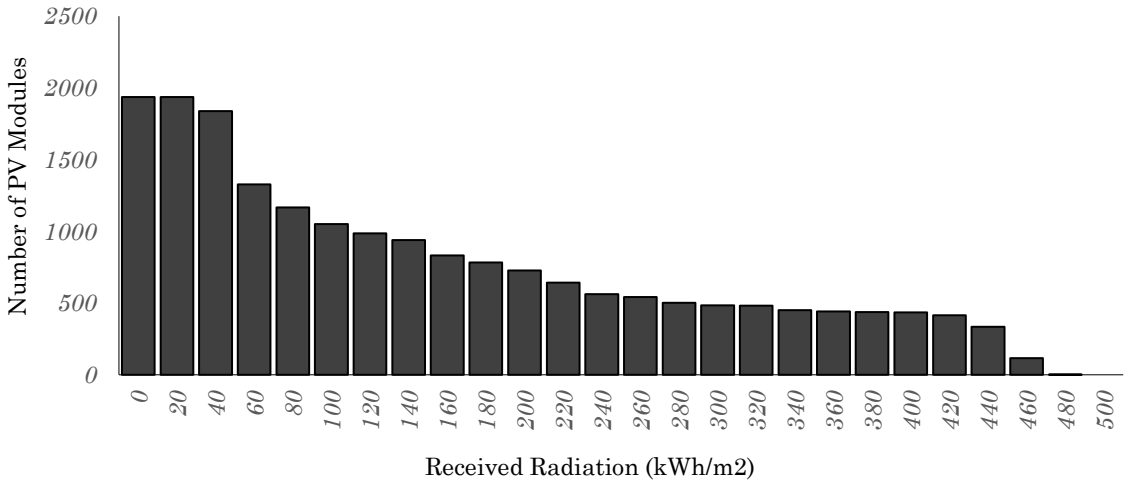

Figure 3-17 Number of PV modules based on the received radiation level

A cost-benefit analysis is performed on Scenario B1 for the curtain wall PV layout using Equations 2~4, considering the following assumptions: (1) the number of modules is 1,937, (2) the average size of the module is 4.5 m^2, (3) a weighted average efficiency of 11% is assumed as the overall efficiency of PV modules in the calculations, (4) two-third of the facade area is considered to be covered by the opaque PV modules with 16% efficiency and the one-third with the semi-transparent modules by 2% efficiency (Aarre Maehlum, 2014), (5) the value of 1 kWh of energy is assumed \$0.5, (6) the discount rate is 5% and the inflation rate is considered 2.15%, and (7) the initial cost is $\$140$, and annual maintenance cost (M) is considered 10% of the module cost (Energysage, Size and weight of solar panels, 2018). All the assumptions are based on conservative estimations. Furthermore, it is assumed that this building consumes all the energy it generates during its operational hours throughout the day.

Figure 3-18 illustrates the radiation threshold for (1) the average annual net profit and (2) the breakeven points at different payback periods for Scenario B1. Also, this figure demonstrates the maximum average annual net profit. This figure indicates that, for instance, the investor will have the maximum average annual net profit for the payback period of two years when the modules that are receiving a radiation level of 360 KWh/m^2 or higher are considered. At this threshold, 441 modules can be installed, which would yield an average annual net profit of \$9,358. Considering the same payback period of two years, the investors cannot consider the installation of PV modules on locations with the radiation of less than 190 KWh/m^2 to break even at the end of this period. In another example, if investors are looking at the payback period of 15 years, they are best to consider the installation of PV modules on locations with the minimum of 100 KWh/m^2 radiation, in which case they will get the maximum average annual net profit of \$40.626. However, for this payback period, investors can install PV modules on all possible locations on the curtain walls and still remain profitable.

Figure 3-19 plots the average annual ROI against the initial investment for different payback period. This plot can be used by the investor to identify the proper investment strategy based on budgetary constraints. For instance, if the available budget for PV module installation at year zero is \$100K, the investor can expect ROI of 18%, 30%, 36%, 37%, 36%, and 34% at payback periods

of 3, 5, 10, 15, 20, and 25 years, respectively. Additionally, the plot indicates that for this capital investment, the location with the radiation threshold of approximately 200 KWh/m2 can be considered.

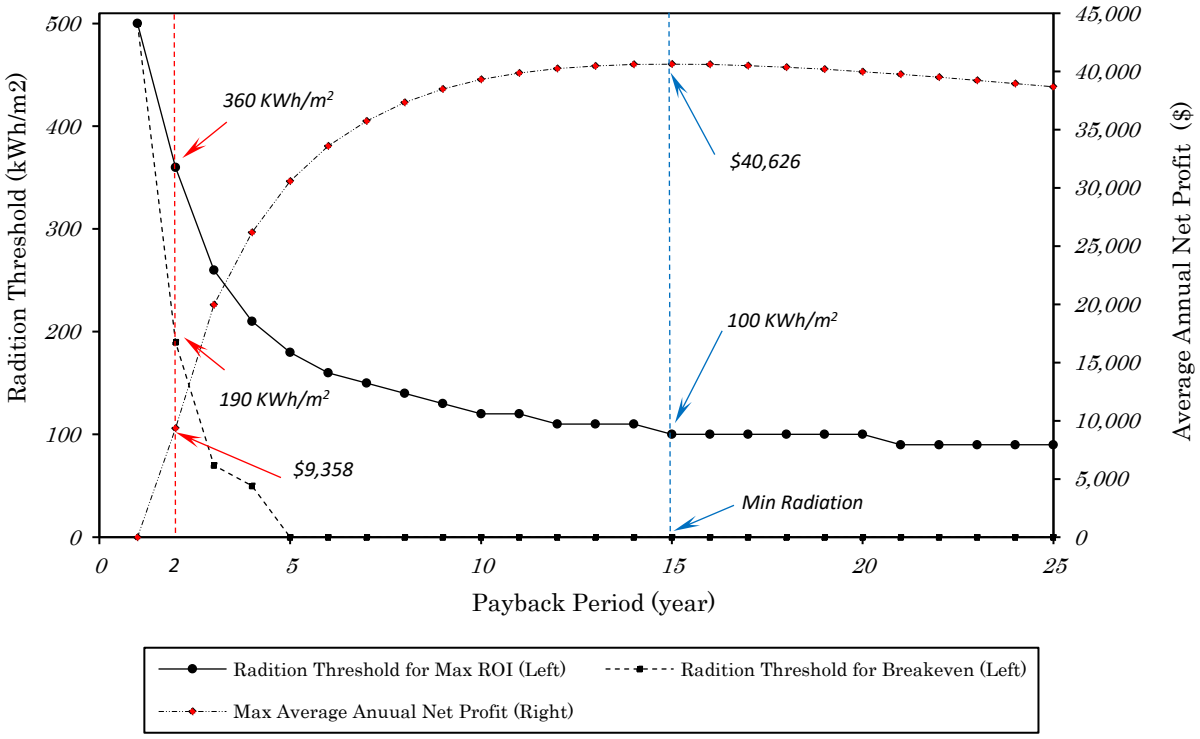

Figure 3-18 Radiation threshold for the maximum net profit at different payback periods (kWh)

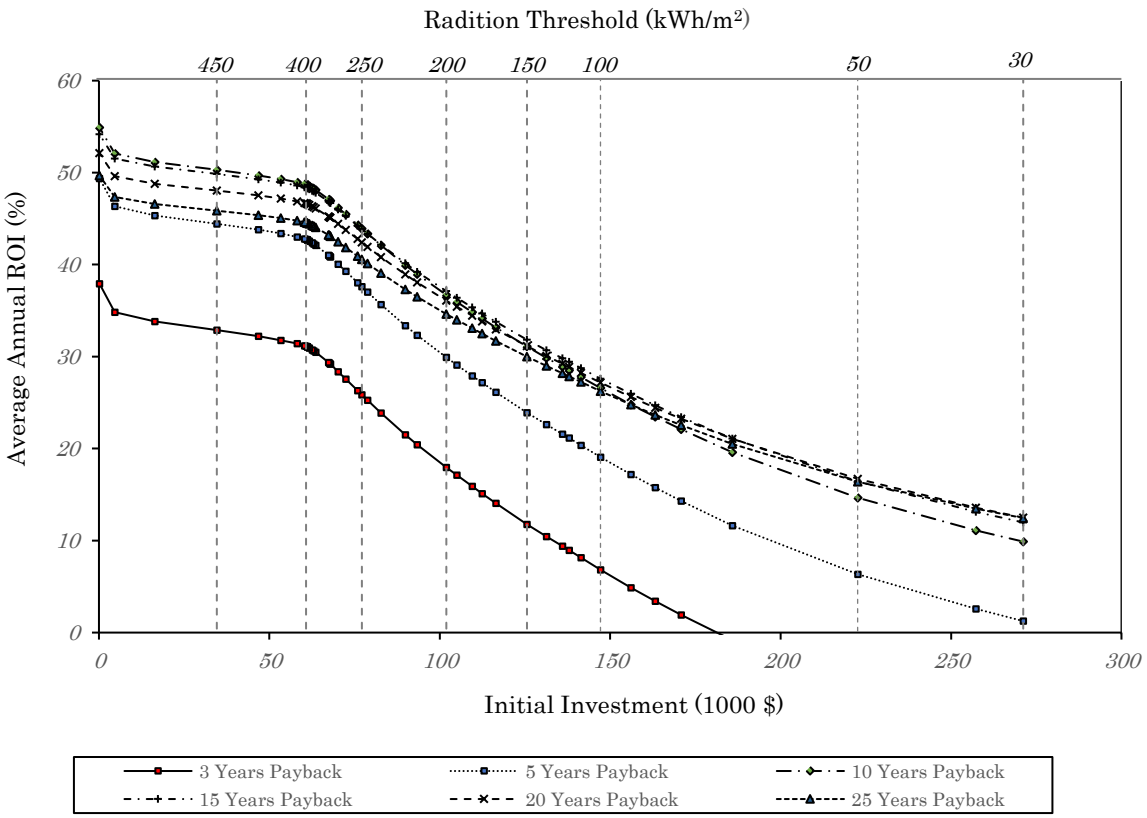

Figure 3-19 Relative return on investment for different payback period at different radiation threshold

Depending on the strategic decision the investor makes based on Figure 3-18 and Figure 3-19, a more detailed analysis of cash flow can be conducted to determine the cash flow of investment during the payback period. Figure 3-20 shows different examples of cash flow analysis for different payback periods and different radiation thresholds, which can be determined based on Figure 3-18 and Figure 3-19. For instance, if the investor decides to consider a 5-year payback period and also radiation threshold of 50 kWh/m^2, i.e., installing 1,590 panels according to Figure 3-17, the breakeven point would occur somewhere around the 4th year. So, the investment will become profitable only in the last year of the investment. Alternatively, if the investor considers the radiation threshold of 400 kWh/m^2, i.e., installing 434 panels according to Figure 3-17, for the same payback period, the investment will become profitable much earlier, i.e., before year 2. Also, the average annual ROI will be considerably higher at the threshold of 400 kWh/m^2 (i.e., 42.7%) compared to 50 kWh/m^2 (6.3%).

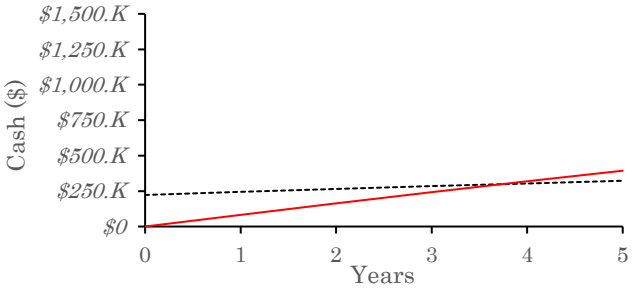

(a) 5 Years Payback Period with Radiation Threshold of 50 KWh/m²

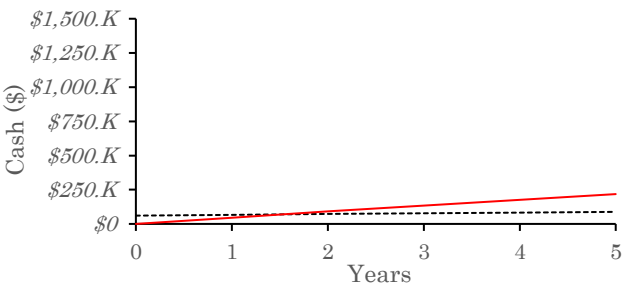

(b) 5 Years Payback Period with Radiation Threshold of 400 KWh/m²

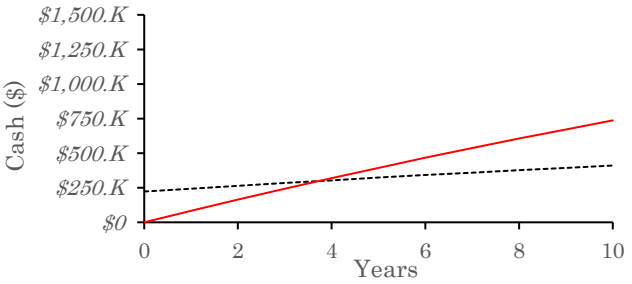

(c) 10 Years Payback Period with Radiation Threshold of 50 KWh/m2

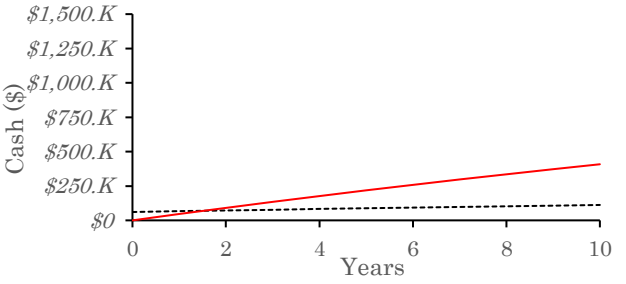

(d) 10 Years Payback Period with Radiation Threshold of 400 KWh/m2

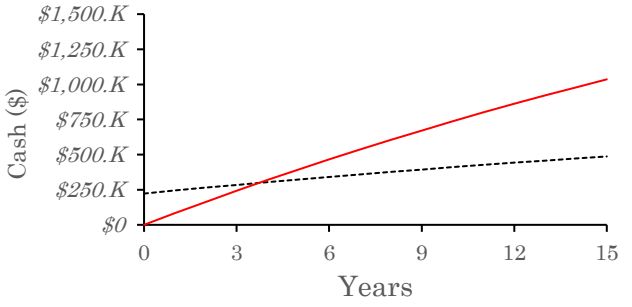

(e) 15 Years Payback Period with Radiation Threshold of 50 KWh/m2

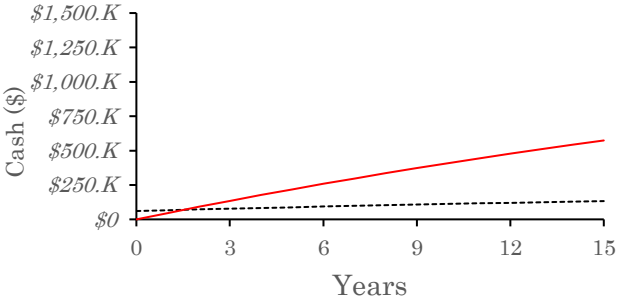

(f) 15 Years Payback Period with Radiation Threshold of 400 KWh/m2

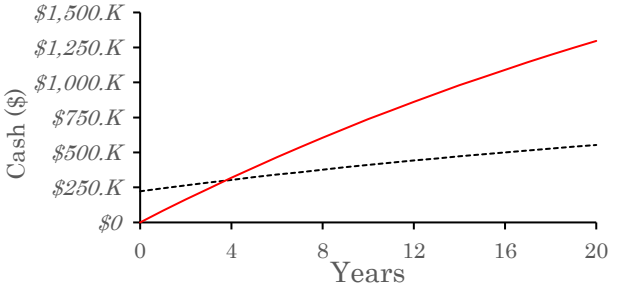

(g) 20 Years Payback Period with Radiation Threshold of 50 KWh/m2

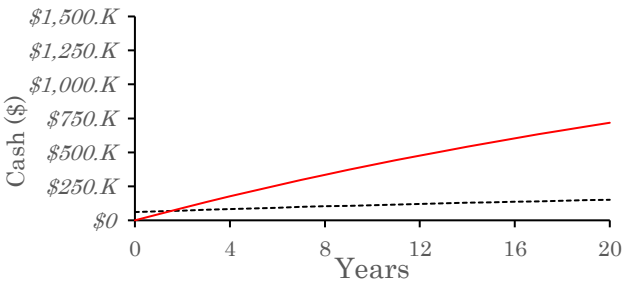

(h) 20 Years Payback Period with Radiation Threshold of 400 KWh/m2

Figure 3-20 Cash flow analysis for different investment plans

3.5 SUMMARY

In this chapter, a BIM-based parametric modeling platform for the design of surface-specific PV module layout on the entire skin of buildings was developed. A prototype was developed using Dynamo visual programming platform to demonstrate the feasibility of the proposed method from geometrical perspective, and a case study was presented for a building in Montreal, Canada. Multiple scenarios were considered for investigating the importance of each factor on the amount of generated energy.

Moreover, in order to examine various investment plans, a cost-benefit analysis was performed for the best scenario as an example. The results of the analysis revealed that, when all the PV modules were parallel to the façades, the energy output was at the lowest level. Furthermore, comparing the results of scenarios with different configurations indicated that the area of the PV modules had a considerable impact on the amount of received cumulative radiation. However, comparing the received radiation per m^2 of modules showed that the larger size of modules caused greater shadow impact on the other modules and reduced the amount of received radiation. The results of the cost-benefit analysis for the case study demonstrated that, despite numerous challenges and limitations, widespread PV modules adoption on the buildings' vertical surfaces was promising.

It is indicated that the developed surface-specific parametric model has a great potential for the analysis of complex PV module layout design on the entire skin of buildings. The platform enables the designers and investors to rapidly generate a wide spectrum of scenarios, perform sensitivity analysis on more promising alternatives, and develop a viable investment plan based on the desired payback period and available budget.

CHAPTER 4 OPTIMIZATION OF PV MODULES LAYOUT ON HIGH-RISE BUILDING SKINS [2]

4.1 INTRODUCTION

As explained in Chapter 3, a BIM-based surface-specific parametric model is developed for the detailed solar simulation on the building using its surface properties. Different factors, such as the location of PV modules on the building surfaces, size, and tilt, and pan angles were considered in the simulation of the solar radiation. However, given the sheer size of the design space for this problem, the parametric model alone is not sufficient because all possible design alternatives cannot be fully explored to find the global near optimum. Therefore, it is imperative to integrate an optimization approach with the BIM-based parametric model and establish a full generative design platform.

This chapter aims to develop a BIM-based generative design framework for the design of PV modules layout on high-rise building skins. In this framework, the surface-specific parametric model of PV modules is integrated with an optimization method to find the optimum design of PV modules layout considering study period, profit margin, harvested PV energy, and cost. This framework will enable designers and investors to apply the generative design paradigm to the use of PV modules on building skin. A case study is developed to investigate the feasibility of the proposed method.

The remainder of this chapter is structured as follows, in accordance with the research methodology explained in Section 1.4. First, the proposed framework is explained. Then, the

[2] This chapter is based on the following paper:
Salimzadeh, N., Vahdatikhaki, F., and Hammad, A. (2021). Optimization of PV Modules Layout on High-rise Building Skins Using a BIM-based Generative Design Approach.
Cleaner Production (Under Review).

validation of the proposed method through implementation and case study is presented. In the end, the summary and conclusions are presented.

4.2 PROPOSED FRAMEWORK

Figure 4-1 presents the overview of the proposed generative design framework. In this framework, a simulation-based generative design approach is used to find the optimum configurations of PV module layout on the building surfaces considering the revenue of the generated energy and the total life cycle cost. As shown in Figure 4-1, the proposed framework consists of two main components, namely GA optimization module, and parametric simulation model. In a nutshell, the optimization module generates the initial population of size *N*. Each member of the population, which represents a specific solution *S*, is then fed into the simulation model as the input. The parametric simulation model is then used as a means to assess the objective functions (i.e., revenue and cost). Subsequently, the evolution mechanism of NSGA-II (i.e., the selection, crossover, and mutation) is applied to the results coming from the parametric model. This process is iterated by *G* generations to identify the optimum solutions, which is represented as a Pareto front.

4.2.1 Parametric Model

The structure of the proposed parametric model and the implementation steps are explained in detail in Section 3.2.2. The parametric simulation model estimates the annual cumulative radiation potential of each panel ($R_{i,k,\theta,\beta}$). This value can then be translated to the required objective values, as will be explained in the next section.

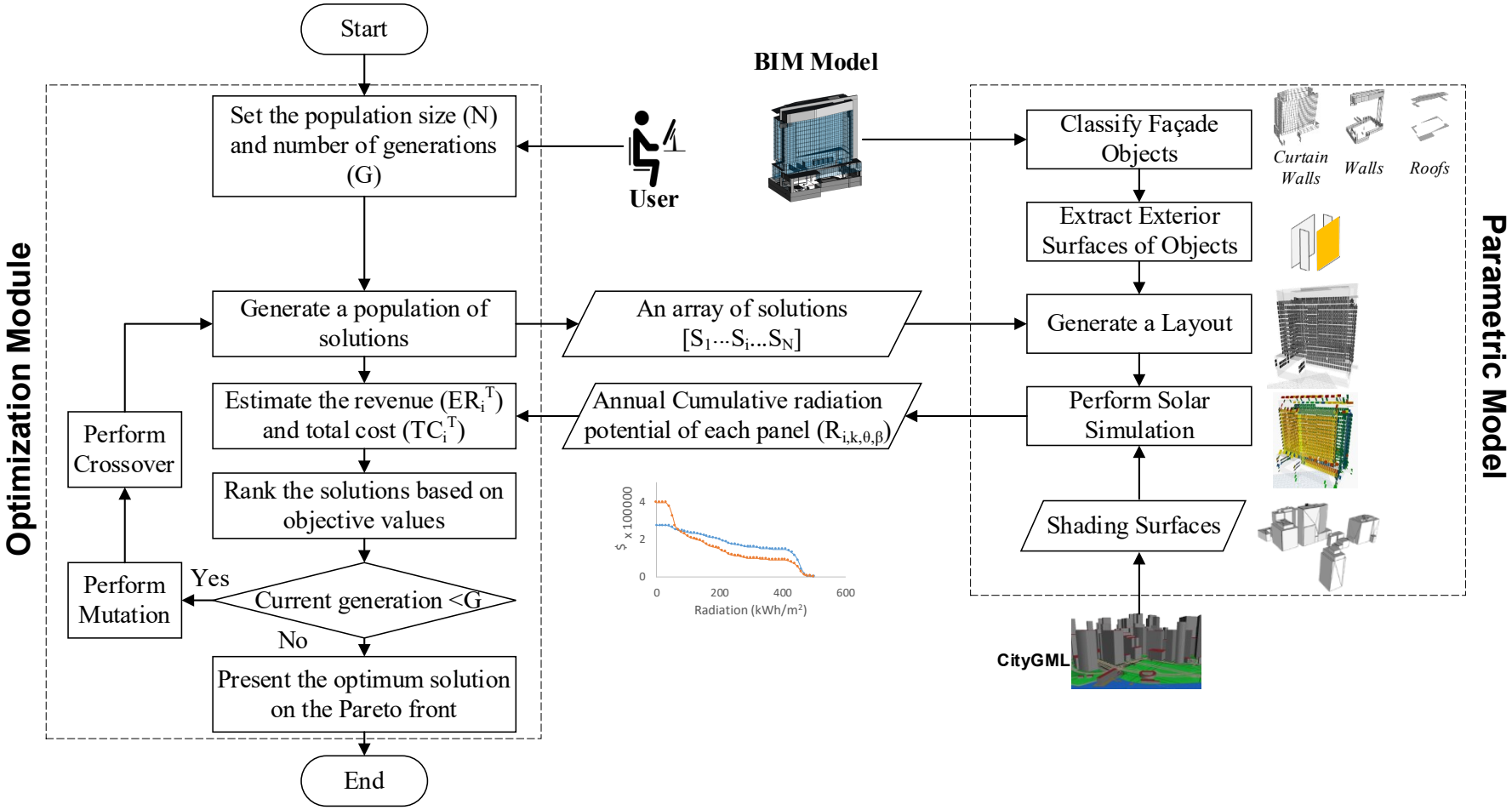

Figure 4-1 Overview of the Proposed Method

4.2.2 Optimization Module

The proposed framework uses Non-Dominated Sorting Genetic Algorithm (NSGA-II) to solve the optimization problem. NSGA-II, which has the ability to effectively solve multi-objective optimization problems, is known as a mature multi-objective optimization algorithm (Wang, 2016). The algorithm aims to find the optimum location, and tilt and pan angles for the PV modules on the building surfaces given predefined sizes and other attributes of panels. The objective of this optimization is to maximize the revenue (i.e., the monetary value of the generated energy) while minimizing the total life cycle cost (i.e., installation and maintenance).

In the first step of the optimization, the user needs to determine the population size *(N)* and maximum number of generations *(G)*. In each generation of the solution, NSGA-II generates *N* number of potential solutions using the chromosome structure shown in Figure 4-2. This structure essentially generates a representation of a solution known to the parametric model (i.e., Equation 3.1).

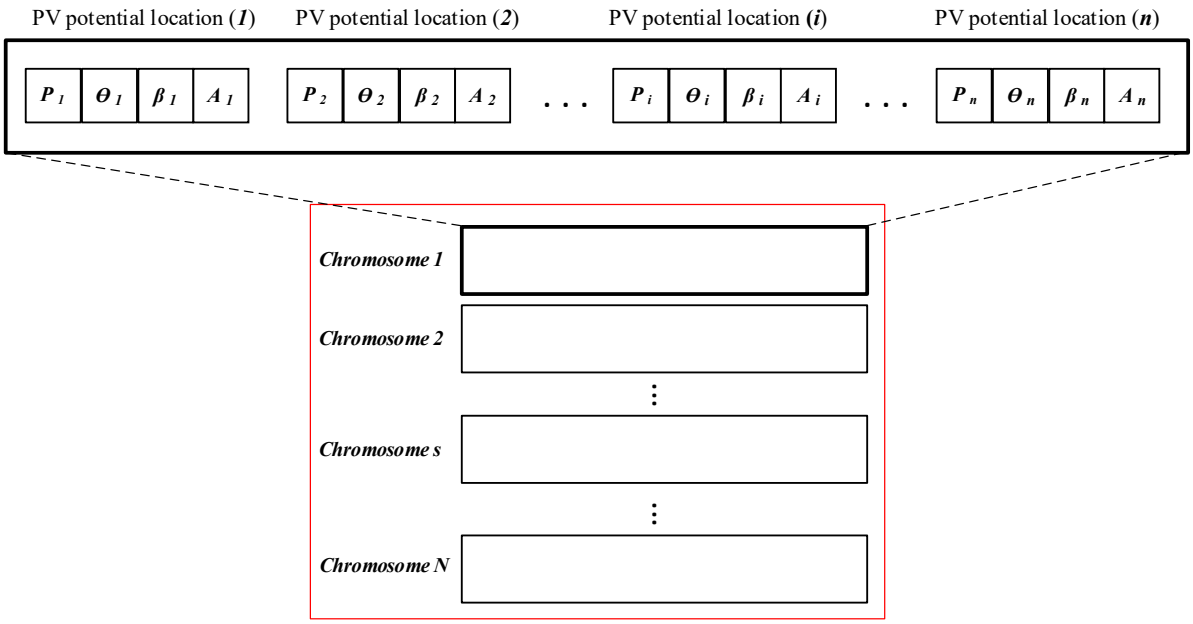

Figure 4-2 Example of GA chromosomes representing the PV potential locations and angles

Each chromosome is then sent to the parametric model where the solar simulation is applied and the annual cumulative solar radiation ($R_{i,k,\theta,\beta}$) of each solution in the generation (i.e., each chromosome) is assessed and returned to the optimization module. Using this value, then, the optimization module estimates the value of the two objective functions.

The first objective function aims to maximize the present value of the generated energy revenue by PV modules during their life cycle of T years for the solution i (ER_{i}^{T}) and is estimated as shown in Equation 4.1. D_T can be calculated using the Equation 3.3.

$$Maximize\ ER_{\mathrm{i}}^{T} = \mathrm{V} \times D_T \sum_{k=1}^{K} P_{i,k} \times R_{ik\theta\beta} \times e_{i,k} \times PR \qquad \text{Eq. 4.1}$$

The second objective function, which is estimated by Equation 4.2, aims to minimize the total life cycle cost of PV modules after T years for the solution i (TC_{i}^{T}). The total life cycle cost of PV modules includes the initial cost (i.e., acquisition and installation) and the maintenance cost. Since the maintenance cost should be considered for the whole life cycle of the PV system, the D_T factor must be considered.

$$Minimize\ TC_i^T = CM \sum_{k=1}^{K} a_{i,k}(1 + \alpha \times D_T) \qquad \text{Eq. 4.2}$$

Once the values of the objective functions are estimated, the evolution mechanism of NSGA-II first filters the top-ranking solutions in the generation and then performs mutation and crossover on them to generate the next generation of the solutions. This process is iterated until the solutions reach a predefined level of convergence or the specified number of generations is reached. In the end, the optimum solutions are presented on a Pareto front. This can be used by the user to identify the non-dominant solutions that can be considered for the design of PV modules. Depending on the available budget, the user can determine the preferred solution.

In case the budgetary constraint is not a dominant factor the optimization problem can be solved as a single objective problem by maximizing the profit of the project, which can be calculated as

the difference between the revenue (ER_i^T) and total cost (TC_i^T) of each solution. In this case, the final outcome of the optimization is a single solution that generates the maximum profit over T years.

4.3 IMPLEMENTATION AND CASE STUDY

4.3.1 Implementation

As shown in Figure 4-3, Revit (Autodesk, Revit, 2021) is used as the BIM authoring platform to model the target building. The neighboring buildings were imported into Revit as a CityGML model. To parametrize the generation of specific PV modules on this building, Dynamo (Dynamo, 2021) is used. Dynamo is a visual programming platform that allows the development of customized scripts and nodes for computational and parametric models. Dynamo runs within Revit and works as an Application Programming Interface (API). Some packages such as Solar Analysis (Solar Analysis, 2021) and LunchBox (LunchBox, 2021) are used in the development process.

The Project Refinery (Autodesk, Project Refinery, 2021) is used as the optimization module in Figure 4-1. The seamless integration of Dynamo and Refinery allows us to get the benefits of automating the design option creation process in Refinery, running the custom nodes in Dynamo, and optimizing the solutions in Refinery.

In line with the framework shown in Figure 4-1, Refinery generates a generation of solutions. These solutions are fed into Dynamo to run the surface-specific solar radiation simulation based on the provided design variables and configurations. Then, the objective functions and the fitness values are calculated within Refinery. The selection, crossover, and mutation are applied to the top-ranking solutions in each generation. This process is repeated until the maximum number of generations is reached.

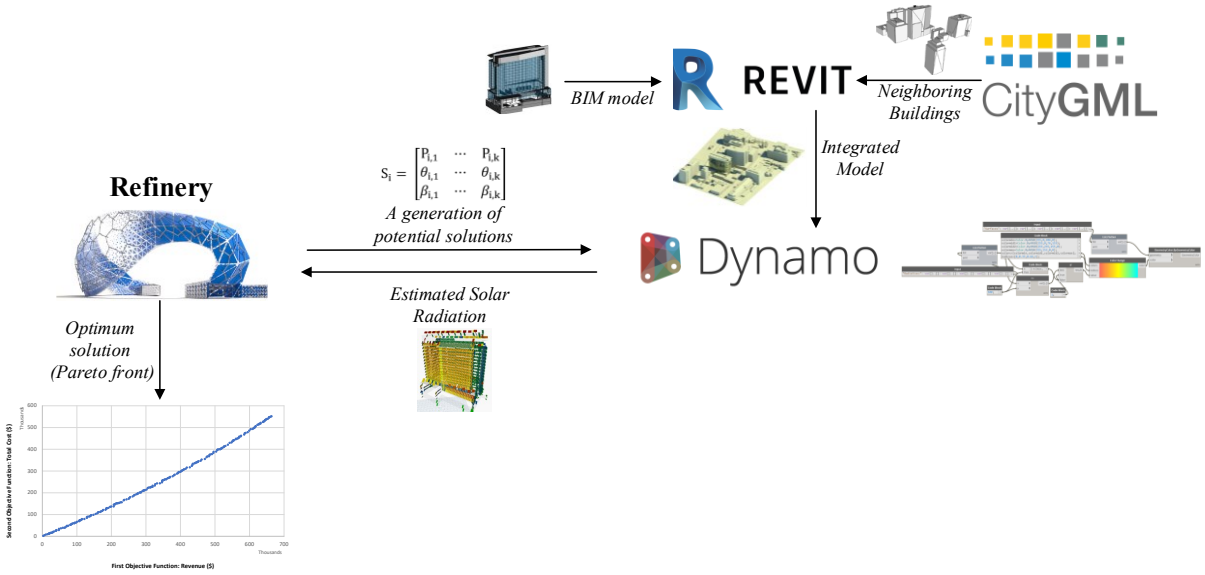

Figure 4-3 Overview of the implementation

4.3.2 Case Study

The same building of JMSB of Concordia University is selected as the case study (Figure 4-4). As explained in Section 3.3, the BIM model of the JMSB building is created using Revit software. To consider the shadow effect of the surrounding buildings in the solar simulation, the city blocks around the JMSB building are extracted from the CityGML model (City of Montreal, 2021). Then these two models are integrated within Revit. Due to the lower probability of receiving solar radiation because of the neighboring buildings' shadow effect, the North-East facade of the building is excluded from the model. The South-West, North-West, and South-East facades and the rooftop surfaces are selected for the optimization process as shown in Figure 4-4.

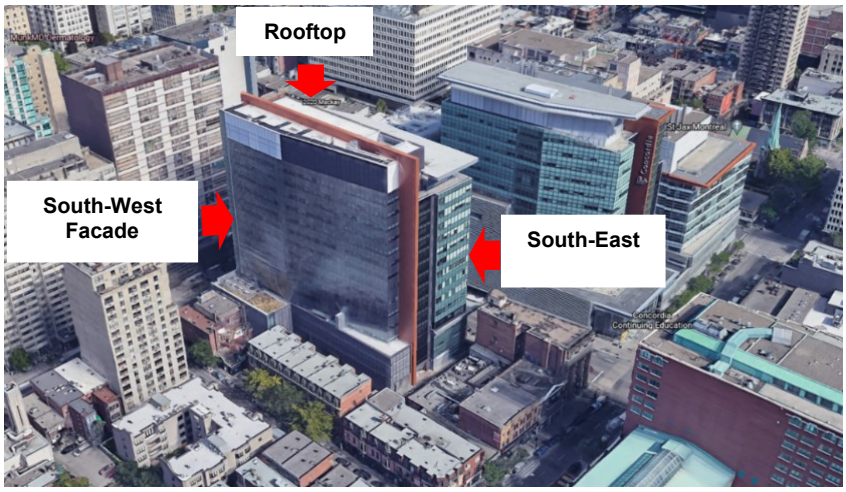

Figure 4-4 John Molson School of Business, Concordia University (Google Earth, 2021)

To calculate the energy generation of the PV system, a performance ratio of PR = 75% is considered to account for losses induced by inverters, temperature, DC and AC cables, weak radiation, dust, snow, etc. (Simulation and design of solar systems, 2021). The average efficiency of 18% is considered (Svarc, 2021). To calculate the present value of a growing annuity of the generated energy, the discount rate and the inflation rate are assumed as r = 5% and g = 2.15%, respectively. To calculate the energy revenue, the average unit cost of electricity is considered V = $0.179 per kWh (Electric Choice, 2021). The average cost of a PV module is assumed as $100/m^2 (Solar Power Farm, 2021). The study period was considered 25 years (i.e. expected service life of the PV system). The maintenance cost is assumed as α = 0.5% of the initial cost. It should be noted that for simplicity, it is assumed that the same type and size of PV module are used for all surfaces. Therefore, the same coefficients are applied to all cases. For more complex scenarios, this assumption can be easily adjusted in Dynamo.

4.3.2.1 Rooftop optimization scenarios

The grid size of the rooftop is generated for PV modules of 3 m × 3 m. This module size resulted in 120 potential points for the installation of panels. Three design scenarios are considered for rooftop PV layout optimization, namely scenarios where PV modules have (1) Non-uniform

orientation (i.e., each panel can have distinctive pan and tilt angles), (2) Uniform orientation (i.e., all panels have the same pan and tilt angles), and (3) Batched uniform orientation (i.e., a group of nearby panels all need to have same pan and tilt angles). In the batch uniform orientation scenario, all the panels with pair-wise Euclidean distances between their center points of less than a predefined threshold are bundled together as a batch. In this study, the threshold was set at 10 m, resulting in 7 distinctive groups of panels. The optimization configurations (N= 60 and G=60) and the PV module size are fixed for all scenarios and are determined through several trials and errors. It was observed that the larger population size and number of generations would not result in significant improvement of the optimization performance. The optimization of the scenarios is done considering all three input parameters as variables including $P_{i,k}$ (placement of PV modules), $\theta_{i,k}$ (tilt angle within the range of 0-90°), and $\beta_{i,k}$ (pan angle within the range of 0-360°).

Figure 4-5(a) shows the Pareto fronts of near-optimum solutions for all three scenarios. As shown in this figure, the overlap between the Pareto fronts is significant. This suggests that all scenarios converged to rather similar solutions. There is a slight convex pattern between cost and revenue, suggesting that as the number of panels increases, the rate of revenue growth declines. This is logical because, at the lower number of panels, the panels are placed at locations where there is maximum radiation potential. By increasing the number of panels installed on the rooftop, panels have to be installed at the location with less radiation potential, resulting in the overall decline in revenue growth. To put this into perspective, Figure 4-5(b) shows the overall cost vs. profit of solutions of all three Pareto fronts. As shown in this figure, although the maximum profit is generated in cases where almost all panels are installed, Return on Investment (ROI) has a generally declining trend. Table 4-1 provides a more detailed account of solutions with maximum profit in each of the scenarios and Figure 4-6 provides an overview of how these scenarios look like. When these scenarios are compared with the baseline case (i.e., PV panels are placed on all possible locations with 0° pan and tilt angles), it is observed that all optimization scenarios offered much higher energy revenue while reducing the overall cost of the project. This indicates the contribution of the generative design approach.

To investigate this further, the hypervolume values and indicators of the three Pareto fronts were calculated and compared using Equation 4.3, as suggested by (Salimi et al., 2018). In the multi-objective optimization problems with two objective functions, the hypervolume indicator can be calculated as the percentage of the area bounded by the Pareto front's points divided by the area created by the selected reference point with respect to the origin.

$$HI_{Par_l} = \frac{HV_{Par_l}}{(Objective\ Function\ 1)_{Max} \times (Objective\ Function\ 2)_{Max}} \times 100\% \qquad \text{Eq. 4.3}$$

where:

HI_{Par_l}: *the hypervolume indicator of Pareto front l*

HV_{Par_l}: *the hypervolume Value of Pareto front l*

As shown in Table 4-2, the hypervolume indicators of all Pareto fronts are very close. This indicates that constraining the solutions to uniformed angles and batching did not contribute to finding better solutions although the search spaces were reduced significantly. This can be an indication of the consistency and proper performance of the optimization module for even non-uniform orientation, where the search space is very large.

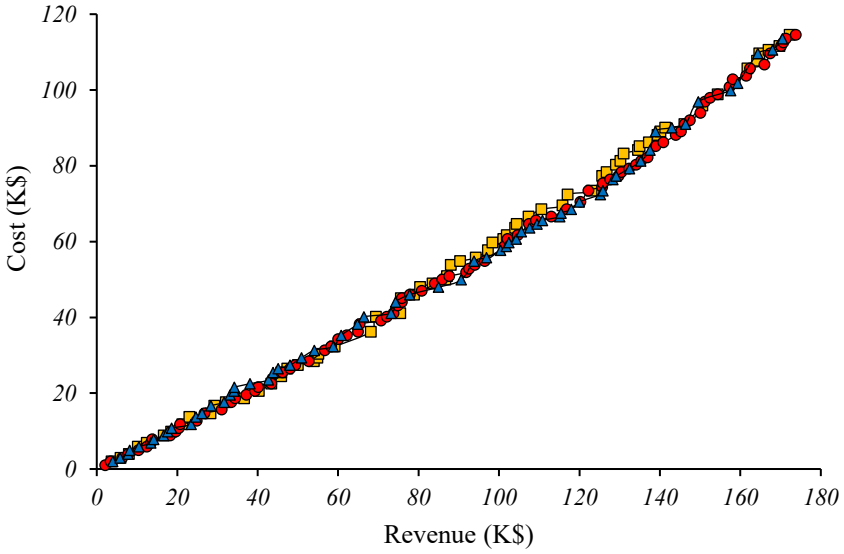

(a)

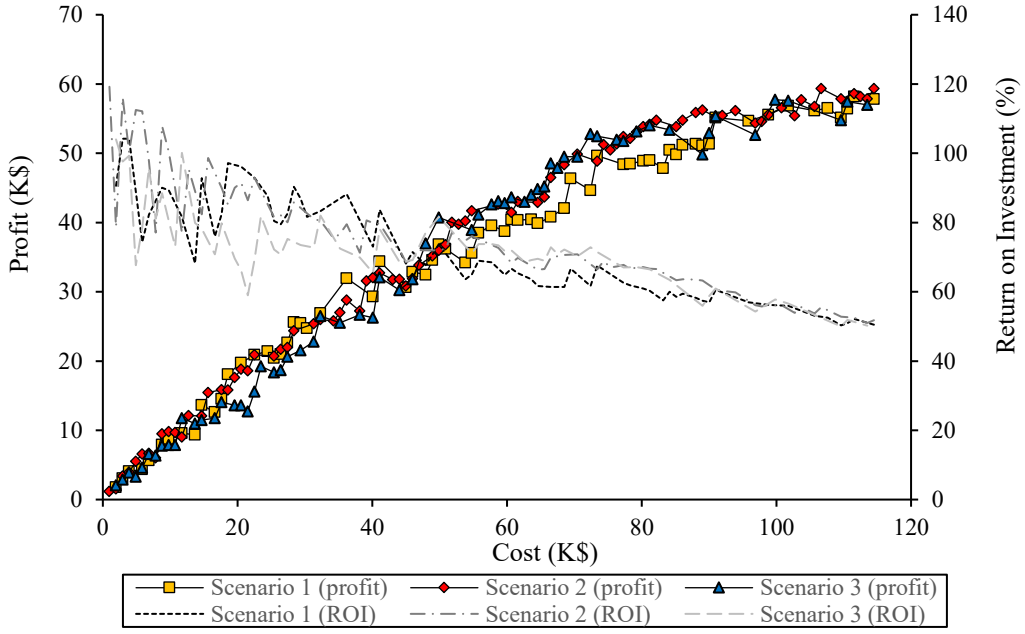

(b)

Figure 4-5 (a) Pareto Fronts, (b) Cost vs. Profit and ROI of solutions of the three different scenarios

Table 4-1 Maximum-profit solutions of the three scenarios for the rooftop design

Rooftop PV design scenarios	Tilt [Mean, std] *(Degree)*	Pan [Mean, std] *(Degree)*	# of panels	Annual Cumulative Radiation *(MWh)*	Average Radiation *(MWh/m²)*	Energy Revenue *(K$)*	Total Cost *(K$)*	Return on Investment *(%)*	Revenue improvement (compared to baseline) *(%)*	Cost improvement (compared to baseline) *(%)*
Baseline scenario	[0 , 0]	[0 , 0]	120	321.88	0.29	135.73	117.42	15.59	N/A	N/A
(1) Non-uniform orientation	[45 , 15]	[230 , 18]	114	402.56	0.39	169.75	111.55	52.2	25.06	5
(2) Uniform orientation	[45 , 0]	[230 , 0]	117	412.21	0.39	173.82	114.49	51.8	28.06	2.49
(3) Batched uniform orientation	[50 , 16]	[240 , 35]	102	373.61	0.40	157.55	99.81	57.8	16.08	15

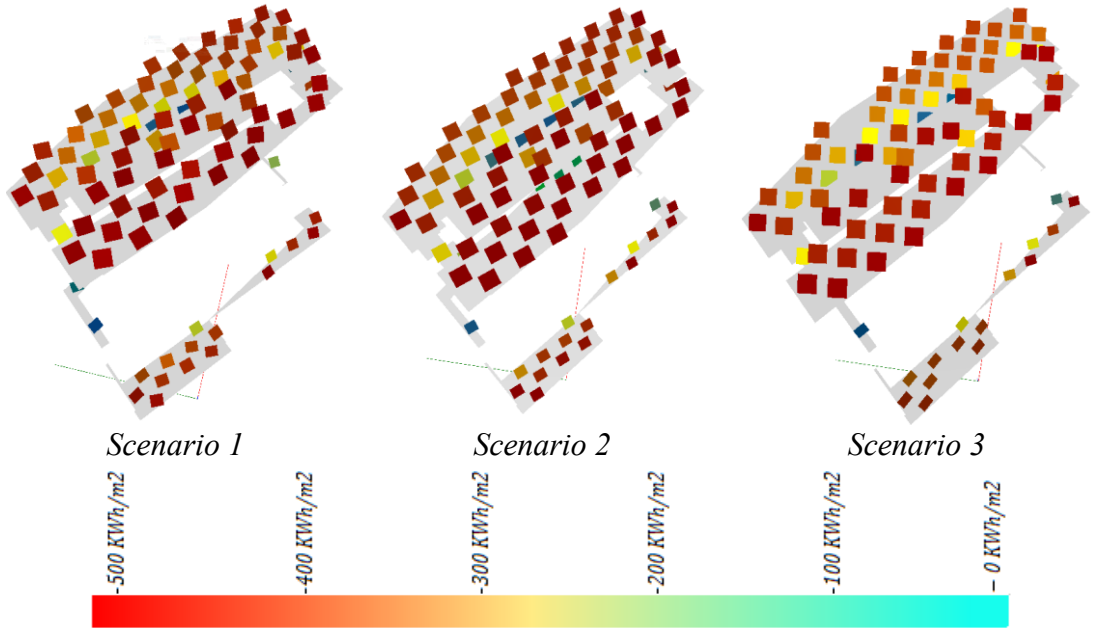

Figure 4-6 Rooftop PV design scenarios

Table 4-2 Comparison of hypervolumes of the rooftop three Pareto fronts

Scenario	Hypervolume Value ($\$^2$)	Hypervolume indicator
Non-uniform orientation	1.029717×10^{10}	0.5377
Uniform orientation	1.048819×10^{10}	0.5476
Batched uniform orientation	1.034960×10^{10}	0.5404

To further investigate the configuration of panels in all pareto solutions of each scenario, the details of panel orientation were analyzed. Figure 4-7 and Figure 4-8 show the distributions of average tilt and pan angles in terms of the relative frequency of different angle ranges and their standard deviations. In addition to the distributions of the solutions of the three scenarios, the distributions of the pool of all solutions combined is also shown. As shown in Figure 4-7(a), 92.6% of all the solutions (i.e., three Pareto fronts combined) have average tilt angles in the range of 35° to 50°. This is consistent with the theoretical optimum tilt angle for the Montreal region, which is 37° (Jacobson & Jadhav, 2018). Figure 4-7(b) suggests that in 89.4% of solutions the standard deviation of the tilt angle is between 5° to 20°. This represents a rather good uniformity of angles in scenarios where angle uniformity is not fully constrained. This can very well be construed as an indication that in general uniform patterns of tilt angles are preferred. This uniformity is more palpable in the first scenario, with 74.6% of solutions only having a standard deviation of 10° to 15°. This is mainly because in the third scenario, the batches are relatively further apart (compared to the first scenario) and this higher level of distinction results in higher variability in the tilt angle of panels. Another observation is that Scenario 2 has a considerably higher concentration of angles around 40° to 45°. This is because in this scenario all the panels have uniform angles and therefore the percentage of average angle becomes more concentrated. In all scenarios, the percentage of average angles of less than 35° and larger than 50° is very small.

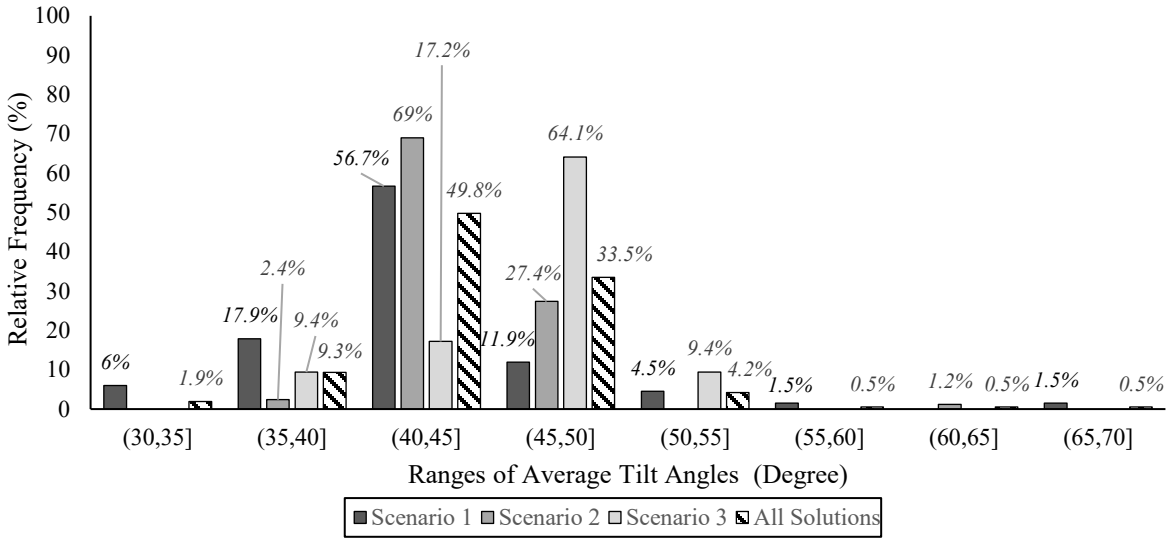

(a)

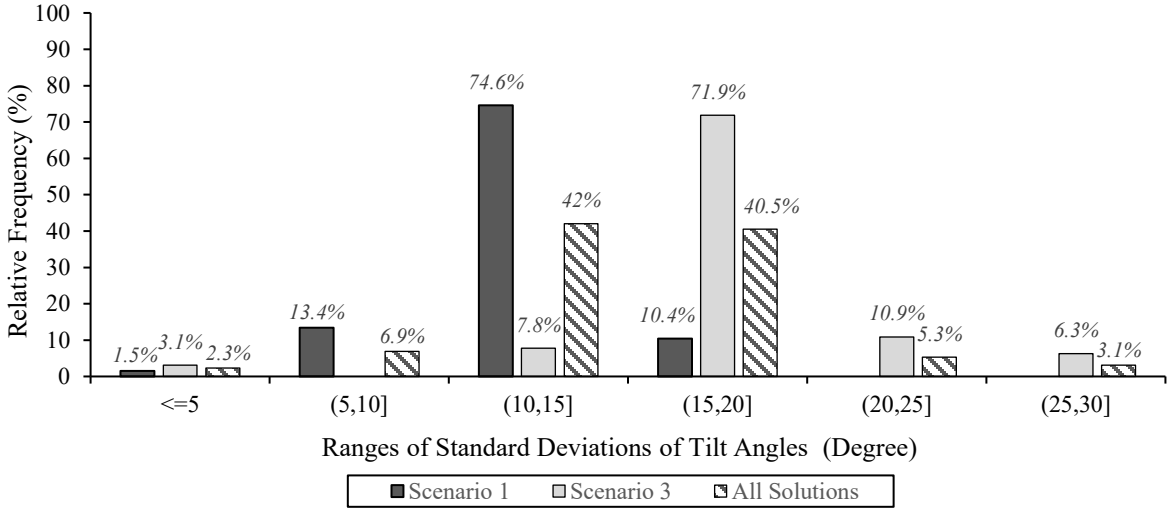

(b)

Figure 4-7 (a) The distribution of average tilt angles, (b) the standard deviation of angles (Rooftop)

Figure 4-8 presents the analysis of the pan angles. As shown in this figure, again 92.1% of all the solutions have average pan angles of 210° to 240°. Compared to tilt angles, pan angles demonstrate a higher degree of variability, with 82.4% of panels having a standard deviation of up to 40°. Again, consistent with the tilt angles, variability in the third scenario is higher than in the first scenario. Nevertheless, the results indicate that all panels are facing the same part of the sky (i.e., [180, 270]).

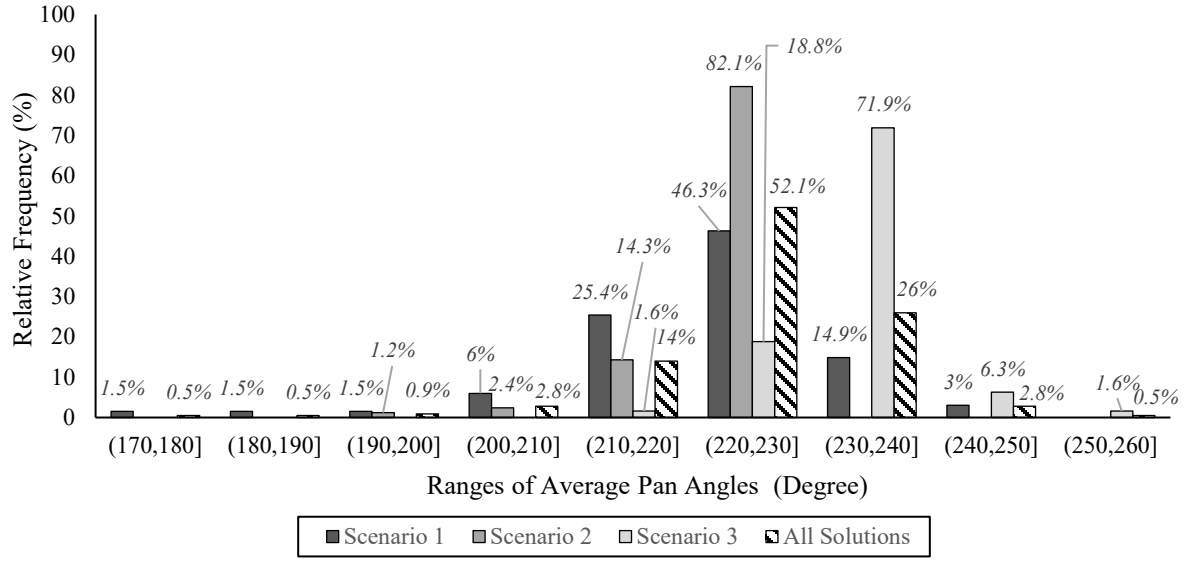

(a)

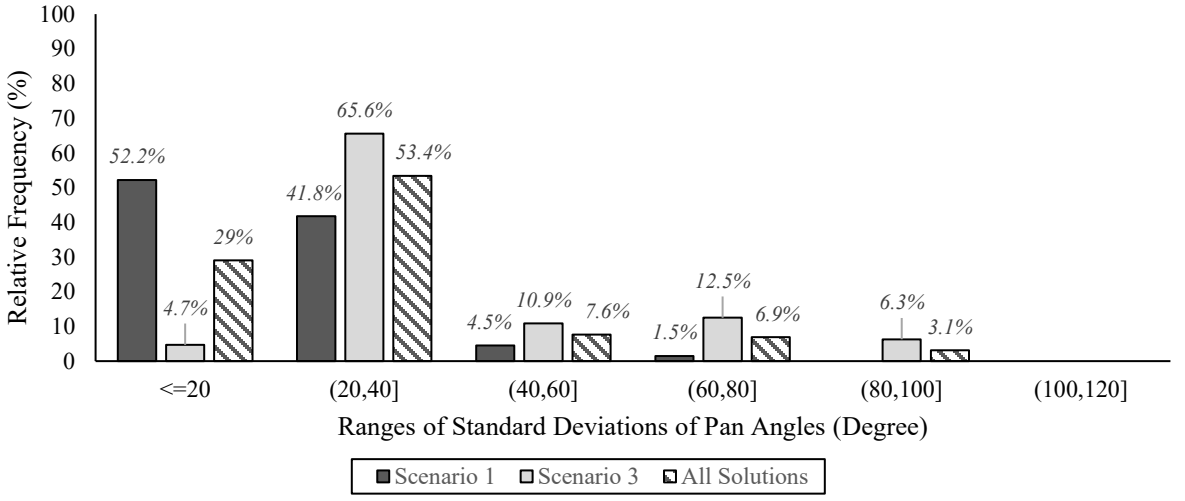

(b)

Figure 4-8 (a) the distribution of average pan angles, (b) the standard deviation of angles (Rooftop)

4.3.2.2 Facade optimization scenarios

As explained in Section 5.4.2, the South-West, North-West, and South-East of the facade surfaces were selected for the optimization process. To show the capability of the proposed BIM-based method to easily distinguish between various surfaces, only the installation of PV modules on the

curtain walls was considered in this study. Based on the BIM model, the distance between two floors on the façade is covered by the curtain panels of 4 m high and 2 m wide. It is assumed that 25% of the floor height is occupied by windows and the remaining part is made of opaque panels. With this assumption, PV modules with the width of 1.5 m and height of 3 m were considered to be installed on the non-window part of each curtain wall, which resulted in a total of 1,137 locations for the installation of panels on the facade based on the generated grid. Similar to the case of rooftops, three different scenarios were considered, i.e., (1) Non-uniform orientation, (2) Uniform orientation, and (3) Batched uniform orientation. In this case, the batching of the panels was considered based on vertical clustering. In total, the entire height of the building was divided into 5 batches. Again, after several trial and error and checking the improvement of solutions' convergence, the optimization configuration was set to (N = 60 and G = 60) panel sizes were kept the same. As explained in Section 3.1, no pan angle was considered for the PV modules on the facade and therefore the optimization decision variables were only $P_{i,k}$ (placement of PV modules), $\theta_{i,k}$ (tilt angle within the range of 0-90°).

The Pareto front of the near-optimum solutions are shown in Figure 4-9(a). Consistent with the observation of rooftop panels, there is a significant overlap between the solutions of the three scenarios. Again, the cost vs. revenue pattern is in a convex form. Figure 4-9(b) shows the profit vs. cost relationship and ROI trend. Unlike the rooftop, the maximum profit for the facade did not happen at the maximum cost, suggesting that after a certain threshold, the cost of additional panels on the facade is not justified. This is because to achieve the full coverage of the curtain walls with PV modules, panels need to be installed at locations where there is not sufficient radiation potential. Therefore, compared to the rooftop, the facade tends to operate at a much lower ROI margin for the majority of solutions on the Pareto fronts. Again, this is a logical pattern because the radiation potential on the vertical surfaces is less than the horizontal surfaces, leading the solutions to yield less revenue for each panel installed. When the maximum-profit cases of the three scenarios are compared, it appears that Scenario 2 offers a slight advantage by offering a higher profit ($117.5K) for a lower cost ($423.7K) resulting in ROI of 27.7%. Figure 4-10 shows the layout of these three designs and Table 4-3 presents their details. When these scenarios are compared with the baseline case (i.e., PV panels are placed on all possible locations without tilt

angles), it is observed that all optimization scenarios offered solutions that are considerably cheaper for more or less similar energy revenue, as shown in Table 4-3. This highlights the significance and added value of the generative design approach towards PV installation.

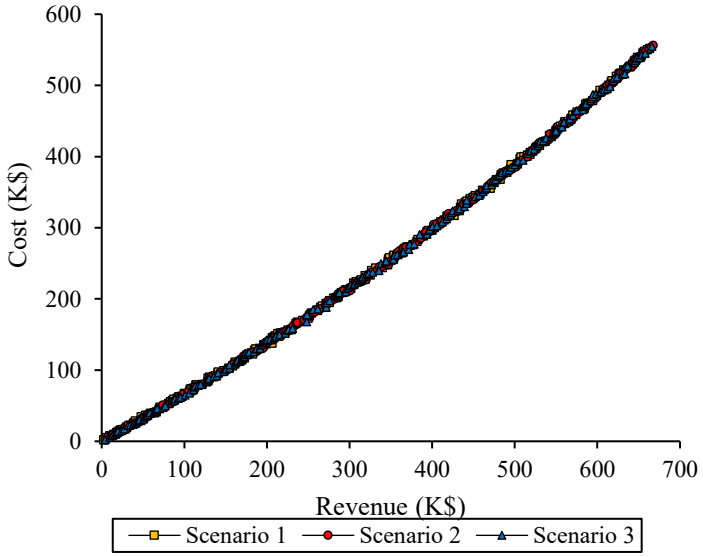

(a)

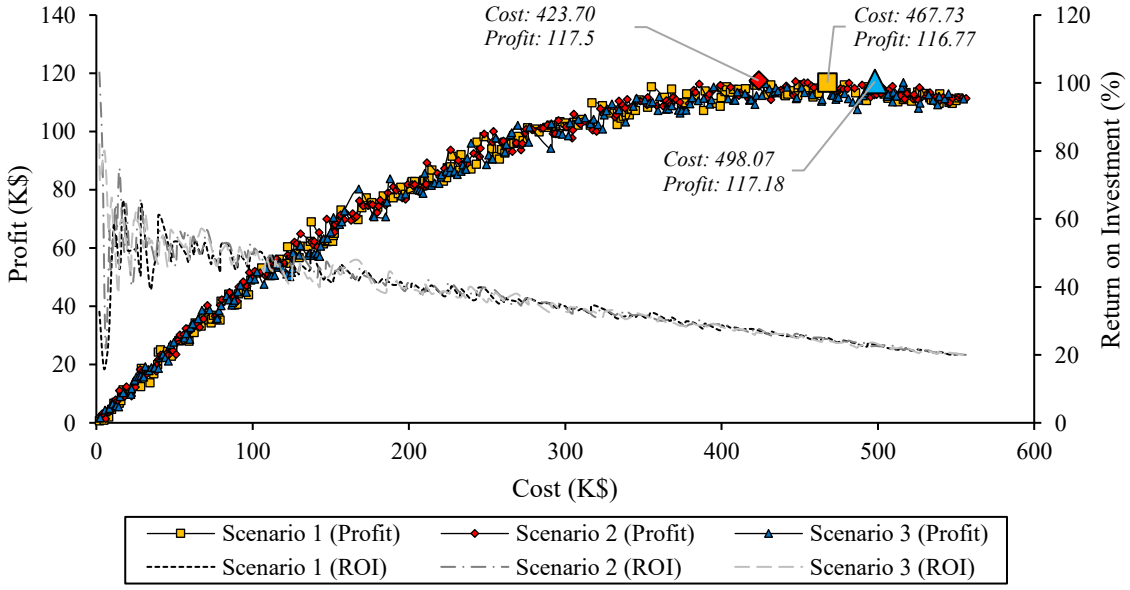

(b)

Figure 4-9 (a) Pareto Fronts, (b) Profit vs. Cost and ROI of solutions of the three different scenarios (Facade)

The hypervolume indicators of the three Pareto fronts are compared in Table 4-4. As demonstrated, again there is no significant difference between the quality of the solutions offered by the three scenarios. This suggests that constraining the problem had little contribution to improving the performance of the optimization module.

Table 4-3 Maximum-profit solutions of the three scenarios for the facade design

Rooftop PV design scenarios	Tilt [Mean, std] *(Degree)*	# of panels	Annual Cumulative Radiation *(MWh)*	Average Radiation *(MWh/m²)*	Energy Revenue *(K$)*	Total Cost *(K$)*	Return on Investment *(%)*	Revenue improvement (compared to baseline) *(%)*	Cost improvement (compared to baseline) *(%)*
Baseline Scenario	[0 , 0]	1137	1360.44	0.26	573.67	556.29	3.12	N/A	N/A
(1) Non-uniform orientation	[45 , 2]	956	1386.12	0.32	584.50	467.73	25	1.89	15.92
(2) Uniform orientation	[45 , 0]	866	1283.43	0.33	541.20	423.70	27.7	-5.66	23.83
(3) Batched uniform orientation	[40 , 4]	1018	1459.06	0.32	615.25	498.07	23.5	7.25	10.47

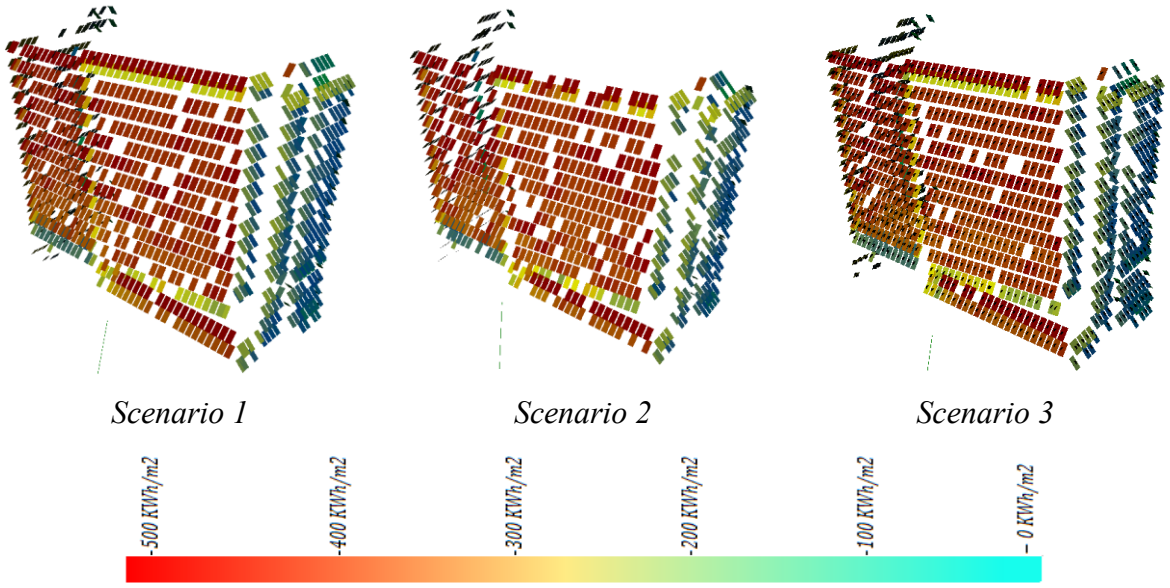

Figure 4-10 Facade PV design scenarios

Table 4-4 Comparison of hypervolumes of the facade three Pareto fronts

Scenario	Hypervolume Value ($\$^2$)	Hypervolume indicator
Non-uniform orientation	1.98428×10^{11}	0.5463
Uniform orientation	1.98862×10^{11}	0.5475
Batched uniform orientation	1.98076×10^{11}	0.5453

Similar to the case of rooftops, the configurations of PV modules on the Pareto fronts was analyzed and plotted in Figure 4-11. This figure represents the distribution of the averages of the tilt angles and the standard deviations of tilt angles of the solutions of all three scenarios. As shown in Figure 4-11(a), very similar to the case of the rooftop, the majority (i.e., 90.6%) of average tilt angles are between 35° to 50°. However, compared to the rooftop, the facade solutions tend to have lower tilt angles, with facade solutions having 31.7% of average tilt angles between 35° to 40° while this rate for the rooftop is only 9.3%. Again, the dominant tilt angles are consistent with the proposed theoretical values. The major difference between the facade and rooftop is the considerably lower variability of tilt angles in the case of the facade. As shown in Figure 4-11(b), 86.1% of solutions have a standard deviation of less than 10°. In the case of the first scenario, 91% of solutions have a standard deviation of less than 5°. This suggests that facade solutions are converging towards uniformity, far more than the rooftop.

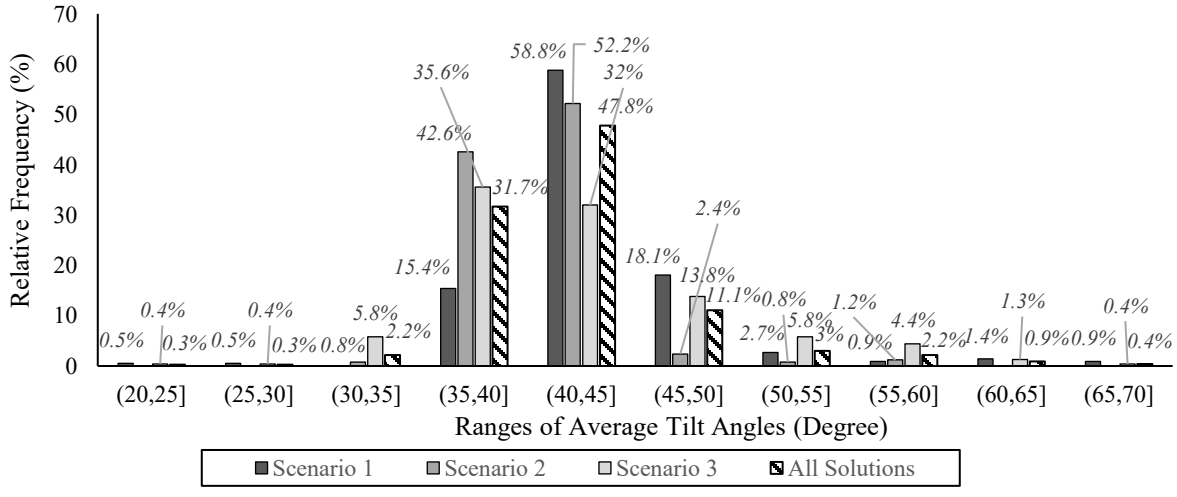

(a)

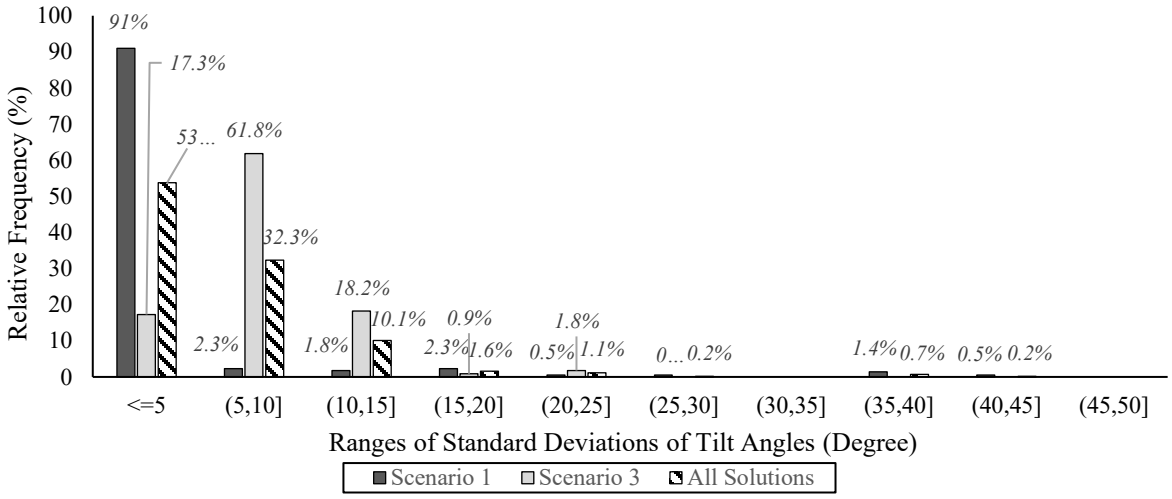

(b)

Figure 4-11 (a) The distribution of average tilt angles, (b) the standard deviation of angles (Facade)

4.3.2.3 Profit analysis for different study periods

In Sections 4.3.2.1 and 4.3.2.2, the optimization of the PV module layout was conducted for the fixed study period of 25 years. Also, the optimization was conducted as a multi-objective optimization that considered revenue and cost. However, different building owners may have different expectations in terms of when their investment needs to be paid back and, in many cases, their final decision is motivated by the generated profit. Essentially, the shorter the expected payback period, the smaller the number of PV modules that need to be considered in order to maximize the profit. To test this hypothesis, the first scenario of non-uniform orientation of panels on the facade was taken to investigate the impact of changing the study period on the optimum solution from the profit perspective. To do so, the multi-objective problem of the previous sections was replaced with a single-objective problem that aims to only maximize profit. Therefore, each optimization run yields a single near-optimum design that maximizes the profit of the building owner. Five different study periods were considered, namely 5, 10, 15, 20, and 25 years. The results are presented in Table 4-5 and Figure 4-12. It should be highlighted that, as can be seen in Table 4-5, the solution with the maximum profit for the study period of 25 years is different from the results shown in Table 4-3. This is because the previous optimization was not searching for the

maximum-profit solutions, but rather for maximum revenue and minimum cost. As can be discerned from the comparison of Table 4-3 and Table 4-5, when the optimization is changed to a single-objective problem focusing on maximizing profit, the identified solution performs better, albeit marginally. As shown in Table 4-5, there is no profit for the first five years of the project even with a minimum number of PV modules. By considering the longer study period, the number of applied PV modules can increase and the project starts to make a profit. As shown in this table, the longer the study period, the higher the ROI and the more profitable the project becomes.

Table 4-5 Profit for different study periods

Study Period (*Years*)	Average Tilt angle (*Degree*)	# of panels	Revenue *(K$)*	Total Cost *(K$)*	Return on Investment (*%*)
25	40	856	537.96	418.81	28.4
20	40	667	374.62	322.44	16.2
15	50	115	63.26	54.82	15.4
10	45	4	2.03	1.88	8.5
5	50	4	1.08	1.84	-41.3

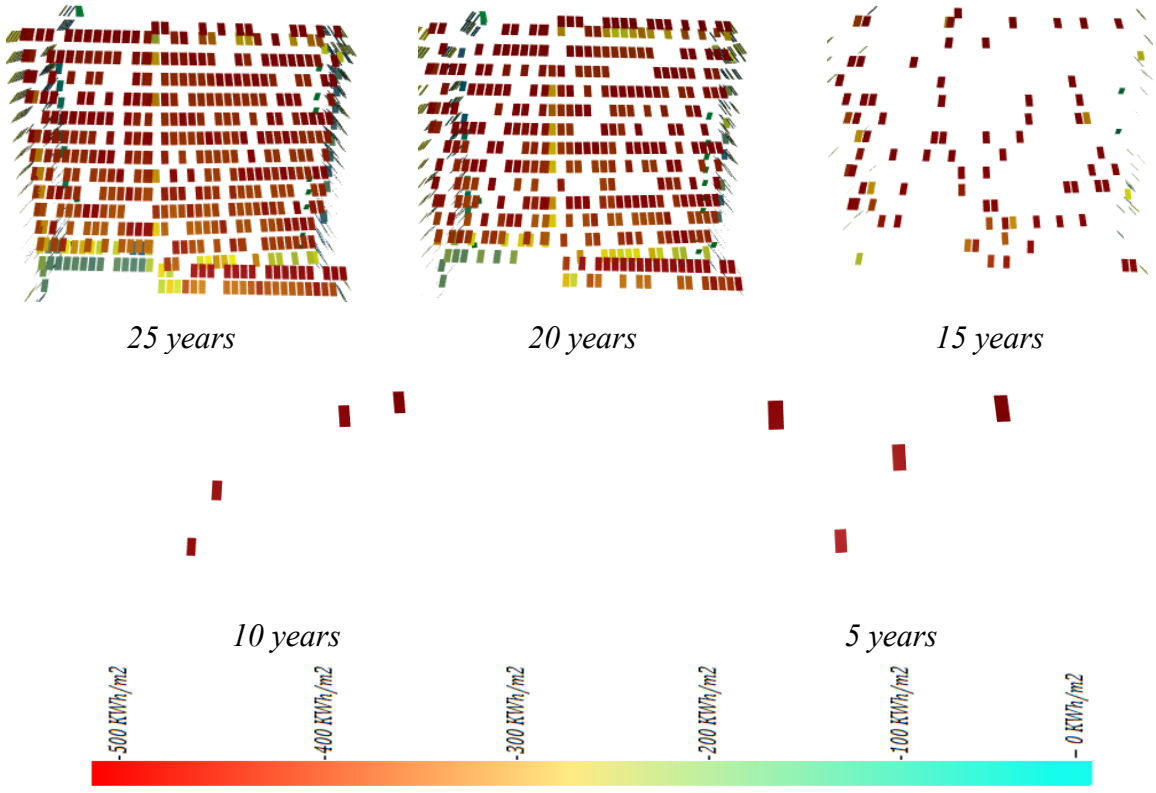

Figure 4-12 Facade PV modules for different study periods

4.3.2.4 Analysis of the impact of PV module size on self-shadowing

As discussed in Section 3, the self-shadowing effect of PV modules needs to be taken into account when considering their use on the buildings' facade. To test this hypothesis, the optimization of facade PV layout was done for three different heights of PV panels, namely, panels with the size of 1.5 m × 2 m, 1.5 m × 3 m, and 1.5 m × 4 m with the same grid spacing. In this case, the problem was defined as a multi-objective optimization problem with the objectives to maximize the revenue and minimize the cost. Figure 4-13 presents the results of this optimization. The details of the most profitable solutions of each scenario are presented in Table 4-6 and Figure 4-14.

The main observation in this analysis is that the maximum profit is achieved when 1.5 m × 3 m panels are used. This is because while smaller panels do not exploit the full potentials of the vertical surfaces, i.e., by covering less area, the performance of PV systems with larger panels is compromised by the increased chance of self-shadowing.

Also, as shown in Figure 4-13(a), as the size of panels increases, the cost of the overall solution also increases. However, the profit does not continuously increase along with the increasing panel sizes. As shown in this figure, the ROIs of different solutions remain almost the same with respect to changes to the panel size. This means that by increasing the panel size, the cost and revenue increase almost at the same rate. The main difference between panel sizes is that although the ROI remains almost intact when the panel sizes are increased, the same profit can be generated by using a smaller number of panels, as shown in Figure 4-13(b).

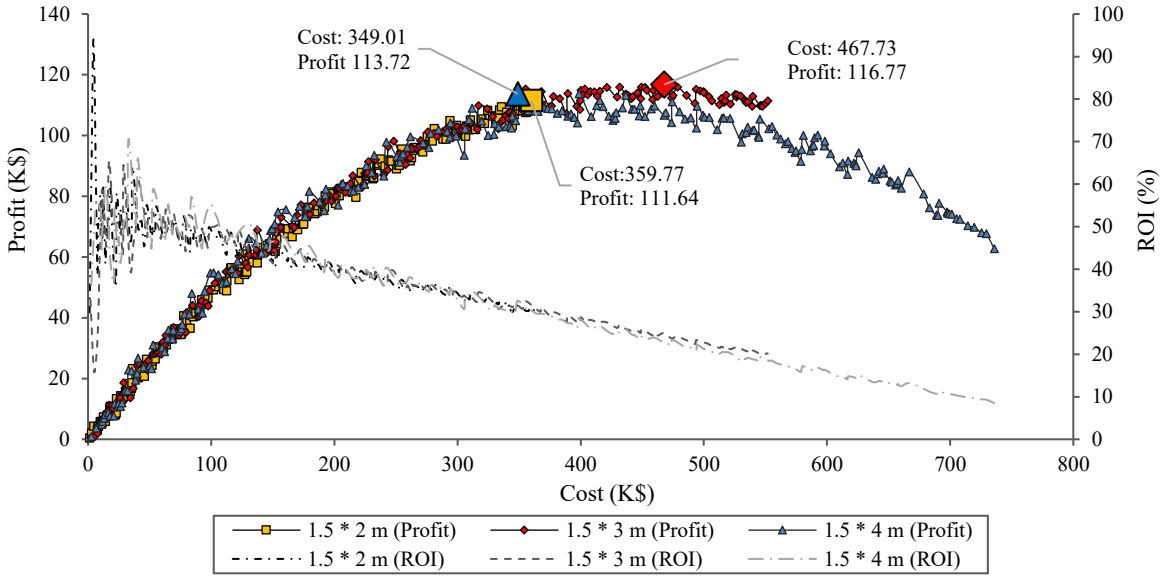

(a)

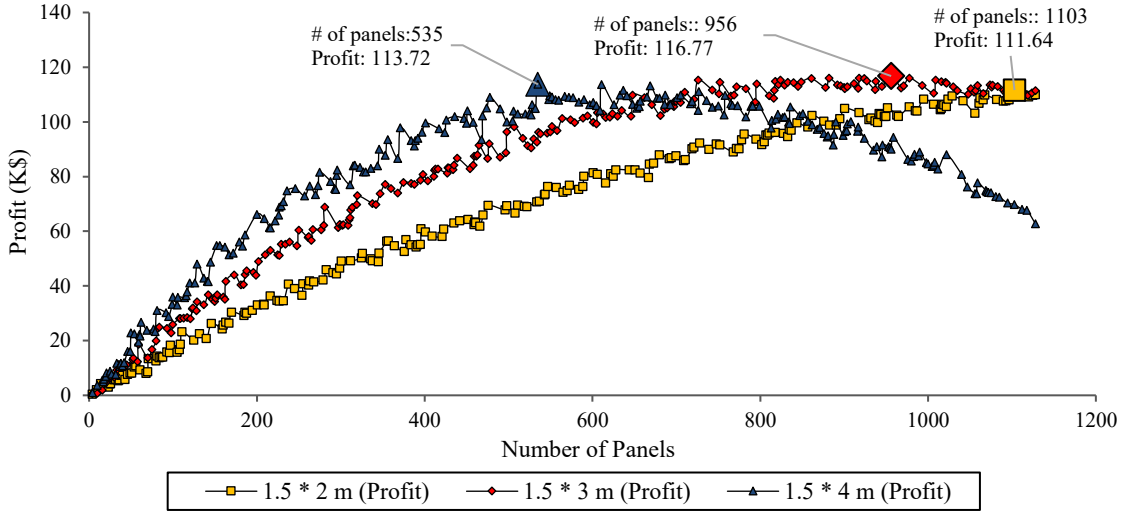

(b)

Figure 4-13 (a) Cost vs. Profit and ROI, (b) number of panels vs. profit of solutions of the three different scenarios with different sizes of panels

Table 4-6 Comparing three different sizes of PV modules to show the self-shadow effect

PV module size *(m^2)*	Tilt [Mean, std] *(Degree)*	# of panels	Annual Cumulative Radiation *(MWh)*	Average Radiation *(MWh/m^2)*	Revenue *(K$)*	Total Cost *(K$)*	Return on Investment *(%)*
1.5 × 2	[40, 1]	1103	1117.93	0.33	471.41	359.77	31
1.5 × 3	[45, 2]	956	1386.12	0.32	584.50	467.73	25
1.5 × 4	[40, 2]	535	1097.35	0.34	462.73	349.01	33

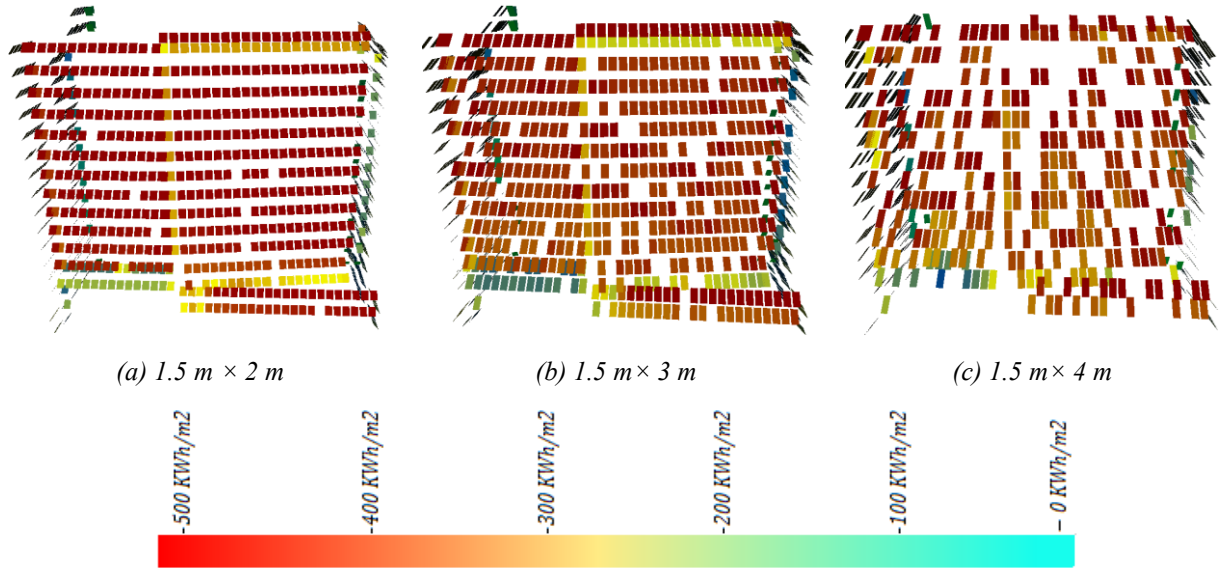

(a) 1.5 m × 2 m *(b) 1.5 m× 3 m* *(c) 1.5 m× 4 m*

Figure 4-14 Optimum PV layouts with three different module sizes

When analyzing the optimum tilt angles of these scenarios, it appears that the panel size does not have a significant impact on the optimal orientation of panels. The average tilt angles and their standard deviation are [46.6, 4.3], [46.2, 3.3], and [47.7, 3.6] for 1.5 m × 2 m, 1.5 m × 3 m, 1.5 m × 4 m sizes, respectively. Again, the optimum tilt angle is consistent with the theoretical recommendations.

4.4 DISCUSSION

The present research made a novel contribution to the body of knowledge by presenting a BIM-based generative design framework for PV module layout design on the whole exterior of high-rise buildings. The main novelty of this framework is that by deploying the semantics of the BIM model, PV layout optimization can be done at a surface-specific level, allowing designers to consider the complex interaction between building surface types (e.g., windows, walls, etc.), type of PV module (e.g., opaque, semi-transparent, etc.), their tilt and pan angles, and the financial aspect of the PV system (i.e., revenue vs. cost at different study periods). The parametric model developed in the previous chapter was seamlessly integrated with an optimization platform to enable a streamlined generative design of the PV module layout.

The most important insight generated by the elaborate case study is that while the we have hypothesized that to gain an optimum yield of the PV system on the facade of buildings, the tilt angles of different arrays of panels need to vary, it was demonstrated that in the majority of the studied scenarios, the optimum solutions favored a more consistent orientation of the panels. The optimum average tilt angles of panels are very much consistent with the theoretical and heuristic recommendations. Nevertheless, it is shown that the high variation of pan angles of PV modules on the horizontal surfaces improves the performance of the PV system. From the aesthetic and installation standpoint, this is more acceptable than the variability in the vertical PV modules because PV modules on horizontal surfaces are less visible and more accessible.

It is also shown that the maximum profit does not always occur when there is a maximum revenue. The installation of panels on any possible location will generate revenue over time; however, if the radiation potential is low, the cost could exceed the revenue and thus push the entire design away from financial optimality. However, it is shown that the expected time horizon for ROI has a major impact on how the optimum PV layout looks and which potential installation locations need to be leveraged. The longer the ROI horizon, the more PV modules can be considered for the installation because even locations with lower radiation potential can become profitable after a certain period of time.

Finally, it was demonstrated that the size of the PV modules has some impact on the optimum layout. The larger the panel sizes, the greater the chance of reduced yield because of the self-shadowing effect but also the higher the amount of energy generated by the panel. Overall, the rate of energy harvested per m^2 of panels changes marginally with the increased size of panels. Nevertheless, given that smaller panels cannot exploit the full potentials of the vertical surfaces and the larger panels have a self-shadow effect, there seems to be a sweet spot in terms of the panel sizes, where the maximum profit can be generated. The proposed framework can help find the optimum size for each building.

4.5 SUMMARY

This chapter proposed a BIM-based generative design approach to optimize the PV modules layout on the building skin. After developing a surface-specific solar radiation simulation model for the building surfaces, an optimization module is integrated with the simulation platform to satisfy two objective functions in the design scenarios. Ultimately, the optimal layout of the PV modules aims to maximize the energy revenue and minimize the life cycle cost. A case study is presented for a high-rise building in Montreal, Canada. Various optimization design scenarios are generated for the rooftop and facade surfaces. Comparing the optimization results for different design scenarios for the rooftops and facades reveals that having a more uniform arrangement in PV layout design increases the chance of using the full capacity of the surface for the installation, because of increasing the generated energy due to less self-shadow effect. In addition to increasing energy revenue, the unified arrangement of the PV modules on the target faced surfaces (i.e. Scenario 2) improves the aesthetic value of the PV layout design and reduces the installation and technical complications.

Since measuring the economic benefit is usually a key step for the building owners and the investors, to investigate the project profit for different study periods, a single objective optimization is conducted to maximize the profit. The results show that the number of the PV modules and the project profit are increased by considering a longer study period.

Based on the above results, it can be concluded that the integration of the surface-specific simulation with the optimization using the generative design approach enables the decision-makers and the investors to consider multiple variables in the design process and find out the optimum solutions based on their needs. The comparison of the results of optimization with the baseline cases indicates the added value of performing optimization for the PV layout design. Overall, a more consistent configuration of PV module is more optimal especially on the façade. It is also discerned that the longer the study period, the more solar panels can be considered for the installation and the higher the return on investment. Also, it appears that constraining the optimization problem, by introducing restrictions on the decision variables, has little impact on the optimality of the solutions identified by the generative design.

CHAPTER 5 SUMMARY, CONTRIBUTIONS, AND FUTURE WORK

5.1 INTRODUCTION

This chapter first summarizes the work done in this research. Then, the contributions and conclusions are explained in detail. Accordingly, the limitations and future work of this research are discussed.

5.2 SUMMARY OF RESEARCH

This research covered a review of the related literature, the current research gaps, the overview of the proposed framework, and a detailed explanation of the proposed methods followed by the implementation to validate and evaluate the applicability of the proposed framework.

In Chapter 2, the current states of the practice and the art in solar radiation evaluation, PV systems, and building PV layout optimization on buildings were discussed. Based on the review, the early research mostly focused on analyzing the solar radiation behavior using numerical and physics models. Then, the introduction of the computational models and various software, as well as the urban developments and the increasing energy demand, propelled researchers and practitioners to move towards investigating solar radiation potential in the built environment. However, simulating the solar radiation potential by considering the complexity of urban structure, was not a simple procedure and required an accurate modeling of the built environment and the surrounding objects. The earlier studies, that investigated the solar radiation behaviour at urban scale, started with GIS-based models. Although the 2.5D models were able to capture the geometries of the objects, the level of detail did not suffice for the surface -specific radiation analysis, which is essential for the more realistic design of PV modules on the building surfaces. Later, by the introduction of BIM, some studies performed the solar radiation simulation based on the building 3D models. However, to optimize the PV layout design on building surfaces, in addition to the 3D semantically-rich models, some other factors (i.e. PV locations, pan and tilt angles, size) should be considered simultaneously, especially when the buildings are located in a dense urban area with the

interference of the shadow effects. Reviewing the exiting research and practices revealed that such an integrated platform which considers all these parameters concurrently to find out where and how to apply or integrate the PV modules on the building surfaces to achieve the optimum performance is still missing.

In Chapter 3, a BIM-based parametric modeling platform was developed for the design of surface-specific PV module layout on the entire skin of a building using the surface properties of the BIM model. A prototype was developed using Dynamo visual programming platform to demonstrate the feasibility of the proposed method from geometrical perspective, and a case study was presented for a building in Montreal, Canada. Multiple scenarios were conducted to accommodate the design variations required for the PV layout design and decision making.

In Chapter 4, a BIM-based GD framework was developed for PV module layout design on the whole exterior of high-rise buildings. For this purpose, the parametric model developed in Chapter 3 was integrated with the optimization module. Integration of the surface-specific solar simulation module with the optimization engine enables the designers to consider multiple design variables, such as the PV modules' location, variety of tilt and pan angles, and PV type with respect to the financial aspect of the generated layouts (i.e., revenue vs. cost at different study periods).

5.3 RESEARCH CONTRIBUTIONS AND CONCLUSIONS

This research work made the following contributions to the body of knowledge:

(1) Demonstrating how BIM can be leveraged towards a more sustainable design of buildings through facilitating the design of complex PV layouts on building skin. By developing a surface-specific solar radiation parametric simulation model for the building surfaces, this research would help designers better harness the potential of solar energy on the vertical surfaces of urban areas. Additionally, it enables the designers to take an analytical approach toward the layout design and application of diverse and upcoming surface-specific PV modules on different surfaces of buildings.

(2) Proposing a BIM-based GD approach to optimize the PV modules layout on the building skin. The parametric model was seamlessly integrated with an optimization module to enable a streamlined GD of the PV module layout to satisfy two objective functions in the design scenarios. The optimal layout of the PV modules aims to maximize the PV energy revenue and minimize the total life cycle cost. With regard to this contribution the following conclusions can be drawn:

- A more uniform PV layout design increases the energy revenue because of less self-shadow effect. In addition, the unified arrangement of the PV modules improves the aesthetic value of the design and reduces the installation and technical complications.
- The results of the single objective optimization for maximizing the profit show that the project profit is increased by considering a longer study period.
- The GD approach enables the decision-makers and the investors to consider multiple variables in the design process and find out the optimum solutions based on their needs.
- The longer the study period, the more solar panels can be considered for the installation and the higher the return on investment.

5.4 ROLES OF MULTIPLE DISCIPLINES IN REALIZING THE VISION OF THE PROPOSED RESEARCH

The practical implications of the proposed research require the collaboration of multiple stakeholders from different disciplines (i.e. remote sensing specialist, architect, energy analyst, owner, contactor) to collect the data necessary for the simulation and contribute to the different levels of decision making with respect to the realization of the research vision.

Figure 5-1 shows the roles of multiple disciplines and modelling requirements in the analysis workflow. Based on the status of the building (i.e. new building, existing building), two different workflows could be considered. For the case of existing buildings, which mostly do not have available as-is BIM model, LiDAR data can be used to generate the facade model of the target building (Catita et al., 2014). Then the required geometric properties of the facade objects, which

are extracted from point cloud data, can be used as an input to perform the surface-specific solar radiation analysis and PV layout design. However, this procedure is less complicated for new buildings, where the BIM model is available. In this case, the clients' requirements can be considered in the design phase. Therefore, the detailed model of the facade can be extracted from the newly designed BIM model. The rest of the procedure is identical for both workflows. In the next step, the energy analyst performs surface-specific radiation analysis and generates various alternatives. Then the optimum PV module layouts will be generated considering the objective functions. The best PV layout will be selected by the owner considering the available budget and the expected payback period. At the end, the installation of the selected PV layout can be done by the contractor.

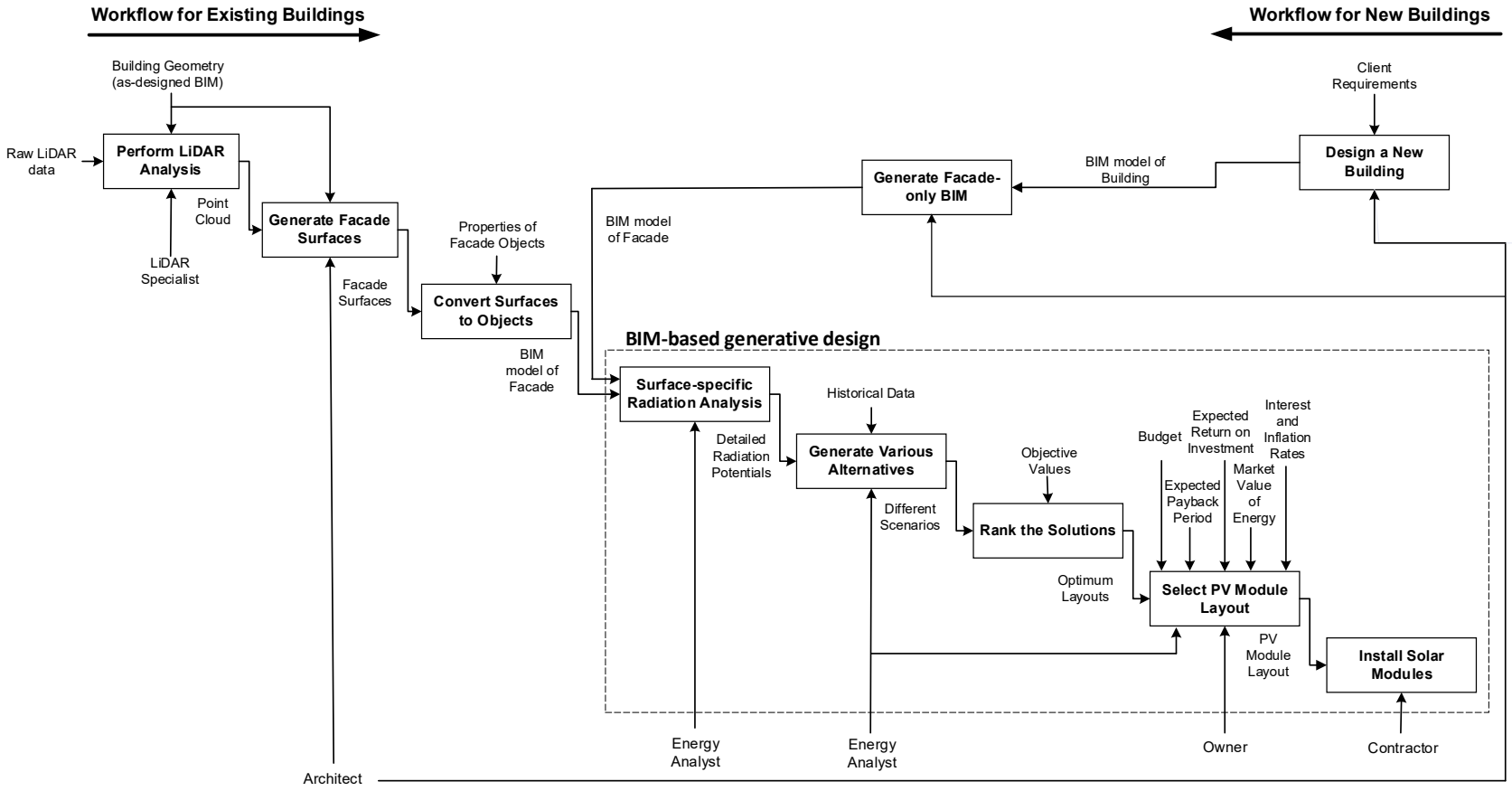

Figure 5-1 Roles of multiple disciplines and modelling requirements in analysis workflow

5.5 LIMITATIONS AND FUTURE WORK

Despite the contributions of this work, there are still some limitations to be addressed in future work as follows:

(1) Although various types of costs are considered in the current cost model, including more details about the soft cost (e.g., permits, the various installation labor fees with respect to the complexity of the surface) and the hard cost (e.g., cost of inverters, electrical and structural components, etc.) can be considered in future studies.

(2) To improve the accuracy of the developed model, some uncertainties (e.g., drastic climate changes, neighborhood developments or an unusual PV market fluctuation) can be considered in future studies.

(3) The proposed methods can be tested in a variety of case studies involving buildings with more complex geometry to further test the full power of the generative design approach.

(4) Due to the lack of control on the hyperparameters of the optimization engine (i.e., Refinery platform), the current optimization process is slow. It can be envisioned that by further improvement of this platform or by replacing it with an open-source alternative, the optimization process can be further enhanced.

(5) Although the panel size was considered in the proposed method, it was not incorporated as a decision variable in the case studies. Considering varying panel sizes in a single solution can potentially generate more favorable solutions.

(6) Although the BIM-based nature of the proposed method offers the apparatus for multi-PV-modules solutions, this research only considered one type of PV modules at a time. This can be changed in the future to better consider the practical and aesthetic aspects of PV layout design.

(7) The current case study considered the installation of PV modules as a design step subsequent to the design of the façade. It can be argued that the design of the façade itself can also be optimized considering the solar radiation potentials. Furthermore, to perform a global and comprehensive optimization of the building skin, some other aspects such as the building energy consumption, daylight access, aesthetic values, and constructability of the design scenarios can be considered in the future research.

(8) It has to be mentioned that, the developed framework in this research is easily applicable if the BIM model of the building is available. However, the main obstacle in using detailed 3D models for solar radiation analysis is the model development, especially for older buildings that usually do not have semantically-rich BIM models at the design phase.

REFERENCES

Aarre Maehlum, M. (2014, May). *Solar Energy Pros and Cons*. Retrieved from Energy Informative: http://energyinformative.org/solar-energy-pros-and-cons/

Abanda, F. H., & Byers, L. (2016). An investigation of the impact of building orientation on energy consumption in a domestic building using emerging BIM (Building Information Modelling). *Energy, 97*, 517-527.

Abraham, A., & Jain, L. (2005). Evolutionary Multiobjective Optimization. *Evolutionary Multiobjective Optimization* (pp. 1-6). London: Springer.

AIA. (2021). *Level of Development Specification.* Retrieved 2018, from The American Institute of Architects: https://bimforum.org/lod/

Al-Janahi, S. A., Ellabban, O., & Al-Ghamdi, S. G. (2020). A Novel BIPV reconfiguration algorithm for maximum power generation under partial shading. *Energies, 13*(17), 44-70.

ArcGIS. (2021). *Esri*. Retrieved from http://www.esri.com/software/arcgis/arcgis-for-desktop

Attoye, D., Tabet Aoul, K., & Hassan, A. (2017). A review on building integrated photovoltaic façade customization potentials. *Sustainability, 9*(12), 1-24.

Autodesk. (2021). *Project Refinery*. Retrieved from https://dynamobim.org/project-refinery-0-62-2-now-available/

Autodesk. (2021). *Revit*. Retrieved from http://www.autodesk.com/education/free-software/revit

Bedrick, J. (2008). *Organizing the development of a building information model.* The American Institute of Architects.

Biyik, E., Araz, M., Hepbasli, A., Shahrestani, M., Yao, R., Shao, L., & Atlı, Y. B. (2017). A key review of building integrated photovoltaic (BIPV) systems. *Engineering science and technology, 20*(3), 833-858.

Bloomberg New Energy Finance. (2018). *Wind & solar to account for 50% of world's power by 2050*. Retrieved from Renewables Now: https://renewablesnow.com/news/wind-solar-to-account-for-50-of-worlds-power-by-2050-bnef-617007/

Brito, M. C., Gomes, N., Santos, T., & Tenedório, J. A. (2012). Photovoltaic potential in a Lisbon suburb using LiDAR data. *Solar Energy, 86*(1), 283-288.

Brown, D. (2016). *How to Run a Solar Radiation Analysis in Revit.* Retrieved from http://dylanbrowndesigns.com/tutorials/how-to-run-a-solar-radiation-analysis-in-revit/

Brown, L. R. (2015). *The Great Transition: Shifting from Fossil Fuels to Solar and Wind Energy.* Washington, D.C: W. W. Norton Company. doi:0393351149, 9780393351149

Bueno, L., Ibliha, M., Vizcarra, B., Chaudhry, G. M., & Siddiki, M. K. (2015). Feasibility analysis of a solar photovoltaic array integrated on façades of a commercial building. *In 2015 IEEE 42nd Photovoltaic Specialist Conference (PVSC)* (pp. 1-4). IEEE.

Byrne, J., Taminiau, J., Kurdgelashvili, L., & Kim, K. N. (2015). A review of the solar city concept and methods to assess rooftop solar electric potential, with an illustrative application to the city of Seoul. *Renewable and Sustainable Energy Reviews, 41*, 830-844.

Caetano, I., Santos, L., & Leitão, A. (2020). Computational design in architecture: Defining parametric, generative, and algorithmic design. *Frontiers of Architectural Research, 9*(2), 287-300.

CanSIA. (2020). *ROADMAP 2020: Powering Canada's Future with Solar Electricity.* Retrieved from http://www.cansia.ca/uploads/7/2/5/1/72513707/cansia_roadmap_2020_final.pdf

Carl, C. (2014). *Calculating solar photovoltaic potential on residential rooftops in Kailua Kona, Hawaii (Doctoral dissertation, University of Southern California).*

Carneiro, C., Morello, E., Desthieux, G., & Golay, F. (2010). Urban environment quality indicators: application to solar radiation and morphological analysis on built area. *In Proceedings of the 3rd WSEAS international conference on Visualization, imaging and simulation* (pp. 141-148). World Scientific and Engineering Academy and Society (WSEAS).

Catita, C., Redweik, P., Pereira, J., & Brito, M. C. (2014). Extending solar potential analysis in buildings to vertical facades. *Computers & Geosciences, 66*, 1-12.

Celik, B., Karatepe, E., Silvestre, S., Gokmen, N., & Chouder, A. (2015). Analysis of spatial fixed PV arrays configurations to maximize energy harvesting in BIPV applications. *Renewable energy, 75*, 534-540.

Charabi, Y., Rhouma, M. B., & Gastli, A. (December 2010). GIS-based estimation of roof-PV capacity & energy production for the Seeb region in Oman. *In Energy Conference and Exhibition (EnergyCon)* (pp. 41-44). IEEE.

Cheng, C. L., Jimenez, C. S., & Lee, M. C. (2009). Research of BIPV optimal tilted angle, use of latitude concept for south orientated plans. *Renewable Energy, 34*(6), 1644-1650.

Chow, A., Fung, A. S., & Li, S. (2014). GIS modeling of solar neighborhood potential at a fine spatiotemporal resolution. *Buildings, 4*(2), 195-206.

City of Montreal. (2021). *Maquette numérique (Bâtiments CityGML LOD2 avec textures).* Retrieved from Portail des données ouvertes: http://donnees.ville.montreal.qc.ca/

CWCT 'Cladding Forum'. (2000). *CURTAIN WALL TYPES.* Retrieved 2018, from http://www.cwct.co.uk/publications/tns/short14.pdf

de Sousa Freitas, J., Cronemberger, J., Soares, R. M., & Amorim, C. N. (2020). Modeling and assessing BIPV envelopes using parametric Rhinoceros plugins Grasshopper and Ladybug. *Renewable Energy, 160*, 1468-1479.

Deb, K., Pratap, A., Agarwal, S., & Meyarivan, T. A. (2002). A fast and elitist multiobjective genetic algorithm: NSGA-II. *Evolutionary Computation, IEEE Transactions, 6*(2), 182-197.

Deb, K., Pratap, A., Agarwal, S., Meyarivan, T., & Fast, A. (2002). A Fast and Elitist Multiobjective Genetic Algorithm:NSGA-II. *IEEE transactions on evolutionary computation, 6*(2), 182-197.

Dezeen. (2017). *dezeen*. Retrieved from https://www.dezeen.com/2017/08/23/copenhagen-international-school-c-f-moller-architects-12000-solar-panels-denmark/

Diwekar, U. (2008). *Introduction to applied optimization* (Vol. 22). Springer Science & Business Media.

Dubayah, R., & Rich, P. M. (1995). Topographic solar radiation models for GIS. *International Journal of Geographical Information Systems, 9*(4), 405-419.

Dynamo. (2021). *Open source graphical programming for design*. Retrieved from http://dynamobim.org/

Eastman, C., Teicholz, P., Sacks, R., & Liston, K. (2011). *BIM handbook: A guide to building information modeling for owners, managers, designers, engineers and contractors.* John Wiley & Sons.

Eke, R., & Demircan, C. (2015). Shading effect on the energy rating of two identical PV systems on a building façade. *Solar Energy, 122*, 48-57.

Electric Choice. (2021). Retrieved from https://www.electricchoice.com/electricity-prices-by-state/

Energysage. (2018). *Size and weight of solar panels*. Retrieved from Energysage: https://news.energysage.com/average-solar-panel-size-weight/

Energysage. (2021). Retrieved from https://news.energysage.com/types-of-solar-panels/

Erdélyi, R., Wang, Y., Guo, W., Hanna, E., & Colantuono, G. (2014). Three-dimensional SOlar RAdiation Model (SORAM) and its application to 3-D urban planning. *Solar Energy, 101*, 63-73.

Esclapés, J., Ferreiro, I., Piera, J., & Teller, J. (2014). A method to evaluate the adaptability of photovoltaic energy on urban façades. *Solar Energy, 105*, 414-427.

ESRI. (2021). *ArcGIS CityEngine*. Retrieved from https://www.esri.com/en-us/arcgis/products/arcgis-cityengine/overview

Fernando, R., Drogemuller, R., & Burden, A. (2012). Parametric and generative methods with building information modelling: Connecting BIM with explorative design modelling. *Proceedings of the 17th International Conference on Computer-Aided Architectural Design Research in Asia* (pp. 537–546). Hong Kong: Association for Computer-Aided Architectural Design Research in Asia (CAADRIA).

Ferreira, B., & Leitão, A. (2015). Generative design for building information modeling. *Computer Aided Architectural Design.* CumInCAD-eCAADe.

Finance Formulas. (2021). *Present Value of a Growing Annuity*. Retrieved from http://financeformulas.net/Present_Value_of_Growing_Annuity.html

Freitas, S., & Brito, M. C. (2015). Maximizing the solar photovoltaic yield in different building facade layouts. (pp. 14-18). Hamburg, Germany: In Proceedings of the European Photovoltaic Solar Energy Conference and Exhibition.

Freitas, S., Serra, F., & Brito, M. C. (2015). PV layout optimization: String tiling using a multi-objective genetic algorithm. *Solar Energy, 118*, 562-574.

Fu, P., & Rich, P. M. (1999). Design and implementation of the Solar Analyst: an ArcView extension for modeling solar radiation at landscape scales. *In Proceedings of the Nineteenth Annual ESRI User Conference*, (pp. 1-31).

Fu, R., Feldman, D., Margolis, R., woodhouse, M., & Ardani, K. (2018). *U.S. Solar Photovoltaic System Cost Benchmark: Q1 2018.* National Renewable Energy Laboratory.

Gastli, A., & Charabi, Y. (2010). Solar electricity prospects in Oman using GIS-based solar radiation maps. *Renewable and Sustainable Energy Reviews, 14*(2), 790-797.

Gooding, J., Edwards, H., Giesekam, J., & Crook, R. (2013). Solar City Indicator: A methodology to predict city level PV installed capacity by combining physical capacity and socio-economic factors. *Solar Energy, 95*, 325-335.

Google Earth. (2021). Retrieved from https://earth.google.com

Gourlis, G., & Kovacic, I. (2017). Building Information Modelling for analysis of energy efficient industrial buildings–A case study. *Renewable and Sustainable Energy Reviews, 68*, 953-963.

Habibi, S. (2017). The promise of BIM for improving building performance. *Energy and Buildings, 153*, 525-548.

Hagerty, K., & Cormican, J. (2019). *Components for solar panel (PV) system*. Retrieved from altestore.com: https://www.altestore.com/howto/components-for-your-solar-panel-photovoltaic-system-a82/

Hassan, R., Cohanim, B., De Weck, O., & Venter, G. (2005). A comparison of particle swarm optimization and the genetic algorithm. *46th AIAA/ASME/ASCE/AHS/ASC Structures, Structural Dynamics and Materials Conference*, (p. 1897).

Hetrick, W. A., Rich, P. M., & Weiss, S. B. (1993). Modeling insolation on complex surfaces. *In Thirteen Annual ESRI User Conference*, *2*, pp. 447-458.

Historical Climate Data. (2018). Retrieved from Government of Canada: http://climate.weather.gc.ca/

Hofierka, J., & Kaňuk, J. (2009). Assessment of photovoltaic potential in urban areas using open-source solar radiation tools. *Renewable Energy, 34*(10), 2206-2214.

Hofierka, J., & Suri, M. (2002). The solar radiation model for Open source GIS: implementation and applications. *In Proceedings of the Open source GIS-GRASS users conference*, (pp. 51-70).

Hofierka, J., & Zlocha, M. (2012). A New 3-D Solar Radiation Model for 3-D City Models. *Transactions in GIS, 16*(5), Transactions in GIS.

Hong, T., Koo, C., Park, J., & Park, H. S. (2014). A GIS (geographic information system)-based optimization model for estimating the electricity generation of the rooftop PV (photovoltaic) system. *Energy, 65*, 190-199.

Husain, A. A., Hasan, W. Z., Shafie, S., Hamidon, M. N., & Pandey, S. S. (2018). A review of transparent solar photovoltaic technologies. *Renewable and Sustainable Energy Reviews, 94*, 779-791.

Hwang, T., Kang, S., & Kim, J. T. (2012). Optimization of the building integrated photovoltaic system in office buildings—Focus on the orientation, inclined angle and installed area. *Energy and Buildings, 46*, 92-104.

International Energy Agency (IEA). (2018). *Renewables.* Retrieved from https://www.iea.org/topics/renewables/subtopics/solar/ .

Introduction to Shading. (2021). Retrieved from www.scratchapixel.com: https://www.scratchapixel.com/lessons/3d-basic-rendering/introduction-to-shading/ligth-and-shadows

IRENA. (2021). *Clean Energy Corridors*. Retrieved from International Renewable Energy Agency: https://www.irena.org/cleanenergycorridors

Jacobson, M. Z., & Jadhav, V. (2018). World estimates of PV optimal tilt angles and ratios of sunlight incident upon tilted and tracked PV panels relative to horizontal panels. *Solar Energy, 169*, 55-66.

Jakubiec, J. A., & Reinhart, C. F. (2013). A method for predicting city-wide electricity gains from photovoltaic panels based on LiDAR and GIS data combined with hourly Daysim simulations. *Solar Energy, 93*, 127-143.

Jelle, B. P., Breivik, C., & Røkenes, H. D. (2012). Building integrated photovoltaic products: A state-of-the-art review and future research opportunities. *Solar Energy Materials and Solar Cells, 100*, 69-96.

Jochem, A., Höfle, B., Rutzinger, M., & Pfeifer, N. (2009). Automatic roof plane detection and analysis in airborne lidar point clouds for solar potential assessment. *Sensors, 9*(7), 5241-5262.

Karteris, M., Slini, T., & Papadopoulos, A. M. (2013). Urban solar energy potential in Greece: A statistical calculation model of suitable built roof areas for photovoltaics. *Energy and Buildings, 62*, 459-468.

Kemery, B. P., Beausoleil-Morrison, I., & Rowlands, I. H. (2012). Optimal PV orientation and geographic dispersion: a study of 10 Canadian cities and 16 Ontario locations. (pp. 1- 4). Halifax, NS, Canada: In Proceedings of the Canadian Conference on Building Simulation.

Kennedy, J., & Eberhart, R. (1995). Particle swarm optimization (PSO). *In Proc. IEEE International Conference on Neural Networks, Perth, Australia*, (pp. 1942-1948).

Kim, H., Asl, M. R., & Yan, W. (2015). Parametric BIM-based energy simulation for buildings with complex kinetic façades. *In Proceedings of the 33rd eCAADe Conference*, *1*, pp. 657-664.

Koo, C., Hong, T., Lee, M., & Kim, J. (2016). An integrated multi-objective optimization model for determining the optimal solution in implementing the rooftop photovoltaic system. *Renewable and Sustainable Energy Reviews, 57*, 822-837.

Kucuksari, S., Khaleghi, A. M., Hamidi, M., Zhang, Y., Szidarovszky, F., Bayraksan, G., & Son, Y. J. (2014). An Integrated GIS, optimization and simulation framework for optimal PV size and location in campus area environments. *Applied Energy, 113*, 1601-1613.

Kumar, L., Skidmore, A. K., & Knowles, E. (1997). Modelling topographic variation in solar radiation in a GIS environment. *International Journal of Geographical Information Science, 11*(5), 475-497.

Ladybug Tools. (2021). Retrieved from https://www.ladybug.tools/ladybug.html

Li, Y., & Liu, C. (2018). Techno-economic analysis for constructing solar photovoltaic projects on building envelopes. *Building and Environment, 127*, 37-46.

Liang, J., Gong, J., Li, W., & Ibrahim, A. N. (2014). A visualization-oriented 3D method for efficient computation of urban solar radiation based on 3D–2D surface mapping. *International Journal of Geographical Information Science, 28*(4), 780-798.

Lin, Q., Kensek, K., Schiler, M., & Choi, J. (2021). Streamlining sustainable design in building information modeling BIM-based PV design and analysis tools. *Architectural Science Review*, 1-11.

Liu, S., Meng, X., & Tam, C. (2015). Building information modeling based building design optimization for sustainability. *Energy and Buildings, 105*, 139-153.

Ludwig, D., Lanig, S., & Klärle, M. (2009). Sun-area towards location-based analysis for solar panels by high resolution remote sensors (LiDAR). *In Proceedings of International Cartograhy Conference.* Santiago de Chile.

LunchBox. (2021). Retrieved from proving ground: https://provingground.io/tools/lunchbox/

Ma, W., Wang, X., Wang, J., Xiang, X., & Sun, J. (2021). Generative Design in Building Information Modelling (BIM): Approaches and Requirements. *Sensors, 21*(16), 5439.

Mallawaarachchi, V. (2021). *Towards Data Science*. Retrieved 2018, from https://towardsdatascience.com/

Mardaljevic, J. (2000). Simulation of annual daylighting profiles for internal illuminance. *International Journal of Lighting Research and Technology, 32*(3), 111-118.

Marsh, A. (2003). *ECOTECT and EnergyPlus.* Building Energy Simulation User News.

Marszal, A. J., Bourrelle, J. S., Musall, E., Voss, K., Sartori, I., & Napolitano, A. (2011). Zero Energy Building–A review of definitions and calculation methodologies. *Energy and buildings, 43*(4), 971-979.

Martín, A. M., Domínguez, J., & Amador, J. (2015). Applying LiDAR datasets and GIS based model to evaluate solar potential over roofs: A review. *AIMS Energy, 11*(2), 326-343.

Mawlana, M. (2015). Improving Stochastic Simulation-based Optimization for Selecting Construction Method of Precast Box Girder Bridges. *PhD thesis*. Concordia University.

McCall, J. (2005). Genetic algorithms for modelling and optimisation. *Journal of Computational and Applied Mathematics, 184*(1), 205-222.

McCormack, J., Dorin, A., & Innocent, T. (2004). Generative Design: A Paradigm for Design Research. *Futureground - DRS International Conference.* Melbourne, Australia: Design Research Society (DRS).

Mellouk, L., Aaroud, A., Benhaddou, D., Zine-Dine, K., & Boulmalf, M. (2015). Overview of mathematical methods for energy management optimization in smart grids. In Renewable and Sustainable Energy Conference (IRSEC), 2015 3rd International (pp. *In Renewable and Sustainable Energy Conference (IRSEC), 2015 3rd International* (pp. 1-5). IEEE.

Melo. (2021). Retrieved from https://www.teses.usp.br/teses/disponiveis/3/3143/tde-21062013-105044/publico/Solar3DBR_SourceCode.pdf

Melo, E. G., Almeida, M. P., Zilles, R., & Grimoni, J. A. (2013). Using a shading matrix to estimate the shading factor and the irradiation in a three-dimensional model of a receiving surface in an urban environment. *Solar Energy, 92*, 15-25.

Mitchell, W. J. (1975). The theoretical foundation of computer-aided architectural design. *Environment planning and design*, 127-150.

Morris, F. A. (2013). Definition and Types of Curtain Walls. In *Curtain Wall Systems.* ASCE.

Natural Resources Canada. (2019). *Solar Photovoltaic Energy in Buildings*. Retrieved from https://www.nrcan.gc.ca/energy/efficiency/data-research-and-insights-energy-efficiency/buildings-innovation/solar-photovoltaic-energy-buildings/3907

Nguyen, H. T., Pearce, J. M., Harrap, R., & Barber, G. (2012). The application of LiDAR to assessment of rooftop solar photovoltaic deployment potential in a municipal district unit. *Sensors, 12*(4), 4534-4558.

Ning, G., Junnan, L., Yansong, D., Zhifeng, Q., Qingshan, J., Weihua, G., & Geert, D. (2017). BIM-based PV system optimization and deployment. *Energy and Buildings, 150*, 13-22.

Ning, G., Kan, H., Zhifeng, Q., Weihua, G., & Geert, D. (2018). e-BIM: a BIM-centric design and analysis software for Building Integrated Photovoltaics. *Automation in Construction, 87*, 127-137.

Norton, B., Eames, P. C., Mallick, T. K., Huang, M. J., McCormack, S. J., Mondol, J. D., & Yohanis, Y. G. (2011). Enhancing the performance of building integrated photovoltaics. *Solar Energy, 85*(8), 1629-1664.

Onyx Solar . (2019). *Photovoltaic Glass for Buildings*. Retrieved from ONYX: https://www.onyxsolar.com/

Ordóñez, J., Jadraque, E., Alegre, J., & Martínez, G. (2010). Analysis of the photovoltaic solar energy capacity of residential rooftops in Andalusia (Spain). *Renewable and Sustainable Energy Reviews, 14*(7), 2122-2130.

Paulescu, M., Paulescu, E., Gravila, P., & Badescu, V. (2012). *Weather modeling and forecasting of PV systems operation.* Springer Science & Business Media.

Peng, C., Huang, Y., & Wu, Z. (2011). Building-integrated photovoltaics (BIPV) in architectural design in China. *Energy and Buildings, 43*(12), 3592-3598.

Perez, R., Ineichen, P., Seals, R., Michalsky, J., & Stewart, R. (1990). Modeling daylight availability and irradiance components from direct and global irradiance. *Solar energy, 44*(5), 271-289.

r.sun. (2006). Retrieved from https://docs.huihoo.com/grass/6.3/manuals/r.sun.html

Raugei, M., & Frankl, P. (2009). Life cycle impacts and costs of photovoltaic systems: current state of the art and future outlooks. *Energy, 34*(3), 392-399.

Redweik, P., Catita, C., & Brito, M. (2013). Solar energy potential on roofs and facades in an urban landscape. *Solar Energy, 97*, 332-341.

Rhinoceros. (2021). Retrieved from https://www.rhino3d.com/6/new/grasshopper/

Robinson, D., & Stone, A. (2004). Irradiation modelling made simple: the cumulative sky approach and its applications. *In PLEA conference* , (pp. 19-22).

Salimi, S., Mawlana, M., & Hammad, A. (2018). Performance analysis of simulation-based optimization of construction projects using high performance computing. *Automation in Construction, 87*, 158-172.

Salimzadeh, N., Sharif, S. A., & Hammad, A. (2016). Visualizing and Analyzing Urban Energy Consumption: A Critical Review and Case Study. *In Construction Research Congress*, (pp. 1323-1331).

Schmitt, L. M. (2001). Theory of genetic algorithms. *Theoretical Computer Science, 259*(1-2), 1-61.

SEIA. (2018). *Solar Means Bussiness.*

S-Energy. (2018). *BIPV Module*. Retrieved from http://www.s-energy.com/epage.php?it_id=1426727258

Shin, D., & Choi, S. H. (2018). Recent Studies of Semitransparent Solar Cells. *Coatings, 8*(10), 329.

Simulation and design of solar systems. (2021). Retrieved from photovoltaic-software.com: https://photovoltaic-software.com/principle-ressources/how-calculate-solar-energy-power-pv-systems

Smith, A., & Gill, G. (2014). *FKI Tower*. Retrieved 2018, from http://smithgill.com/work/fki/

Solar Analysis. (2021). Retrieved from Autodesk: https://knowledge.autodesk.com/support/revit-products/learn-explore/caas/CloudHelp/cloudhelp/2021/ENU/Revit-Analyze/files/GUID-925CBF1E-2B91-41A7-8CA8-C87F69F7BBC1-htm.html

Solar Power Farm. (2021). Retrieved from https://www.solarpowerfam.com/cost-of-solar-panels-per-square-meter/

Solconpro. (2018). Retrieved from solconpro: http://www.solconpro.de

Srinivas, N., & Deb, K. (1994). Muiltiobjective optimization using nondominated sorting in genetic algorithms. . *Evolutionary computation, 2*(3), 221-248.

SUNMetrix. (2021). *Cost of Solar Panels*. Retrieved from SUNMetrix: https://sunmetrix.com/cost-of-solar-panels/#solar1

Šúri, M. H., & Dunlop, E. D. (2005). PV-GIS: a web-based solar radiation database for the calculation of PV potential in Europe. *International Journal of Sustainable Energy, 24*(2), 55-67.

Šúri, M., Huld, T. A., Dunlop, E. D., & Ossenbrink, H. A. (2007). Potential of solar electricity generation in the European Union member states and candidate countries. *Solar energy, 81*(10), 1295-1305.

Svarc, J. (2021). *Clean Energy Reviews.* Retrieved from https://www.cleanenergyreviews.info/blog/most-efficient-solar-panels

Sydora, C., & Stroulia, E. (2020). Rule-based compliance checking and generative design for building interiors using BIM. *Automation in Construction*(120).

The eco experts. (2021). *Solar panels*. Retrieved from The eco experts: https://www.theecoexperts.co.uk/solar-panels/how-much-electricity

Tooke, T. R., Coops, N. C., Christen, A., Gurtuna, O., & Prévot, A. (2012). Integrated irradiance modelling in the urban environment based on remotely sensed data. *Solar Energy, 86*(10), 2923-2934.

Touloupaki, E., & Theodosiou, T. (2017). Energy performance optimization as a generative design tool for nearly zero energy buildings. *Procedia engineering, 180*, 1178-1185.

Traverse, C. J., Pandey, R., Barr, M. C., & Lunt, R. R. (2017). Emergence of highly transparent photovoltaics for distributed applications. *Nature Energy, 2*(11), 849–860.

United Nations. (2015). *World Urbanization Prospects: The 2014 Revision.* Department of Economic and Social Affairs, Population Division.

Vermeulen, D., & El Ayoubi, M. (2021). *Using generative design in construction applications*. Retrieved from Autodesk University: https://medium.com/autodesk-university/using-generative-design-in-construction-applications-e268c785b004

Wang, J. L., & Chen, X. (2010). Parametric design based on building information modeling for sustainable buildings. *International Conference on Challenges in Environmental Science and Computer Engineering. 2*, pp. 236-239. IEEE.

Wang, R. (2016). An Improved Nondominated Sorting Genetic Algorithm for Multiobjective Problem. *Mathematical Problems in Engineering* (pp. 1-7). Hindawi Publishing Corporation.

Wang, X., Song, Y., & Tang, P. (2020). Generative urban design using shape grammar and block morphological analysis. *Frontiers of Architectural Research, 9*(4), 914-924.

Ward, G. J. (1994). The RADIANCE lighting simulation and rendering system. *In Proceedings of the 21st annual conference on Computer graphics and interactive techniques* (pp. 459-472). ACM.

Wiginton, L. K., Nguyen, H. T., & Pearce, J. M. (2010). Quantifying rooftop solar photovoltaic potential for regional renewable energy policy. *Computers, Environment and Urban Systems, 34*(4), 345-357.

Yoon, J. H., Song, J., & Lee, S. J. (2011). Practical application of building integrated photovoltaic (BIPV) system using transparent amorphous silicon thin-film PV module. *Solar Energy, 85*(5), 723-733.

Zhang, J., Liu, N., & Wang, S. (2021). Generative design and performance optimization of residential buildings based on parametric algorithm. *Energy and Buildings, 244*, 111033.

APPENDICES

Appendix A. GENERATING PV LAYOUT ON CURTAIN WALL

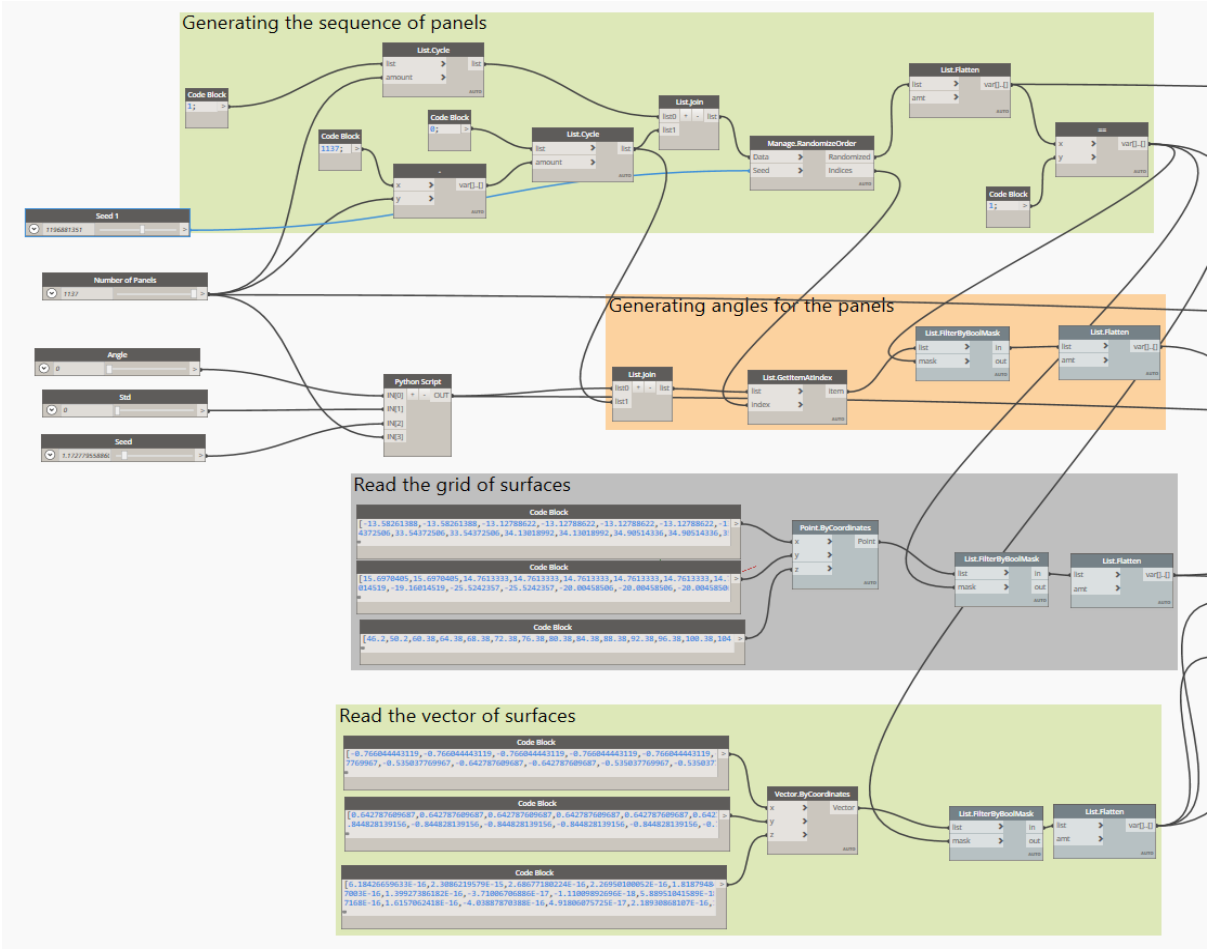

Figure A-1 Generating the sequence of panels

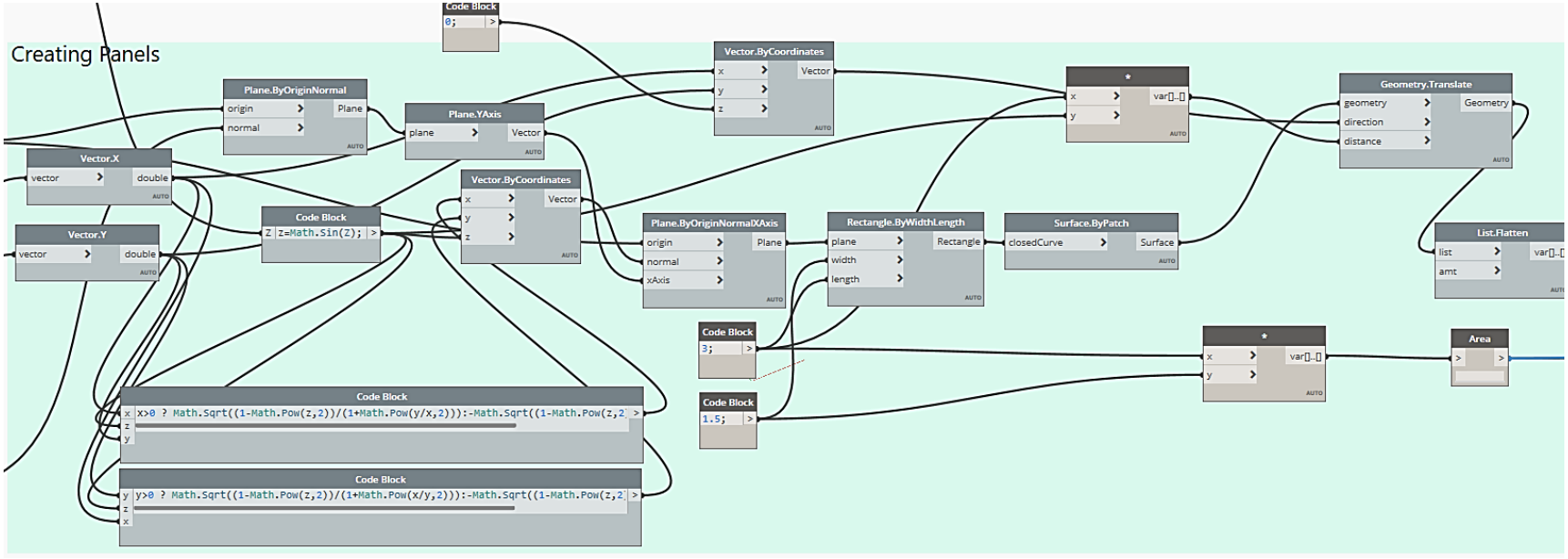

Figure A-2 Creating panels with tilt angle

Appendix B. SHADING ANALYSIS

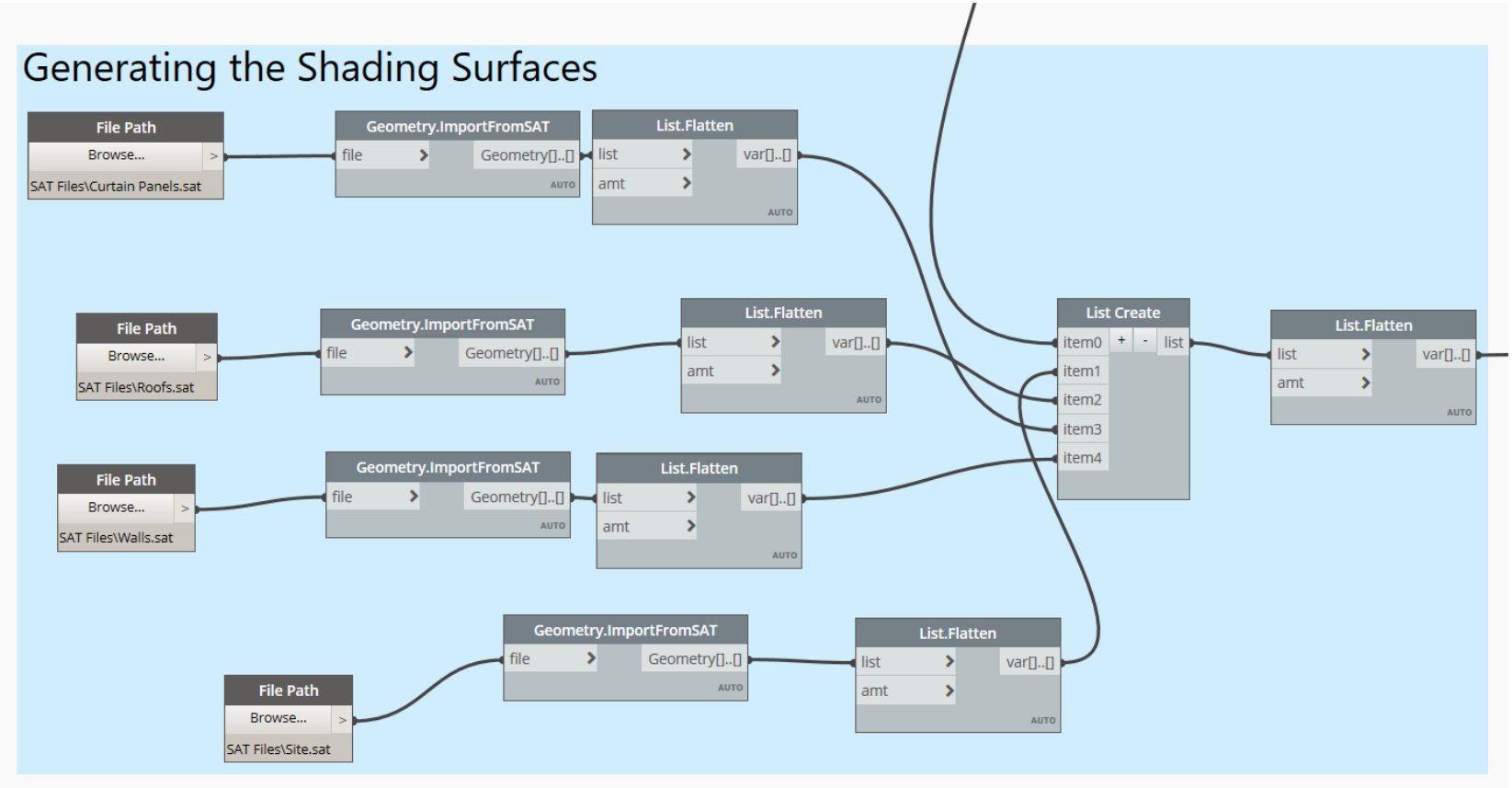

Figure B-1 Generating the shading surfaces

Appendix C. SOLAR SIMULATION

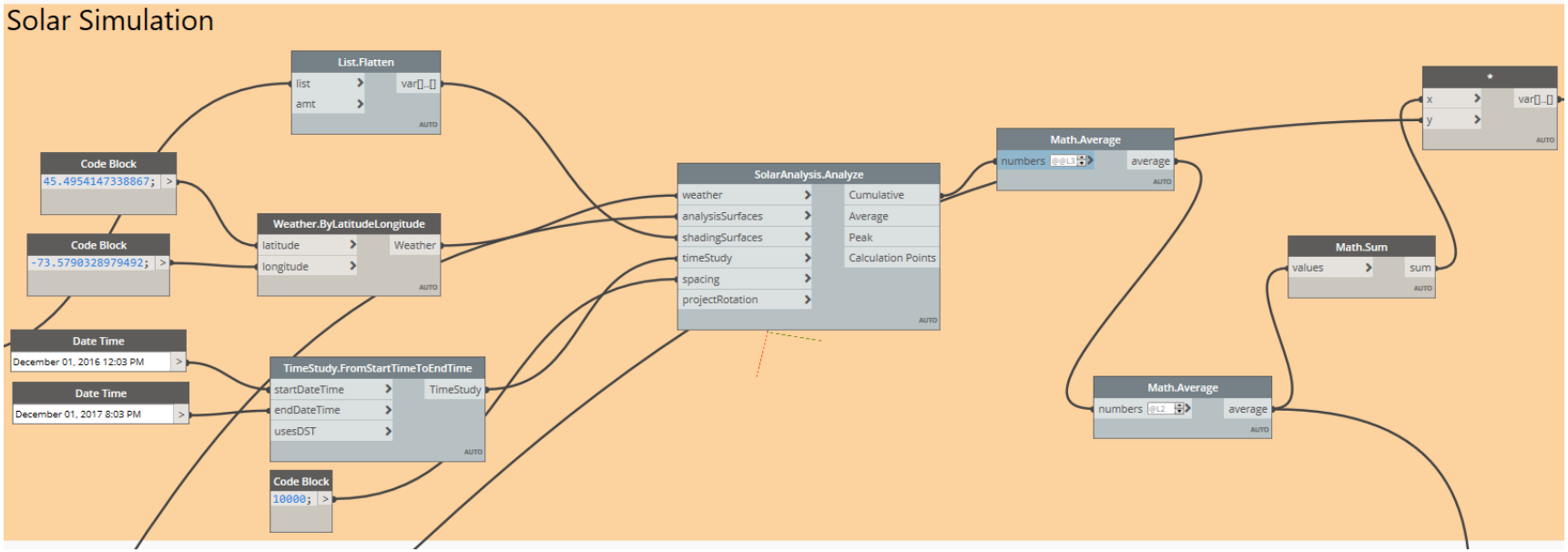

Figure C-1 Solar simulation

Appendix D. GENERATING PV LAYOUT ON ROOFTOP

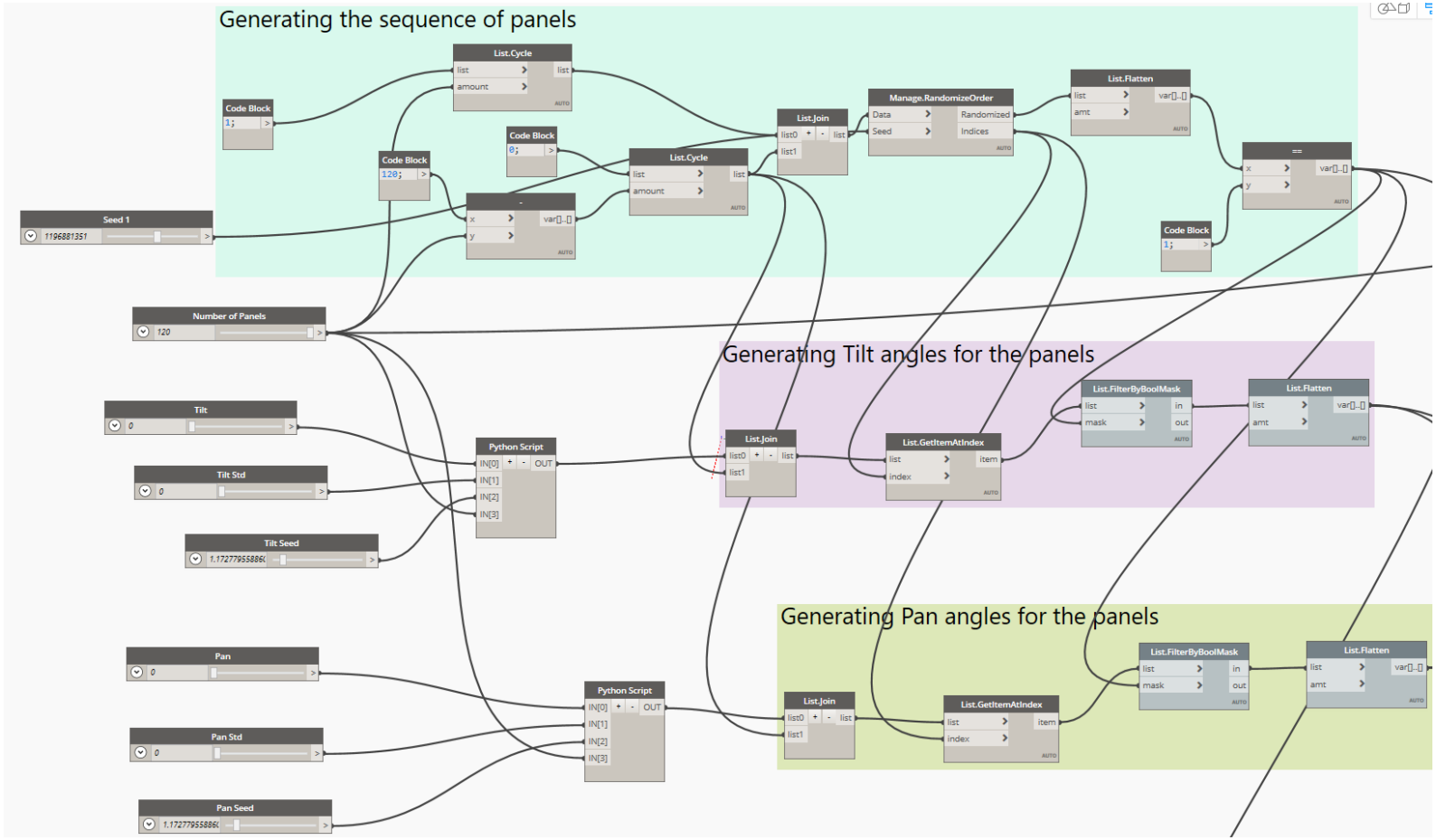

Figure D-1 Generating the sequence of panels, defining pan and tilt angles

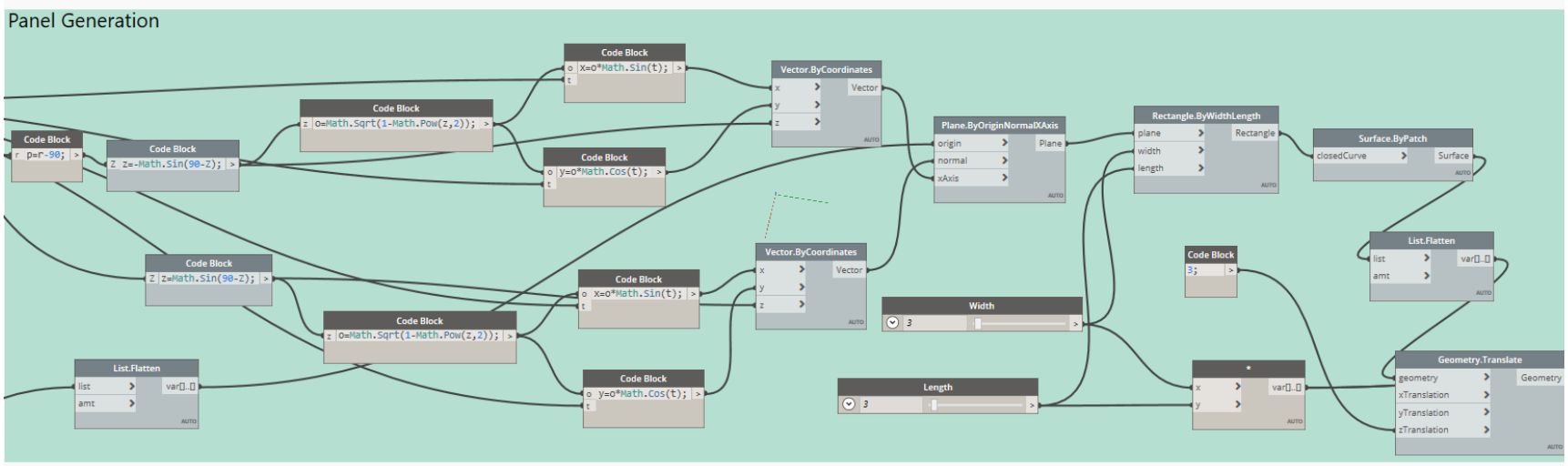

Figure D-2 Panel creation with pan and tilt angle

Appendix E. LIST OF PUBLICATIONS

Journal Papers

- Salimzadeh, N., Vahdatikhaki, F., and Hammad, A. (2021). Optimization of PV Modules Layout on High-rise Building Skins Using a BIM-based Generative Design Approach. *Cleaner Production* (Under Review).

- Salimzadeh, N., Vahdatikhaki, F., and Hammad, A. (2020). Parametric Modelling and Surface-specific Sensitivity Analysis of PV Module Layout on Building Skin Using BIM. *Energy and Buildings,* 216, 109953.

Conference Papers

- Salimzadeh, N., Vahdatikhaki, F., and Hammad, A. (2018). BIM-based Surface-specific Solar Simulation of Buildings. In *ISARC. Proceedings of the International Symposium on Automation and Robotics in Construction* (Vol. 35, pp. 1-8). IAARC Publications.

- Salimzadeh, N., Hammad, A. (2017). High-level Framework for GIS-Based Optimization of Building Photovoltaic Potential at Urban Scale Using BIM and LiDAR. In *International Conference on Sustainable Infrastructure 2017* (pp. 123-134).

- Salimzadeh, N., Sharif, S. A., and Hammad, A. (2016). Visualizing and analyzing urban energy consumption: A critical review and case study. In *Construction research congress 2016* (pp. 1323-1331).